1506
UNIVERSITÀ
DEGLI STUDI
DI URBINO
CARLO BO

DIPARTIMENTO DI SCIENZE PURE E APPLICATE
CORSO DI DOTTORATO DI RICERCA IN SCIENZE DI BASE E APPLICAZIONI
Curriculum SCIENZE CHIMICHE E SCIENZE FARMACEUTICHE
Ciclo XXXII

Design and Development of Novel Biocompatible Nanosystems for *Drug Delivery*

Settore scientifico disciplinare: CHIM/09

RELATORE

Chiar.mo Prof. Luca Casettari

DOTTORANDO
Dott.ssa Francesca Biondo

Anno accademico 2018-2019

A me, "che cerco sempre di fare
ciò che non sono capace di fare,
per imparare a farlo"
P. Picasso

TABLE OF CONTENTS

SECTION I

Polymeric Nanoparticles in Drug Delivery

SECTION II

Phospholipid Nanoparticle in Drug Delivery

SECTION III

Glycolipid-Mediated Liposome Targeting in Zebrafish Embryos

Abstract

In recent years, pharmaceutical research has focused on the development on nanotechnology systems applicable in different fields of medicine, especially in the field of drug delivery. Nanotechnology is an emerging branch of sciences for designing tools and devices of nanoscale size with specific function at the cellular, atomic and molecular levels. Nanocarriers, owing to their high surface area volume ratio, have the ability to alter basic properties and bioactivity of drugs. Improved the pharmacokinetics and biodistribution, decreased toxicities, improved solubility and stability, controlled release and site-specific delivery of therapeutic agents are some of the features that nanocarriers can incorporate in drug delivery system. The composition of the nanocarriers, (e. g. organic, inorganic, and hybrid materials) and the form in which drugs are associated with them, such as core-shell system or matrix system, are also fundamental for understanding their drug delivery profile.

Considering the above facts, this dissertation aims to design novel nano-based drug delivery systems and to develop new control process strategies, such as modified the shape, chemical composition, internal structure and morphology of the nanocarriers so as to obtain new levels of product performance in the targeted drug delivery system.

Firstly, we designed a new nano-formulations to enhance the therapeutic efficacy and bioavailability of ocular drugs, for glaucoma therapy. An amphiphilic di-block copolymer, composed of methoxy poly(ethylene glycol) (mPEG) and poly(ε-caprolactone) (PLC), that can self-assemble into polymeric micelles (PMs), was synthesized. mPEG-PLC PMs bearing the hydrophobic drug, Methazolamide (MTZ) were formulated and fully characterized. In *vitro* and in *vivo* studies were carried out to verify ocular tolerability and to evaluate anti-glaucoma activity in a glucocorticoid-induced glaucoma model. The results showed that, a better in *vivo* inhibitory effect of MTZ-PMs was achieved, compared to MTZ solution on glaucoma induction in experimental rabbits. Hence, these newly developed nano formulations have characteristics which are appropriate for ocular nanodelivery.

Secondly, in effort to develop improved nano-liposomal carriers for in *vivo* application on Zebrafish embryo models, in collaboration with Leiden University, we focused on preparation of new glico-liposome formulations, obtained by combining the advantages of synthetic sugar fatty acid esters and liposomes, in order to use this nano drug delivery system to target the Mannose receptor (mrc1) and to study their receptor specificity and potential for intracellular delivery in Liver sinusoidal endothelial cells (LSECs). We have successfully generated a

LSECs-targeted glycol-liposomal drug delivery system with precise and in *vivo* confirmed specificity towards LSECs through interaction with the **mrc1** receptor.

Another work carried out, was based on the formulation and characterization of a novel mixed/chimeric liposomal system. The bock copolymer methoxy polytylene glycol-co-poly (δ-decalactone) ($mPEG_x$-PDL_y) was incorporated into 1,2-dipalmitoyl-sn-glycero-3-phosphocholine (DPPC) and 1,2-diasteroyl-sn-glycero-3phosphocholine (DSPC) lipid bilayers. The chimeric liposomes were studied in regards with their physicochemical properties, their colloidal stability and their *in vitro* toxicity. As a result, depending on their thermodynamic, physicochemical and toxicity profiles, these chimeric polymer-grafted liposomes could be promising candidates for further in *vitro* and in *vivo* investigation for future nano drug delivery applications.

Introduction

1. History and definition of nanotechnology

Numerous fields, such as physics, chemistry, biology and medicine, are converging to study science at a very fundamental or building block levels, namely nanoscience. In particular, nanoscience is the study of atoms, molecules and objects on the nanoscale. The application of nanoscience, leading to the use and development of new nanomaterials and nanosized components, in useful product, is named nanotechnology.[1,2]

In 1959, the physicist Richard Feynman was the first that proposed the idea of nanotechnology. In his lecture titled, "There's Plenty of Room at the Bottom", Feynman described a process in which scientists would be able to manipulate and to control individual atoms and molecules.[3] For this reason, Feynman is considered the father of modern nanotechnology.[4] Over a decade later, Professor Norio Taniguchi, in his explorations of ultraprecision machining, coined the term 'nano-technology' to describe the manipulation of materials at the nano (10^{-9}) scale. Also, he advocated that nanotechnology consisted "*of the processing, separation, consolidation and deformation of materials by one atom or one molecule"*.[5]

The growth of nanotechnology, in modern era, occurred through the invention of the scanning tunnel microscope, which provided the possibility to see and to manipulate the individual atoms and bonds. In 1986, Heinrich Rohrer with his colleague Gerd Binning, at IBM Zurich Research Laboratory, won the Nobel Prize for Physics for this discovery.[6,7] Drexler and Robert Freitas Junior, in the 1990s, to signify the application of nanotechnology in medicine, they introduced the term 'nanomedicine'.[8,9] It is a branch of nanotechnology and nanoscience, that refers to highly specific medical intervention at molecular scale for diagnosis, prevention and treatment of diseases.[10]

---

1 P. D. Otto, M. M. de Villers et al., *Nanotechnology in Drug Delivery*, Springer, **2009,** Vol. *1*.
2 V. Balzani, Nanoscience and Nanotechnology: A personal view of a chemist, Wiley-VCH, **2005**, 1, 278-283.
3 D. Schaming, H. Remita, *Nanotechnology: from the ancient time to nowadays*, *Foundations of Chemistry*, **2015**, *17* (3), 187-205.
4 P. R. Feynman, *There is Plenty of Room at the Bottom*, Engineering and Science magazine, California Institute of Technology, **1960**, XXIII, 5.
5 N. Taniguchi, *On the Basic Concept of 'Nano-Technology'*, Proceedings of the International Conference on Production Engineering, Tokyo, **1974**, 18-23.
6 G. Binning, H. Rohrer, Scanning tunneling microscopy, IBM J. of Res. and Development, **1986**, 30,355-69.
7 The 1986 Nobel Prize in Physics, Press Release, **1986**. Nobelprize.org
8 R. A. Jr. Freitas, Nanomedicine, Vol. I: Basix Capabilities. Austin, TX: Landes Biosciences, 1999.
9 K. E. Drexler, Nanosystems: Molecular Machinery, Manufacturing, and Computation, John Wiley & Sons, Inc, New York, **1992**.
10 NIH Roadmap Initiatives. http://nihroadmap.nih.gov/initiatives.asp

The interdisciplinary field of nanotechnology and nanomedicine has gained considerable attention from academia, pharmaceutical industry and various national and international agencies and has made a significant progress in the last 15 years. The beginning of the 21st century indeed saw an increased interest in the emerging fields on nanoscience and nanotechnology.

The National Nanotechnology Initiative (NNI), that was launched in 2001 in the US, defined nanotechnology and nanomedicine as follows: "*Nanotechnology is the understanding and control of matter at dimension between approximately 1 and 100 nanometers (nm), where unique phenomena enable novel application, encompassing nanoscale science, engineering, and technology, nanotechnology involves imaging, measuring, modelling, and manipulating matter at this length scale. Nanomedicine is the application of nanotechnology to medicine*".[11] This is a commonly used definition, which describes nanotechnology as the production of material and systems with a dimension or manufacturing limit less than 100 nm. The size in the above range, is not a rigid boundary, it varies according to the application.

For this reason, a more satisfactory definition of nanoscience and nanotechnology can be achieved by focusing on the intrinsic properties of the nanoscale objects and on the possibility of using, manipulating or organizing them into appropriate formulations in order to perform specific functions.

2. Nanotechnology in nanomedicine.

Today, the nanotechnology field is continuously growing and has become the foundation for remarkable industrial applications. This technological field has several outstanding advantages compared to standard technologies. Nanotechnology improves performance and acceptability of dosage forms, by increasing their effectiveness, safety, patient adherence, as well as ultimately reducing health care costs. It may also enhance the performance of drugs that are unable to pass clinical trial phases.

Nanotechnology definitely promises to serve as drug deliver carrier of choice for the more challenging conventional drugs used for the treatment and management of chronic diseases.[12] The nanotechnology aims is to realize the anticipated improved understanding of the patho-physiological basis of disease, bring more sophisticated diagnostic opportunities and yield

11 NNI, National Nanotechnology Initiative, **2004**, Nanotechnology resources page: http://www.nano.gov/nanotech-101/what/definition

12 P. Ulrich, W. Tobias, G. Micheal, A. G. David, *Nanomedicine for respiratory diseases*, *European Journal of pharmacology*, **2006**, 533, 341-350.

improved therapies.[13] Besides, nanotechnology takes advantage of analytical techniques and methodologies of multiple disciplines and also it is able to fabricate nanoscale building blocks that could be functional, on their own or in combination with other materials, for the creation of new tools, constructs, devices and nanosystems, that are ideally suited for applications in medicine and in Drug Delivery.

In the field of the medical products, nanotechnological process are used to formulate medications, to develop new tools and diagnostic research to prevent and treat disease in the nanomedicine therapy.[14] Nanomedicine includes three main areas: nanodiagnosis, regenerative medicine and nanotherapy. Nanodiagnosis is the development of systems and image analysis to detect a disease or cellular malfunction. Regenerative medicine aims to repair or replace damaged tissues and organs using nanotechnology tools.[15]

The nanotherapy purports to address active nanosystems containing recognition elements to act or transport and release drugs exclusively in cells or effected areas in order to achieve a more effective treatment while minimizing side effect. A new area which combines diagnostics and therapy termed theranostics is emerging and is a promising approach which holds in the same system both the diagnosis/imaging agent and the medicine.[16,17] Nanomedicine is also useful to study the benefits and risks of nanomaterials used in medicine and medical devices. [18,19]

Some of the potential benefits of medical nanomaterials used, include improved drug delivery, antibacterial coatings of medical devices, reduced inflammation, better surgical tissue healing, and detection of circulating cancer cells. Therefore, nanomedicine relates to medical research and intervention on the nanoscale of diagnosing, treating and preserving and improving human health, using molecular tools and molecular knowledge of the human body. Nanomedicine has the potential to provide numerous benefits: improved efficacy,

13 M. Ferrari, *Cancer nanotechnology: opportunities and challenges*, *Nat. Rev. Cancer.,* **2005**, *5*, 161, 7.
14 P. Boisseau and B. Loubaton, *Nanomedicine, Nanotechnology in Medicine*, *ComptesRendus de l'Académie des Sciences*, **2011**, 1-27.
15 K. Chaudhury et al., *Regenerative nanomedicine: current perspettive and future directions*, *International Journal of Nanomedicine*, **2014**, *9*, 4153-4167.
16 S. D. Caruthers, S. A. Wickline, G. M. Lanza, *Nanotechnological applications in medicine*, *Curr. Opin. Biotechnol.*, **2007**, *18*, 26-30.
17 J. Xie, S. Lee, X. Chen, *Nanoparticle-based theranostic agents*, *Adv. Drug Delivery Rev*., **2010**, 62, 1064-1079.
18 S. P. Egusquiaguirre, M. Igartua, R. M. Hernandez, et al., *Nanoparticle delivery systems for cancer therapy: advances in clinical and preclinical research*. *Clin. Transl. Oncol*., **2012**, *14*, 83-93.
19 X. Chen and H. J. Schluesener, *Nanosilver: a nanoproduct in medical application*., *Tixicol. Lett.*, **2008**, *176*, 1-12.

bioavailability, dose-response, targeting ability, personalization and safety compared to conventional medicines.[20,21]

The application of nanotechnology to medicine raises new issues because if new uses are allowed, it can contribute to the development of personalized medicine both for diagnosis and therapy. Based on the above findings, nanomedicine encompasses the monitoring, repair, construction and control of human biological systems at the molecular level, using engineered nanodevices and nanostructures.[22] The design and development of multifunctional nanoparticle complexes can simultaneously deliver diagnostic and therapeutic agents to targeted specific sites. These capabilities are unprecedented and represent tremendous progress toward improving patient diagnosis treatment and follow up.[23]

3. Nanoparticle, basic component of nanotechnology

The etiology to the term 'nano' comes from the Greek word "Nanos" meaning "extremely small or dwarf". Scientifically, it implies to the unit of length that equates to 1 billionth of a meter or 10^{-9} m and represented as 'nm' in SI units.[24]

Nano-sized materials are emerged as one of the focal points of modern nanotechnology research and have received much recent attention because of they are expected to be used in various application based on their excellent and unique optical, electrical, magnetic, catalytic, biological, chemical and mechanical properties. Against this background, nanoscale materials have brought about many great changes and new research opportunities in physics, chemistry, material science, biology, etc.[25]

The use of nanoscale dimension to optimize material properties is not new. The present high visibility and definition of this field is mainly attributable to the pioneering work of Gleiter and co-workers in the early 1980s.[26] They synthesized nanoscale grain size materials by the *in-situ* consolidation of atomic clusters.[27]

---

20 D. J. Bharali, S. A. Mousa, *Emerging nanomedicines for early cancer detection and improved treatment: Current perspective and future promise*, *Pharmacol. Ther.* **2010**, *128* (2), 324-335.

21 H. K. Sajja, M. P. East, H. Mao, et al. *Development of multifuctional nanoparticles for targeted drug delivery and noninvasive imaging of therapeutic effect, Curr. Drug Discov. Technol.* **2009**, *6* (1), 43-51.

22 L. Gommersall, I. S. Shergill, H. U. Ahmed, D. Hayne, M. Arya, H. R. H. Patel, M. Hashizume and I. S. Gill, *Nanotechnology and Its Relevance to the Urologist*, *European Urology*, **2007**, *52*, 368-375.

23 R. Seigneuric, l. Markey, D. S. Nuyten et al. *From nanotechnology to medicine: Applications to cancer research, Curr. Mo. Med.,* **2010**, *10* (7), 640-652.

24 W. H. De Jong, A. J. P. Borm, *Drug delivery and nanoparticles: applications and hazards*, *Int. J. Nanomed*, **2008**, *3*(2), 133-149.

25 P. Tartaj, M. Morales, S. Verdaguer, T. Carreno and C. Serna,*The preparation of macnetic nanoparticles for applications in biomedicine*, *Rev. J. Phys*., **2003**, *36* (13), 182.

26 H. Gleiter, *Nanocrystalline materials*, *Progress in Materials Science*, **1989**, *33*, 223-315.

27 R. Uyeda, Studies of ultrafine particles in Japan: *Crystallography. Methods of preparation and technological applications*, *Progress in Materials Science*, **1991**, *35*, 1-96.

The process for producing nanomaterials can be characterized as two main approaches, "top-down" or "bottom-up".[28] The top-down approach starts with large particles that are chopped to a nanometric size through the application of high-energy forces. This is the classical approach for the majority of nanoparticle production process. Top-down approaches require highly precise control of the variables of the process in order to obtain the narrow particle size, lithography is the classical example of this technique.[29] Other high-energy processes include grinding, high impact homogenization, ultrasound waves, and extrusion through nanopores membranes.[30] Bottom-up approaches are based on the self-assemble of molecules under thermodynamic control, generating nanostructures from atoms and molecules as a result of the effects of the chemical, physical and process interventions on the balance of the intermolecular and intramolecular forces of the system components. [31] Bottom-up approaches focus on the construction of functional materials, mimetizing the organization of the molecules in living organisms.

The concept of particle existence at nanoscale levels has long existed also in nature. For example, the human body consists of several nanostructures. The biological moieties such as proteins, enzymes, cyto-skeletal polysaccharides, cell membrane channels, the blood cells, (neutrophils, eosinophils, basophils and lymphocytes), double-stranded DNA are considered nanometer size particles. [32,33] Fabrication of biomimetic nanoscale materials can serve as a powerful tool in the studying biological mechanisms of all living cells. It is important to unify the terminology used for describing particle size in nanotechnology, health and environmental sciences.

The materials under discussion, can be classified as particles, regardless of their source. The size of these particles varies between 1 nm to several microns, and they can therefore be classified as either nanoparticles (NPs), any dimension smaller than 1 micron, or microparticles (MPs), all dimension larger than one micron.[34,35]

28 P. Iqbal, J. A. Preece and P. M. Mendes, *Nanotechnology: The "Top-Down" and "Bottom-Up" approaches*, *Supramolecular Chemistry, Molecules to Nanomaterial, John Wiley & Sons*, Ltd., **2012**, 1-14.

29 D. Mijatovic, J. C. T. Eijkel and A. van den Berg, *Technologies for nanofluidic systems: Top-down vs. Bottom-up a review*, *Lab on Chip*, **2005**, *5*, 492-500.

30 B. K. Teo and X. H. Sun, *From Top-Down to Bottom-Up to Hybrid Nanotechnologies: Road to Nanodevices, J. Cluster Sci*., **2006**, *17*, 529.

31 L. Wang, Y. Sun, Z. Li, A. Wu, G. Wei, Materials, *Bottom-up Synthesis and Sensor Applications of Biomimetic Nanostructures,* **2016**, *9*, 53.

32 D. L. Nelson, A. L. Lehninger, M. M. Cox*, Lehninger principles of biochemistry*, *Macmillan: London*, UK, **2008**.

33 F. M. Fernandes, T. Coradin, C. Aimé, *Self-Assembly in Biosilicification and Biotemplated Silica Materials*,*Nanomaterials*, **2014**, *4*, 792-812.

34 C. N. R. Rao, A. Muller and A. K. Cheetham, *The Chemistry of Nanomaterials: Synthesis, Properties and Applications*, *Wiley-VCH verlag GmbH*, Germany, **2004**.

35 "ISO/TS 80004-2: *Nanotechnologies – Vocabulary – Parte 2: Nano-objects*" International Organization for Standardization, **2015**. (Retrieved 18 January 2018)

NPs and MPs can be classified as natural, incidental or synthetic, based on their origin. Natural nanomaterials are produced in nature either by biological species or through anthropogenic activities. Incidental nanoparticles are formed as a by-product of industrial or natural processes. The synthetic ones are made by physical, chemical, biological or hybrid methods. Usually, they are engineered nanomaterials which have been manufactured by humans to have certain required properties for desired applications. Besides nanoparticles and microparticles can be also organized into four different material-based categories: Carbon-based nanomaterials, that are particles contains carbon;[36] Inorganic-based nanomaterials, that include metal and metal oxide;[37,38] Organic nanomaterials, made mostly from organic matter, and in the end composite-based nanomaterials, made by any combinations of carbon-based nanoparticles with any form of metal, ceramic or polymer bulk materials.[39,40]

For nanomaterials, the surface to volume ratio dramatically increases with decreasing size and thus the surface plays a major role in the interaction with its surroundings.[41] Changes of surface properties, for example by modification with other substances, would result in the change of the nanomaterial's behaviour and resulting effects. Therefore, surface properties and their changes must not be neglected in the consideration of different forms of nanoscaled substances.[42] Not only the chemical composition, but also morphological properties and surface properties determine the special characteristics.[43] These properties do not only differ in comparison to the corresponding bulk material counterparts, but also between different nanoforms of the same substance. It is important to know that the nanoparticle's physico-chemical characteristics, for example chemical composition, crystal structure, surface area and energy, reactivity, (photo)-catalytic activities and energetic properties can be modified in order to fit formulation's specific needs and requirements.

36 M. F. L. De Volder, S. H. Tawfich, H. R. Baughman, A. Hart, *Carbon Nanotubes: Present and future commercial application*, *J. Science*, **2013**, *339*, 535-539.

37 S. Sieben, C. Bergemann, A. S. Lubbe, B. Brockmann, D. Rescheleit, *Comparison of different particles and methods for magnetic isolation of circulating tumor cells*, *J. of Magnetism and Magnetic Materials*, **2001**, *255*, 175-179.

38 W. Paul, C. P. Sharma, *Inorganic nanoparticles for targeted drug delivery*, *Biointegration of Medical Implant Materials, Science and Design*, **2010**, 204-235.

39 J. Jeevanandam, A. Barhoum, Y. S. Chan, A. Dufrense and M. K. Danquah, *Rewiew on nanoparticles and nanostructured materials: history, sources, toxicity and regulation*, *Beilstein J. Nanotechnol.*, **2018**, *9*, 1050-1074.

40 G. Romero, S. E. Moya, *Synthesis of Organic nanoparticles*, *Frontiers of Nanoscience*, **2012**, *4*, 115-141.

41 M. V. Yezhelyev et al. *Emerging use of nanoparticles in diagnosis and treatment of breast cancer*, *Lancet Oncol.*, **2006**, *7*, 657-667.

42 A. Hoschino et al., *Use of fluorescent quantum dot bioconjugates for cellular imaging of immune cells, cell organelle labeling, and nanomedicine: surface modification. Regulates biological function, including cytotoxicity*, *J. Artif. Organs*, **2007**, *10*, 149-157.

43 Y. Lu, Y. Yin, B. T. Mayers, Y. Xia, *Modify the surface properties of superparamagnetic iron oxide nanoparticles through a sol- gel approach, Nano Letters - ACS Publications*, **2002**, *2* (3), 183-186.

Design considerations, such as size, shape, surface coating and dosing, can be manipulated to prolong blood circulation, distribution and enhance treatment efficacy.[44] Before that, these new and promising nanoparticle technologies can translate into clinical applications, pharmacological studies as well as the plausible side effects investigations, related to their use, are needed.[45] Nanoparticles must be evaluated on a particle-by-particle basis and a rational characterisation strategy must include adsorption, distribution, metabolism and excretion (ADME) tests and physicochemical and toxicological characterisation, involving both *in vitro* and *in vivo* studies. The use of material at nano-scale sizes, on the one hand allow for featuring molecular properties and on the other hand permit to design tools and construct devices whit specific function at the cellular, atomic and molecular levels.[46,47] Using structures designed at extremely small scales there exists opportunities that can not only enhance existing technologies but also offered a novel feature with potentially far reaching technical medical and scientific implication.

The capacity to engineer at the nanoscale confers the ability to combine several beneficial features into multicomponent multifunctional nanoparticles, that are useful as novel tools for molecular imaging, diagnosis, drug discovery and delivery formulations.[48,49]

4. Nanosystem for Drug Delivery

The application of nanomaterials and nanotechnology to biomedical research, nanomedicine, has had a major impact on the development of new types of diagnostic, imaging, therapeutic agents and drug delivery systems. The term drug delivery covers a very broad range of approaches, formulations technologies and techniques used to transport a pharmaceutical compound into the human (or animal) body as needed, to safely achieve its desired therapeutic effect.[50] By definition, drug delivery systems (DDS) are supramolecular assemblies incorporating agents intended to treat a disease. For this reason, advanced DDS present indubitable benefits for drug administration, they are used to overcome the

44 J. P. M: Almeide, A. L. Chen, A. Foster and R. Drezek, *In vivo biodistribution of nanoparticles*, *Rev.* Nanomedicine, **2011**, *6* (5), 815-835.

45 Y. Hu, J. Xie, Y. W. Tong and C. Wang, *Effect of PEG conformation and particle size on the cellular uptake effiency of nanoparticles with the HepG2 cells, J. of Controlled Release*. **2007**, 118 (1), 7-17.

46 H. W. Kroto, J. R. Heath, S. C. Obrien, et al., *Nature*, **1985**, *318*, 162;

47 J. Nye, A. Greenberg and A. Jones, *Nanoscience in Healthcare: Prevention, Treatment and Prosthetics*, *Nanoscale Science and Engineering Center*, Wisconsin Madison University, **2010**.

48 A. Z. Wang, F. Gu, L. Zhang, J. M. Chan, A. Radovic-Moreno, M. R: Shaikh, O. C. *Biofunctionalized Targeted Nanoparticles for Therapeutic Application*, *Expert Opin. Biol. Ther*., **2008**, *8*, 1063-1070.

49 V. Wagner et al*, The emerging nanomedicine landscape*, *Nat. Biotechnol*, **2006**, 24, 1211-1217.

50 K. K. Jain, *Drug Delivery Systems –An Overview*, *Methods in Molecular Biology, Springer (MIMB)*, **2008**, *437*, 1-50.

shortcomings of the conventional drugs, such as unfavourable pharmacokinetics, poor solubility, instability, high toxicity, drug resistance and low cellular uptake.[51,52,53]

Several methods of drug administration were employed in delivery nanotechnological product, for example: Intravenous that is the most reliable method for delivering drug to the systemic circulation, because it bypasses many of the absorption barriers, efflux pumps, and metabolic mechanisms;[54] Inhalation, method to administer drugs through the respiratory system; [55] In the oral administration, the drug first reaches the stomach, where it usually disintegrates and dissolves in the gastric lumen. Drugs given orally must be acid stable or protected from gastric acid; [56] Transdermal is the local application of the drug through the skin and the ocular delivery have also been developed for localized side specific drug administration without unwanted systemic side effects.[57,58] These methods are still most widely used today, yet each has its disadvantages.

Oral delivery via tablets or capsules is largely inefficient due to exposure of the pharmaceutical agent to the metabolic process of the body. Therefore, a larger than necessary dose is often required, and the maximum effectiveness of the drug is limited. Traditional intravenous (IV) administration is much more problematic. Effectiveness specially for IV injectable drugs is often low, necessitation large amounts of a drug to be injected into the body creating a high concentration of the drug in the blood stream that could potentially lead a toxic side effects.[59] Therefore, several factors must be taken into consideration when administrating a drug, namely its own properties, the disease to be treated and the desired therapeutic time.[60] Traditional drug administration cannot resolve the problems of toxicity and or bioavailability for numerous effective drugs, thereby limiting their use in therapeutics. The pharmacokinetic and pharmacodynamic properties of the drug, toxicity, immunogenicity,

51 G. A. Hughes, *Nanostructure mediated drug delivery*, *Nanomedicine*, **2005**, *1*, 22-30.
52 R. Ravichandron, *Nanotechnology based drug delivery systems*, *Nanobiotechnol*., **2009**, *5*, 17-33.
53 B. Mishra, B. Bhavesh, B. Patel, S. Tiwari, *Colloidal nanocarriers: a review on formulation technology types and applications toward targeted drug delivery*, *Nanomedicine*, **2010**, *6*, 9-24.
54 K. Peters, S. Leitzke, J. E. Diederichs, K. Borner, H. Hahn, R. H. Muller, S. Ehlers, *Preparation of clofazimine nanosuspension for intravenous use and evaluation of its therapeutic efficacy in murine Mycobacterium avium infection*, *J. Antimicrob. Chemother*., **2000**, *45*(1), 77-83.
55 L. D. Mastrandrea, *Vascular Health and Risk Management Dovepress inhaled insulin overview of a novel route of insulin administration, Vasc. Health Risk Manag*., **2010**, *6*, 47-58.
56 J. P. Bai, L. L. Chang, J. H. Guo, *Targeting of peptide and protein drugs. To specific sites in the oral route, Crit. Rev. Ther. Drug Carr. Syst*. **1995**, *12*, 339-371.
57 G. Cevc, I. U. Vier, *Nanotechnology and the transdermal route. A state-of-the-art review and critical appraisal, J. Contol. Rel*., **2010**, *141*, 277-299.
58 P. I. Siafaka, A. Titopoulou, E. N. Koukaras, M. Kostoglou, E. Koutris, E. Karavas, D. N. Bikiaris, *Chitosan derivates as effective nanocarriers for ocular release of timolol drug*, *Int. J. Pharm*., **2015**, 495, 249-264.
59 J. Leroux, E. Allemann and Da. Jaeghere, *Biodegradable nanoparticles-from sustained release formulations to improved site specific drug delivery, J. Cont. Rel*., **1996**, *39*, 339-350.
60 D. E. Golan, H. Armen, J. Tashjian, E. J. Armstrong, et al., Principles of pharmacology: *The pathophysiological basis of drug therapy, Lippincott Williams&Wilkins*, Philadelphia, **2008**.

biorecognition ability and thus increase efficiency could be modified by using drug delivery systems.[61]

In recent years, biocompatible micro- and nanoparticles have been reported as potential drug carrier systems.[62,63] In terms of size one can divide the carrier systems to micrometric, one to several micrometres, and sub-micrometric particles, called nanocarriers, whose dimensions should be maintained from the point of preparation till the point of application. The expected advantages of utilizing nanoparticles for drug delivery stem from the particle's ability to: 1) protect the drug from plasma-induced deactivation; 2) optimize drug pharmacokinetics and biodistribution; 3) enhance drug delivery to the disease site via passive and active mechanisms; 4) modulate drug release mechanisms via diffusion, degradation, and other unique stimuli-trigged processes; and 5) biodegrade or get eliminated safely from the body.[64] Nanocarriers are used to aim therapies directly and selectively at diseased tissues or cells, thereby preventing toxicity and unwanted side effects. The nano-sized particles improve the solubility of poorly water soluble drugs, modify pharmacokinetics, increase drug half-life by reducing immunogenicity increase specificity toward the target cell or tissue, therefore reducing side effects, improve bioavailability, diminish drug metabolism and enable a more controllable release of therapeutic compounds and the delivery of two or more drugs simultaneously for combination therapy.[65,66,67]

Nanosystems are multifunctional systems engineered at the nanoscale and are comprise of distinctive physicochemical properties with massive prospects in theranostic applications.[68] In the last two decades, these systems with novel properties and flexibility in tailoring their fabrication have evolved as indispensable scaffolds for improving efficacy via targeted drug delivery of anticancer agents, immunosuppressant, antimicrobials, topicals, ophthalmic and nasal actives, peptides and nucleic acids in diverse therapeutic diagnostic implications, as well as for renewal of conventional therapies.[69]

---

61 S. T. Yang, J. Luo, Q. Zhou, H. Wang, *Pharmacokinetics, Metabolism and Toxicity of Carbon Nanotubes for Biomedical Purpose*, *Theranostics*, **2012**, *2*, 271-282.

62 G. M. Barratt, *Therapeutic applications of colloidal drug carriers, Pharmaceutical Science & Technology Today*, **2000**, *3*(5), 163-171.

63 H. Parhiz, M. Khoshnejad, J. W. Myerson, at al., *Unintended effects of drug carriers: Big issues of small particles, Adv. Drug Deliv. Rev*., **2018**, *130*, 90-112.

64 A. Bettencourt, A. J. Almeida, *Poly(methyl methacrylate) particulate carriers in drug delivery, J. Microencapsul*., **2012**, *29*, 323, 367.

65 D. F. Emerich, C. G. Thanos, *The pinpoint promise of nanoparticle-based drug delivery and molecular diagnosis. Biomol. Eng*., **2006**, *23*, 171-184.

66 T. M. Allen and P. R. Cullis, *Drug delivery systems: entering the mainstream*, *Science*, **2004**, *303*, 1818-1822.

67 W. Wang, *Oral protein drug delivery, J. Drug Target*, **1996**, *4*, 195-232.

68 Z. Zhang, L. Wang, J. Wang, X. Jiang, X. Li, Z. Hu, Y. Ji, X. Wu, and C. Chen, *Mesoporous silica-coated gold nanorods as light-mediated multifuctional theranostic platform for cancer treatment, Adv. Mater*, **2012**, *24*, 1418-1423.

69 S. C. Balmert, S. R. Little, *Biomimetic delivery with micro- and nanoparticles, Adv. Mater*, **2012**, *24*, 3757-3778.

Nanosystems have developed well as target-specific platforms, either as nanocarriers or as active agents themselves. Nanosystems explored in drug delivery consist of two inherent components: an active molecule and a carrier device. Any one of them should have, at minimum, one nanodimension. The active moiety may be a therapeutic drug or gene and/or functional group for complementary effects.[70] The nanoplatforms serve as carrier to load the drug and carry it to the targeted site, where it will be released safely. The therapeutic molecules to be delivered range from anti-inflammatory, anticancerous, antibacterial, antifungal, and antiviral drugs, herb-based drugs, viral and non-viral vectors, antibodies and genes.[71] Diverse nanoparticulate systems exists for biomedical and pharmaceutical applications.[72,73] They differ in their make, synthesis method, and physicochemical properties as well as their applications. Numerous types of nanoparticulate systems have emerged from different materials such as lipid, polymer, organometallic, organic and inorganic compounds.[74,75] The structures of polymer-based-nanocarriers are assorted and offer the most flexibility in fabrication as well as functionalization strategies. Controlled release modulation, simultaneous diagnosis-treatment, shielding of active molecules, and improved targeting potential and therapeutic windows make these nanocarriers more beneficial than their counterparts.[76] Lipid nanocarriers, that contains either solid or liquid lipids or an optimized combination, are selective for tagging and are more biocompatible, which, in turn, enhances their cell uptake and nullifies the possible side effects originating from the synthetic compounds.[77]

Furthermore, they are also being designed to respond to internal stimuli such as pH, redox potential, enzymatic activity, and temperature.[78,79] Inorganic nanosystems are versatile vectors

70 R. Lehner, X. Wang, M. Wolf, P. Hunziker, *Designing switchable nanosystems for medical applications, J. Control. Release*, **2012**, *161*, 307-316.

71 K. L. Nair, A. K. T. Thulasidasan, G. Deepa, R. J. Anto, G. S. V. Kumar, *Purely aqueous PLGA nanoparticulate formulations of curcumin exhibit anhanced anticancer activity with dependence on the combination of the carrier, Int. J. Pharm.*, **2012**, *425*, 44-52.

72 S. Bose, B. Michniak-Kohn, *Preparation and characterization of lipid based nanosystems for topical delivery of quercetin, Eur. J. Pharm. Sci*., **2013**, *48*, 442-452.

73 L. Montenegro, F. Lai, A. Offerta, M. G. Sanpietro, L. Micicche, A. M. Maccioni, D. Valenti, A. M. Fadda, *From nanoemulsion to nanostructured lipid carriers: a relevant development in dermal delivery of drugs and cosmetics, J. Drud Delivery Sci. Technol*. **2016**, *32*, 100-112.

74 C. S. Kim, G. Y. Tonga, D. Solfiell, V. M. Rotello, *Inorganic nanosystems for therapeutic delivery: status and prospects, Adv. Drug Del. Rev*. **2013**, *65*, 93-99.

75 N. Habibi, N. Kamaly, A. Memic, H. Shafiee, *Self- assembled peptide-based nanostructures: smart nanomaterials toward targeted drug delivery, Nano Today*, **2016**, 11, 41-60.

76 C. I. C. Crucho, M. T. Barros, *Polymeric nanoparticles: a study on the preparation variables and characterization methods, Mater Sci. Eng*. **2017**, *80*, 771-784.

77 Y. Wang, L. Miao, A. Satterlee, L. Huang, *Delivery of oligonucleotides with lipid nanoparticles, Adv. Drug Deliv. Rev.* **2015**, *87*, 68-80.

78 M. Kanamala, W. R. Wilson, M. Yang, B. D. Palmer, Z. Wu, *Mechanisms and biomaterials in pH-responsive tumor targeted drug delivery: a review, Biomaterials*, **2016**, *85*, 152-167.

79 Z. Dan, H. Cao, X. He, L. Zeng, L. Zou, Q. Shen, Z. Zhang, *Biological stimuli-responsive cyclodextrin-based host-guest nanosystems for cancer therapy, Int. J. Pharm*., **2015**, 483, 63-68.

for multifunctional drug delivery with therapeutic, imaging and theranostic applications. Metal oxides, gold nanorods, and silica nanoparticles, are inorganic nanocarriers that have unique advantages.[80] Nanocrystal are nanocolloidal systems that involve nanosized drug particles with a stabilizer or surfactant shield.[81] These several formulations have been widely used over the years as drug containers and drug delivery systemsbecause of its easy method of preparation. Moreover, the surface of these nanosystems can be functionalized with a wider range if ligands, like antibodies, liposomes or biodegradable polymeric nanoparticles, that make them even more specific for active targeting.[82]

The primary objectives of nanoparticles-mediated delivery of several drugs with therapeutic formulation are: 1) to resolve the problems of delivery to targets prevented by biological barriers;[83,84] 2) to enhance the carriers blood circulation lifetime;[85] 3) to improve poor targeting selectivity. Clearly, these goals can be achieved by both improving and optimizing the physicochemical properties of the drug carriers, as well as by conjugation of the drug carriers to biomolecular targeting ligands. Ligands together with drugs can be covalently attached to carrier's coating surface for targeting. This strategy is normally referred to "multifunctional nanoparticles" where the carrier is comprised of delivery, imaging, and therapeutic agents.[86]

Drug-carrying NPs can be synthesized using a variety of materials and techniques. Commonly used techniques are precipitation, emulsion, and lipid extrusion. Besides, the drugs can be loaded in different ways for example, dispersed in a matrix, encapsulated by a NP or in a vesicle, dissolved in a hydrophilic or hydrophobic core, and attached covalently to the surface of the NP. According to this knowledge, the drug delivery nanosystems with modulatory controlled release profiles have been rightly classified as conventional and advanced nanocarriers.[87] Liposomes, nanotubes, and micelles either functionalized or non-functionalized are examples of conventional systems, while advanced systems combine

80 L. Sun, D. Wang, Y. Chen, L. Wang, P. Huang, Y. Li, Z. Liu, H. Yao, J. Shi, *Core-Shell hierarchical mesostructured silica nanoparticles for gene/chemo-synergetic stepwise therapy of multidrug-resistant cancer, Biomaterials*, **2017**, *133*, 219-228.

81 L. Peltonen, J. Hirvonen, *Drug Nanocrystals-versatile option for formulation of poorly soluble materials*, *Int. J. Pharm*., **2018**, *537*(1-2), 73-83.

82 E. S. Dzunuzovic, M. T. Marinovic-Cincovic, J. V. Dzunuzovic, K. B. Jeremic, J. M. *Nedelikovic, Influence of the way of synthesis of poly(methyl methacrylate) in the presence of surface modified TiO2 nanoparticles on the properties of obtained nanocomposites*, *Hem. Ind*. **2010**, *64*(6), 473-489.

83 T. Lammers, F. Kiessling, W. E. Hennik, and G. Storm, *Drug targeting to tumors Principles, pitfalls and (pre-) clinical progress*, *J. Control. Release*, **2012**, 161-187.

84 D. R. Groothuis, *The blood-brain and blood-tumor barriers: A review of strategies for increasing drug delivery*, *Neuro-Oncology*, **2000**, *2*, 45-59.

85 R. K. Jain, *Determinants of tumor blood flow: A review*, *Cancer Res*, **1988**, *48*, 2641-2658.

86 K. Kogure, H. Akita, and H. Harashima, *Multifuctional envelope-type nano device for non-viral gene delivery: Concept and applications of Programmed Packaging, J. Control. Release*, **2007**, *122*, 246-251.

87 C. Demetzos, N. Pippa, *Advanced drug delivery nanosystems (aDDnS): a mini-review, Drug Deliv*., **2014**, *21*, 250-257.

different modalities with different kinds of biomaterial with multimodal functionality, as show in Figure 1.

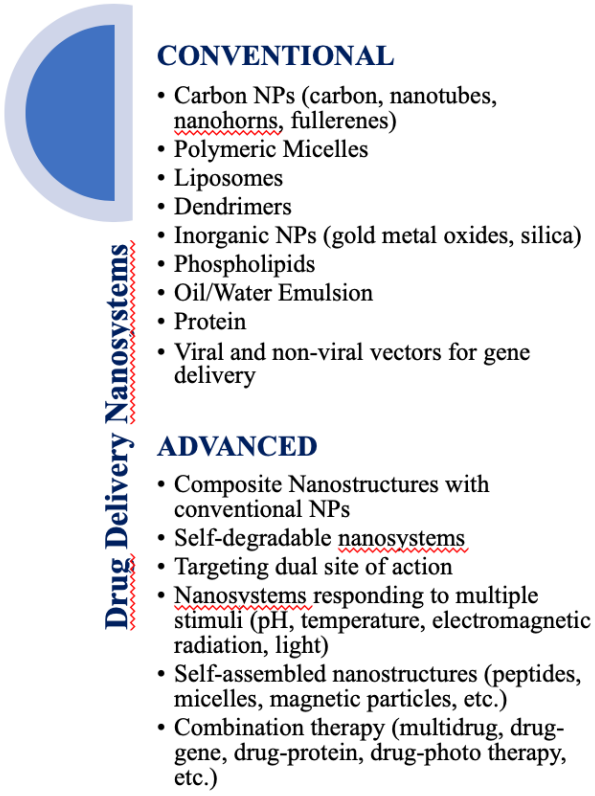

Figure 1. Conventional and Advanced drug delivery systems

It has been well established that, manufacturing methods have influence on the physicochemical properties of nanoparticles and nanosystems such as size, charge, lamellarity and so forth. These physicochemical properties need to be fully characterized in order to predict *in vitro* and *in vivo* performances of the nano-based drug delivery systems and fully understand their chemistry.[88]

Scanning electron microscopy (SEM), Transmission electron microscopy (TEM and Cryo-TEM) and other modern microscopic techniques are used to determine morphology of the formulation.[89] Dynamic light scattering (DLS) and Nanoparticle Tracking Analysis (NTA) rapidly assess size, Zeta potential and possible aggregation of the particle in nanosystems.[90] Crystalline nature and thermal stability of nanocarriers are defined by differential scanning calorimetry (DSC), thermogravimetric analysis (TGA) and X-ray diffraction (XRD)

88 D. Bennet, S. Kim, *Application of Nanotechnology in Drug Delivery, Ed. Sezer, A. D. In Tech*, **2014**, 257-310.

89 J. Panyam, S. Sahoo, S. Prabha, T. Bargar, V. Labhaetwar, *Fluorescence and electron microscopy probes for cellura and tissue uptake of poly(D-, L-lactide-coglycolide)nanoparticles, Int. J. Pharm.* **2003**, 262, 1-11.

90 S. Bhatia, *Nanoparticles types, classification, characterization, fabrication methods and drug delivery applications, In: Natural polymer drug delivery systems, Switzerland: Springer Int. Publishing*, **2016**, 33-93.

techniques. UV spectroscopy or high or ultra-performance liquid chromatography (HPLC or UPLC) post ultracentrifugation or ultrafiltration define the loading efficacy of a nanocarrier.[91] Biological characterization of nanoparticles basically includes the *in vitro* and *in vivo* analysis of the sample in various biological conditions. *In Vitro* experiments can provide an initial cost-effective assessment of the toxicity, and the efficacy of a nanomaterial-based therapeutic and inform the design of animal studies. *In vitro* studies also enable the elucidation of biomedical mechanism under controlled conditions.[92] Nanoparticle's binding, pharmacology and uptake properties can be monitored by common cell and molecular biology methods such as ELISA (enzyme-linked immunosorbent assay) and fluorescence microscopy.[93,94] After the *in vitro* analysis, the nanomaterials are intended for *in vivo* diagnostic and therapeutic purposes. The primary goal of the *in vivo* characterization is to elucidate the nanomaterial's safety, efficacy, and toxicokinetic properties in animal models. *In vivo* assays can supply essential information regarding what append when the NPs are inside the body. Some in *vivo* tests which are important in nanocarriers analysis include dose-response, biodistribution, acute and multi dose safety and efficacy, administration route determination, adsorption, distribution, metabolism and excretion (ADME). These data must be obtained prior to transitioning the nanoparticles to clinical applications.[95]

Nanosystems have extensively developed well as target-specific platforms, either as nanocarriers or as active agents themselves. A large selection of ingredients certainly enables one to shape and to design the parameters of nanoparticles like the composition of the polymer, the architecture, the backbone stability, the water solubility, and hence the activity of nanocarriers. The emerging development of novel multifunctional nanosystems, in which the combination of different functions in a single nanoparticle affords biocompatibility, biostability and biodistribution, provides new potential for therapeutic applications that undoubtedly will revolutionise the medical and research landscape.[96]

---

91 M. Gumustas, S. Kurbanoglu, B. Uslu, S. A. Ozkan, UPLC versus HPLC on Drug Analysis: Advantageous, Applications and their Validation Parameters, Chromatographia, 2013, 76, 1365-1427.

92 M. Maskos, R. H. Stauber, *Characterization of nanoparticles in biological environments*, P.Ducheyne, editor, *Comprehensive biomaterials. Oxford, UK, Elvesier*, **211**, 329-339.

93 A. Voller, A. Bartlett, and B. E. Bidwell, *Enzyme immunoassays with special reference to ELISA techniques, J. Clin. Pathol.* **1978**, *31*(6), 507-520.

94 X. Yun, V. D. Maximov, J. Yu, G. Zhu, A. A. Vertegel, and M. S. Kindy, *Nanoparticles for targeted delivery of antioxidant enzymes to the brain after cerebral ischemia and reperfusion injury, J. of Cerebral Blood Flow & Metabolism*, **2013**, *33*(4), 583-592.

95 W. G. Kreyling, D. Fertsch-Gapp, M. Schaffler, B. D. Johnston, N. Haberl, C. Pfeiffer, J. Diendorf, C. Schleh, S. Hirn, M. Semmler-Behnke, M. Epple and W. J. Parak, *In vitro and in vivo interactions of selected nanoparticles with rodent surum proteins and their consequences in biokinetics, BeilStein J. Nanotechnology*, **2014**, *5*, 1699-1711.

96 J. Shi, Z. Chen, L. Wang, B. Wang, L. Xu, L. Hou, Z. Zhang, *A tumor-specific cleavable nanosystem of PEG-modified C60@Au hybrid aggregates for radio frequency-controlled release, hyperthermia, photodynamic therapy and X-ray imaging, Acta. Biomater*. **2016**, *29*, 282-287.

Aim

The advent of nanosciences, nanotechnologies and nanomaterials, have gained a major turning point in twentieth and twenty-firs century industrial and technological development. Nanotechnology is a field of research and development that focuses on structures, devices, and processes based on the atomic, molecular, or supramolecular modelling of matter at scales typically of the order of one to one hundred nanometers (1-100 nm).

The constituent of this field are nanomaterials that include nanoparticles, nanostructured coatings, dense bulk materials, and nanocomposites, with an organic, inorganic or metal matrix. In particular, nanoparticles show unique size-dependent physical and chemical properties. Several materials are used for the production of NPs, based on this, they are reported to be nontoxic, highly biocompatible, and non-immunogenic. With their ability of encapsulation, they serve as an essential tool of targeted delivery. Regardless of the nature of the chemical agents, encapsulation protect compounds against elimination and degradation, while preserving their chemical stability.

Nanoparticles improve the cellular penetration and cellular uptake of molecules. Delivery in nanoparticles provides solubility to molecules or pharmaceutical agents, which otherwise display limited solubility in aqueous media. For instance, anticancer agents like Doxorubicin or Acyclovir can attain concentrations well above their aqueous solubility, when harboured within liposomes.[97,98] Also, targeted delivery of nanoparticles evidently magnifies the effective concentration of the pharmaceutical agents at a specific organ. The release of the active compound from nanoparticles could be achieved by external stimulus such as light, magnetic field, temperature and heat, or the environmental stimuli, such as pH.

The application of nanoparticulate formulations are feasible in various forms, including solution, colloidal solution, aerosol, and in solid or semi solid forms. Nanoparticles can be given to the body via numerous routes, such as parenteral, topical and pulmonary routes of administration. During the past few decades, NPs have emerged as a powerful tool for biomedical applications, as far as drug delivery is concerned. Nanosize drug delivery systems generally focus on formulating bioactive molecules in biocompatible nanosystems, such as

97 G. Storm, F. H. Roerdink, P. A. Steenrenberg, W. H. de Jong, D. J. Crommelin, *Influence of lipid composition on the antitumor activity exerted by doxorubicin-coating liposomes in a rat solid tumor model, Cancer Res*. **1987**, *47*, 3366-3372.

98 B. Bareiss, M. Ghorbani, Li. Fengfu, J. A. Blake, J. C. Scaiano, Z. Jin, D. Chao, K. Merrett, J. L. Harden, F. Diaz-Mitoma, M. Griffith, *Controlled release of acyclovir through bioengineered corneal implants with silica nanoparticles carriers, Open. Tissue Eng. Regen. Med. J*., **2010**, *3*, 10-17.

nanocrystals, solid lipid nanoparticles, nanostructure lipid or polymeric carriers, micelles, lipid drug conjugates, nanoliposomes, dendrimers, nanoshells, emulsions, nanotubes, quantum dots, etc. Extensively versatile molecules, from synthetic chemicals to naturally occurring complex macromolecules such as nucleic acids and proteins, could be dispensed in such formulations, maintaining their stability and efficacy.[99]

Drug delivery nanosystems provides many advantages such as enhance drug-therapeutic efficiency and pharmacological characteristics; improve the solubility of poorly water-soluble drugs; modify pharmacokinetics; increase specificity towards the target cell or tissue, therefore reducing side effects; improve bioavailability; diminish drug metabolism and enable a more controllable release of therapeutic compounds and the delivery of two or more drugs simultaneously for combination therapy. Considering the above facts, this dissertation aims to design novel nano-based drug delivery systems and to develop new control process strategies, such as modified the shape, chemical composition, internal structure and morphology of the nanocarriers so as to obtain new levels of product performance in the targeted drug delivery system.

In the ***Section I***, the synthesis of amphiphilic block copolymers, as a building block of nanocarriers for potential drug delivery applications was examined. In particular, an amphiphilic di-block copolymer, composed of methoxy poly(ethylene glycol) (mPEG) and poly(ε-caprolactone) (PLC), that can self-assemble into polymeric micelles (PMs), was synthesized and fully characterized.

The mPEG-PLC micelles were amply used as drug carriers for delivery of anti-glaucoma drug methazolamide (MTZ). MTZ-PMs were prepared using the thin film hydration procedure and optimized using a Design of Experiment (DoE) approach. *In vitro* drug release, thermal analyses and FT-IR characterization were evaluated. MTT assay and histopathological assessment were carried out to verify the ocular tolerability as well as Draize irritancy test. *In vivo* studies were conducted on rabbits to evaluate anti-glaucoma activity in a glucocorticoid-induced glaucoma model.

The results showed successful entrapment of MTZ inside PMs matrix as reflected by the complete vanishing of drug melting peak in DSC thermogram and the possible formation of hydrogen bonding between MTZ and mPEG-PLC copolymer in FT-IR spectrum. The selected formula exhibited a particle size of 60 nm, entrapment efficiency of 93% and discrete

99 B. Murkherjee, *Nanosize drug delivery system, Curr. Pharm. Biotechnol*., **2013**, *14*(15), 1221.

spherical particles. Moreover, sustained release of MTZ, cellular and tissue biocompatibility and marked anti-glaucoma efficacy, as compared to MTZ solution, were realized. The combined results show that PMs could potentiate the therapeutic outcome of nanotechnology ocular delivery.

The ***Section II*** focuses on the synthesis, physicochemical characterization of three innovative sugar fatty acid monoesters, that are surfactants, belonging to glycolipid molecules, which play an important role in the solubilization and stabilization of drugs in different preparation. These compounds can also be included in several formulations to modify the bioavailability of drugs, and to be used as drug delivery systems.

For instance, in effort to develop improved nano-liposomal carriers for in *vivo* application on Zebrafish embryo models, in collaboration with Leiden University, we focused on preparation of new glico-liposome formulations, obtained by combining the advantages of synthetic sugar fatty acid esters and liposomes, in order to use this nano drug delivery system to target the Mannose receptor (**mrc1**) and to study their receptor specificity and potential for intracellular delivery in Liver sinusoidal endothelial cells (LSECs).

Three different glycolipids were synthetized by one reaction step. Oleic esters of Glucose and Mannose were obtained by enzymatic reaction using Novozym 435. Fucose oleic ester, instead, was synthesized by chemical reaction under basic conditions using pyridine and TBTU as catalyst. Nuclear magnetic resonance ^{1}H-NMR and ^{13}C-NMR analysis were performed to characterize these synthetic glycolipids. These molecules were then incorporated into florescent DOPC liposomes. The size, Z-potential and PDI of the glycol-liposomes, were measured by DLS. NTA-analysis were performed to study the distribution of the nanoparticle in Milli-Q water suspension. Cryo-TEM analysis were carried out to study the morphological properties of glyco-liposome formulations. The results confirmed the formation of small unilamellar liposomes with size of about 100 nm.

In vivo studies were conducted on two days old Zebrafish embryos to study the biodistribution and the pharmacokinetics of the injected glico-liposomes. The results obtained showed that we have successfully generated a LSECs-targeted glycol-liposomal drug delivery system with precise and *in vivo* confirmed specificity towards LSECs through interaction with the **mrc1** receptor.

In conclusion, in the ***Section III*** a mixed/chimeric liposomal nanosystem, composed of phospholipids and block copolymers, was developed and evaluated in regards with its feasibility as a drug delivery system.

These innovative nano-platforms combine advantages from both classes of biomaterials. Thermal analysis was performed in order to offers an insight into the interactions. Between these materials and consequently into their physicochemical characteristics. In addition, colloidal stability was assessed by monitoring Z-potential and size.

Distribution over time. Finally, their suitability as carries for biomedical applications was evaluated by carrying out in vitro toxicity studies. As a result, depending on their thermodynamic, physicochemical and toxicity profiles, these chimeric polymer-grafted liposomes could be promising candidates for further in *vitro* and in *vivo* investigation for future nano drug delivery applications.

SECTION I

POLYMERIC NANOPARTICLES IN DRUG DELIVERY

1. Introduction

Conventional drug delivery systems of active agents present a number of critical issues such as the sensitive toxicity, poor specificity followed by an uncontrollable release of therapeutics, low bioavailability, and drug resistance induction, which sensitively decrease the therapeutic efficiency of many drug systems.[100,101] The versatile and favourable properties of polymeric nanostructures, including stealth micelles, liposomes, dendrimers, carbon nanotubes, and quantum dots, make them promising nanocarriers to overcome or at least minimize the drawbacks of traditional therapies.[102,103,104,105]

Polymeric nanoparticles (PNPs) provide several advantages in drug delivery, that include high biocompatibility and biodegradability, increasing the stability of any volatile pharmaceutical agents, improving targeted drug delivery, and non-immunogenicity.[106] Besides, they have the best protection ability of encapsulated therapeutic from physiological factors. In these systems, a good retention of drug at the targeted site and an improvement of the efficacy at reduced dose was observed.[107] The first efforts to deliver an anticancer drug, such as doxorubicin, using poly (alkyl-cyanoacrylate) NPs, took place in 1979.[108] These revolutionary developments several reports, for the delivery of therapeutic agents via PNPs, have been published.[109] Due to their design, polymeric nanoparticles are versatile, and they can be made with a wide range of polymers from natural and synthetic sources.

---

100 B. J. Borm, *Particle toxicology form coal mining to nanotechnology, Inhal. Toxicol.,* **2002**, *14*(3), 311-324.

101 L. Huang, C. Perrault, J. Coelho-Martins, C. Hu, C. Dulong, M. Varna, J. Liu, J. Jin, C. Soria, L. Cazin, A. Janin, H. Li, R. Varin, H. Lu, *Induction of acquired drug resistance in endothelial cells and its involvement in anticancer therapy, J. of Hemat. & Onc*., **2013**, *6*(49), 1-11.

102 A. Kumari, S. K. Yadav, S. C. Yadav, *Biodegradable polymeric nanoparticles-based drug delivery systems, Colloids Surf. Biointerfaces*, **2010**, *75*, 1-18.

103 M. Bagheri, E. Bigdeli, Z. Pourmoazzen, *pH-responsive stealth micelles composed of cholesterol-modified PLA as a nano-carrier for controlled drug release, Prog. Biomater*, **2014**, *3*(22), 1-12.

104 E. C. Wiener, M. W. Brechbiel, H. Brothers, R. L. Magin, O. A. Gansow, D. A. Tomalia, P. C. Lauterbur, *Dendrimer-based metal chelates: a new class of magnetic resonance imaging contrast agents, Magn. Reson. Med*., **1994**, *31*, 1-8.

105 M. S. Dresselhaus, G. Dresselhaus, J. C. Charlier, E. Hernandez, *Electronic, thermal and mechanical properties of carbon nanotubes, Philos. Trans. A. Math. Phys. Eng. Sci.*, **2004**, *362*, 2065-2098.

106 S. Dumitriu, *Polymeric biomaterials II ed., CRC Press*, New York, USA, **2002**.

107 F. Alexis, E. Pridgen, L. K. Molnar, O. C. Farokhazad, *Factors affecting the clearance and biodistribution of polymeric nanoparticles, Mol. Pharmaceutics*, **2008**, *5*(4), 505-515.

108 D. Peer, J. M. Karp, S. Hong, O. C. Farokhazad, R. Margalit, R. Langer, *Nanocarriers as an emerging platform for cancer therapy, Nat. Nanotechnol*., **2007**, *2*, 751-760.

109 F. Alexis, E. M. Pridgen, R. Langer, O. C. Farokhzad, *Nanoparticle technologies for cancer therapy*, M. Shafer-Korting, editor. *Drug Delivery, Berlin, Heidelberg: Springer Berlin Heidelberg*, **2010**.

Multifunctional PNPs for different diseases treatment, having particular size, shapes and surface modifications, can be prepared by controlling the physico-chemical properties of polymers, such as molecular weight, dispersity index, hydrophobicity and crystallinity. Their degradation that determine the drug release and their responsiveness to internal or external stimuli, can be accurately controlled. These leading to more accurate and programmable polymer nano-based drug delivery systems in nanomedicine field.[110]

Based on the beneficial properties of polymeric nanoparticles, this ***Section I*** focuses on the synthetic techniques to obtain these nano-vectors. In addition, drug delivery systems based on proteins and polysaccharides as natural polymers, as well as, DDS that consist of polyester poly(lactic acid) (PLA), poly(D,L- lactide- coglycolide) (PLGA), poly(e-caprolactone) (PCL), and poly(d-decalactone) (PDL) were studied. In the end the formulations and characterization of block copolymer micelles (mPEG-PCL) have been considered. The experimental methods of their *in vitro* and *in vivo* behaviours have been extensively analysed.

2. Procedure for the manufacture of polymeric nanoparticles

Polymeric nanoparticles are fairly easily and cheaply synthesized in large quantities by a multitude of methods.[111] PNPs are generally prepared by either encapsulating, entrapping, or adsorbing therapeutic molecules.[112,113] Two type of PNPs can be produced: nanocapsules and nanospheres. The first one is a vesicular system in which the drug is located into a cavity, called core, surrounded by a polymer membrane, shell. Nanospheres are matrix systems where the drug is physically and uniformly dispersed.[114,115] The procedures for the manufacture of nanoparticles are divided up into two categories. The first techniques taking advantage of performed polymers, and the last ones are based on polymerization of monomers. The synthetic procedures that using performed polymers, to obtain polymeric nanocarriers are:[116]

110 N. Rapoport, *Physical stimuli-responsive polymeric micelles for anticancer drug delivery, Prog. Polym. Sci*., **2007**, *32*(8-9), 962-990.

111 F. Bally, C. A. Serra, V. Hessel et al., *Homogeneous polymerization: benefits brought by microprocess technologies to the synthesis and production of polymers, Macromol. React. Eng*., **2010**, *4*, 543-561.

112 P. Couvreur, G. Barrat, E. Fattal, P. Legrand, C. Vauthier, *Technology Nanocapsule*, Crit. Rev. *The Drug Carrier Syst*., **2002**, *19*, 99-134.

113 S. R. Shaffazick, S. S. Guterres, L. L. Freitas, A. R. Pohlamann, *Physicochemical characterization and stability of the polymeric nanoparticles systems for drug administration, Quimica Nova*, **2003**, *26*, 726-737.

114 W. E. Bawarski, D. Pharm, E. Chidlowsky, D. J. Bharali, S. A. Mousa, *Emerging nano-pharmaceuticals, Nanomed. Nanotech. Biol. Med*., **2008**, *4*, 273-282.

115 M. T. Peracchia, et al., *PEG-coated nanospheres from amphiphilic deblock and multiblock copolymers: Investigation of their drug encapsulation and release characteristics*, *J. Controlled Release*, **1997**, *46*, 223-231.

116 J. P. Rao, K. E. Greckeler, *Polymer nanoparticles: preparation techniques and size-control parameters, Prog. Polym. Sci.,* **2011**, *36*(7), 887-913.

- **Nanoprecipitation:** or solvent displacement technique is based on interfacial turmoil between miscible organic and aqueous phase. Polymeric excipients and drug dissolved in a water-miscible organic solvent diffuse from organic to aqueous phase with spontaneous accumulation into nanocrystals.[117]

- **Solvent evaporation:** that involves preparation of polymeric solutions in volatile organic solvents, such as dichloromethane, chloroform, or ethyl acetate, followed by formulating emulsions.[118] The organic solvent is then removed from the system through stirring at different temperature or by reduced pressure. This method enables the incorporation of lipophilic drugs with high loading efficiencies through controlling the mixing speed and the mixing conditions.

- **Solvent diffusion:** this technology allows the encapsulation into polymeric nanoparticles od lipophilic and/or hydrophilic active molecules. Polymer, drug and oil are dissolved into partially water-miscible organic solvent. Then, in the emulsification step of the organic phase in the aqueous phase under vigorous agitation is observed.The addition of water, to this system, causes the diffusion of the dissolver into the aqueous phase, resulting in the formation of nanocapsules.[119,120]

- **Salting out:** can be considered as a modification of the emulsification/solvent diffusion. Polymer and drug are initially dissolved in an organic solvent, which is. Subsequently emulsified into an aqueous gel containing the salting-out agent such as electrolytes and colloidal stabilizer, for example hydroxyethylcellulose or poly (vinyl-pyrrolidone). This oil/water emulsion is diluted with a sufficient volume of water or aqueous solution to enhance the diffusion of organic solvent into the aqueous phase, thus inducing the formation of nanospheres. This method is used in the preparation of PLA.[121]

- **Dialysis:** for preparation of polymeric nanoparticles with narrow distribution. Drug, and polymer are placed inside a dialysis tube/ membrane after dissolving with water miscible organic solvents with appropriate molecular weight cut off. The organic

117 G. Varan, J. M. Benito, C. O. Mellet, E. Bilensoy, *Development of polycationic amphiphilic cyclodextrin nanoparticles for anticancer drug delivery*, *Beilstein J. Nanotechnol*., **2017**, *8*, 1457-1458.

118 E. Allemann, R. Gurny, E. Doelker, *Drug-loaded nanoparticles: preparation methods and drug targeting issues, Eur. J. Pharm. Biopharm*., **1993**, *39*, 173-191.

119 G. D. Quintanar, E. Alleman, H. Fessi, *Preparation techniques and mechanisms of formation of biodegradable nanoparticles from performed polymers, Drug Dev. Ind. Pharm*., **1998**, *24*, 1113-1128.

120 S. Z. U. Quasim, A. Naveed, M. M. Athar, S. Irfan, M. I. Ali, M. M. Ahmed, R. B. Reddy, *Materials for drug & gene delivery, Nanobiotechnology*, D. A. Phoenix, W. Ahmed, Eds. *One Central Press, Ltd*, Manchester, UK, **2014**.

121 E. Allemann, R. Gurny, E. Doelker, *Preparation of aqueous polymeric nanodispersions by a reversible salting-out process: influence of process parameters on particle size, Int. J. Pharm*., 1992, *87*, 247-253.

phase diffuses out through the dialysis membrane into the aqueous phase which decrease the interfacial tension between them. The homogeneous suspension of NPs is formed by the displacement of solvent inside the membrane followed by progressive aggregation of polymer due to the loss of solubility. The nanosuspension produced can be lyophilized to obtain a fine powder of NPs.[122]

- **Supercritical fluid technology:** this technique avoids the use of organic solvent. A supercritical fluid is any substance where distinct liquid, gas phases do not exist.[123] Drug and polymer are dissolved in a supercritical fluid to form a solution, followed by the rapid expansion of the solution across an orifice or a capillary nozzle into ambient ait. High degree of super saturation accompanied by the rapid pressure reduction in the expansion, results in the homogenous nucleation and well dispersed uniform sized NPs.[124,125]

Instead, the methods that involve polymerization of monomers are as follow:

- **Emulsion polymerization:** is one of the widely used strategies for the preparations of polymeric. Nanoparticles. This technique is divided into two categories conventional and surfactant-fee emulsion polymerization. The conventional method involves the use of water, used as the main dispersion medium, a monomer, an initiator, and a surfactant. The polymerization starts with the collision of monomers with the initiatior molecules in continuous phase. [126] Surfactant-free emulsion polymerization is a conventional method employs. The use of organic solvents that must be eliminated at the end of the process. The reagents used in this method are water, initiator, and acryl or vinyl monomers.[127]

- **Mini- and microemulsion polymerization:** Miniemulsion consists of water, monomer mixture, co-stabilizer, surfactant and initiator. The difference between the emulsion polymerization is the use of low molecular mass co-stabilized and high shear device to reach an interfacial tension greater than zero. Microemulsion

122 M. Liu, Z. Zhou, X. Wang, J. Xu, K. Yang, Q. Cui et al., *Formation of poly(L, D,-lactide) spheres with controlled size by direct dialysis*, *Polymer*, **2007**, *48*(19), 5767-5779.

123 L. Padrela, M. A. Rodri Gues, S. P. Velaga, H. A. Matos, E. G. Azevedo, *Formation of indomethacin-saccharin cocrystals using supercritical fluid technology, European J. of Pharmaceutical Sciences*, **2009**, *38*(1), 9-17.

124 J. Varshosaz, F. Hassanzadeh, M. Mahmoudzadeh, A. Sadeghi, *Preparation of cefuxorime axetil nanoparticles by rapid expansion of supercritical fluid technology, Powder Technol*., **2009**, *189*(1), 97-102.

125 B. S. Sekhon, *Supercritical fluid technology: An overview of pharmaceutical applications, Int. J. Pharm. Tech. Res.*, **2010**, *2*(1), 810-826.

126 P. Couvreur, B. Kante, M. Roland, P. Guiot, P. Bauduin, P. Speiser, *Polycyanoacrylate nanocapsules as potential lysosomotropic carriers: preparation, morphological and sorptive properties, J. Pharm. Pharmacol*., **1979**, *31*, 331-332.

127 M. Egen, R. Zentel, *Surfactant-free emulsion: Polymerization of various methacrylates: towards monodisperse colloids for polymer opals, Macromol. Chem. Phys.*, **2004**, *205*, 1479-1488.

polymerization of monomers may be achieved by incorporating a monomer in any of the water and oil phases of the system. Replacing dispersed phase by a monomer in an o/w microemulsion produces spherical particles of optimum diameter.[128]

- **Interfacial polymerization:** the reaction takes places at the interface of the liquids. In this method two reactive monomers are dispersed in two phases: continuous and dispersive phase. Its limit is the synthesis of small-sized nanoparticles. In the same way, the controlled/living polymerization (C/LRP), was introduced in order to control the molar mass distribution, architecture, and function of polymeric nanoparticles. This technique uses solvents such as water or supercritical carbon dioxide. [129]

The choice of a specific synthetic method to obtain polymeric nanoparticles, depends on the particular physicochemical properties that need to be achieved in the formulation, such as desired diameter of the particles, the degree of biocompatibility and biodegradability, and specific surface properties as well as permeability, charge, and the targeted drug release profiles and rates.[130]

3. Drug delivery systems based on biodegradable polymers

Polymers used for drug delivery are classified according to their chemical nature, their matrix architecture stability of the backbone chain and their solubility in physiological environments.[131] Biodegradable and biocompatible polymers of synthetic or natural origin, used in drug delivery are considered to be biologically inert materials that protect the drug from enzymatic degradation, provide a specific target drug delivery, enhancing the drug bioavailability, reducing the systemic side effects and drug toxicity, in order to increase a high patient compliance.[132]

Natural polymer, or biopolymers, are compounds that occur naturally or are produced by living organisms such as cellulose, silk, chitin, protein and DNA. In the past, natural polymers

128 M. Antonietti, R. Basten, S. Lohman, *Polymerization in microemulsions-a new approah to ultrafine, higly functionalized polymer dispersions, Macromol. Chem. Phys.*, **1995**, *196*, 441-466.

129 E. Drioli, A. Criscuoli, E. Curcio, *Membrane contactors and catalytic membrane reactors in process intensification, Chem. Eng. Technol.*, **2003**, *26*, 975-981.

130 A. Chowdhury, S. Kunjiappan, T. Panneerselvam, B. Somasundaram, C. Bhattacharjee, *Nanotechnology and nanocarrier-based approaches on treatment of degenerative disease, International Nano Letters*, **2017**, *7*(2), 91-122.

131 F. Raza, H. Zafar, Y. Zhu, Y. Ren, A. Ullah, A. U. Khan, X. He, H. Han, Md Aquib, K. O. Boajye-Yiadom, L. Ge, *A review on recent advances in stabilizing peptides/proteins upon fabrication in hydrogels fro biodegradable polymers*, *Pharmaceutics*, **2018**, *10*(16), 1-21.

132 R. Song, M. Murohy, C. Li, K. Ting, C. Soo, Z. Zheng, *Current development of biodegradable polymeric materials for biomedical applications, Drug Des. Devel. And Therapy*, **2018**, *12*, 3117-3145.

have been preferred, due to their abundance in nature and biocompatibility.[133] However, they have some disadvantages that progressively limited their application, such as high batch to batch variability and risk of infection. Synthetic polymers can be used to overcome these issues, because they are promising materials for biomedical applications.[134] Besides, they have an advantage of being easy to prepare, having good mechanical strength, and giving reproducible results that are not observed in the case of natural polymers.[135] Most commonly used synthetic polymers are poly(ethylene-glycol) (PEG), polyester poly(lactic acid) (PLA), poly(D,L- lactide- coglycolide) (PLGA), poly(ε-caprolactone) (PCL), and poly(δ-decalactone) (PDL). Their characteristics and uses are described below.

- **Poly(ethylene-glycol) (PEG):** is the most popular hydrophilic polymer. It is a synthetic material with major characteristics of biocompatibility, water solubility and low cost.[136] It has numerous applications such as drug delivery and tissue engineering.[137] PEG can be used to coat nanoparticles to extend their circulation time by reducing protein adsorption through the hydrophilicity or steric properties of PEG which are thought to minimize uptake by RES cells and mononuclear phagocytic systems (MPS).[138,139] Furthermore, PEGylated nanoparticles exhibit longer circulation time, because they can remain invisible to phagocytic cells since they do not bind opsonin proteins.[140]

- **Poly(lactic acid) (PLA):** is synthetic, thermoplastic, and biodegradable polyester. The traditional method of PLA synthesis performs by ring opening polymerization (ROP), using Sn(II) 2-ethylhexanoate as initiator.[141] Polymers obtained from lactic acid have found numerous application in medicine and in systems for controlled drug release. For the application as drug carriers, PLA should be defined molecular weight. In

133 S. Kulkarni Vishakha, D. Butte Kishor, S. Rathod Sudha, *Natural Polymers-a comprehensive review, Int. J. of Research in Pharm. and Biomed. Sci.*, **2012**, *3*(4), 1597-1613.

134 J. M. Lu, X. Wang, C. Marin-Muller, H. Wang, P. H. Lin, Q. Yao, C. Chen, *Current advances in research and clinical application of PLGA-based nanotechnology, Expert Rev. Mol. Diagn*., **2009**, *9*, 325-341.

135 J. Sharma, M. Lizu, M. Stewart, K. Zygula, Y. Lu, R. Chauhan, X, Yan, Z. Guo, E. Wujcik, S. Wei, *Multifunctional nanofibers towards active biomedical therapeutics, J. Polym.*, **2015**, *7*, 186-219.

136 J. F. Lutz, A. Hoth, *Preparation of ideal PEG analogues with a tunable thermosensitivity by controlled radical copolymerization of 2-(2-methoxyethoxy) ethyl methacrylate and oligo (ethylene glycol) methacrylate*, *Macromolecules*, **2006**, *39*, 893-896.

137 P. Ni, Q. Ding, M. Fan, J. Liao, Z. Qian, J. Luo, et al., *Injectable thermosensitive PEG-PCL-PEG hydrogel/acellular bone matrix. Composite for bone regeneration in cranial defects, Biomaterials*, **2014**, *35*, 236-248.

138 F. Alexis, E. Pridgen, L. K. Molnar, O. C. Farokhazad, *Factors affecting the clearance and biodistribution of polymeric nanoparticles, Mol. Pharm*., **2008**, *5*(4), 505-515.

139 D. E. Owens, N. A. Peppas, *Opsonization, biodistribution and pharmacokinetics of polymeric nanoparticles, Int. J. Pharm*., **2006**, *307*(1), 93-102.

140 S. M. Moghimi, A. C. Hunter, J. C. Murray, *Long-circulating and target-specific nanoparticles: theory to practice, Pharmacol. Rev*., **2001**, *53*(2), 283-318.

141 M. S. Lopes, L. A. Jardini, R. M. Filho, *Synthesis and characterizations of poly (lactid acid) by ring-opening polymerization for biomedical applications*, *Chemical Engineering Transactions*, **2014**, *38*, 331-338.

literature, the performance of PLA nanoparticles in the controlled delivery of various bioactive molecules such as conventional and antitumor drugs, peptides and genes for the treatment of a variety of illness have been extensively reported.[142,143]

- **Poly(d-decalactone) (PDL):** synthesized via ROP of δ-decalactone monomers.[144] The polymerized δ-decalactone structure is characterized by the presence of the polyester alkyl side chain that have potential value in drug delivery applications. The side-chain is expected to disrupt backbone packing in condensed structures, which might also favour increased drug incorporation. Furthermore, this polymer should generate a highly hydrophobic core when formulated as micellar or NPs delivery system, which may be useful to achieve better drug loading than is possible with other used polymers.[145,]

- **Poly(ε-caprolactone) (PCL):** is another biodegradable, biocompatible synthetic polyester.[146] It is a promising polymer for pharmaceutical and biomedical applications. PCL is important to develop polymeric nanoparticles that can, eventually, success in clinical trials.[147] For example, encapsulation of amphotericin B, a polyenoic antifungal agent and drug for treatment of leishmaniosis, in the PCL nanospheres can reduce drug toxicity and enhance activity, by increasing the available drug concentration at the side of action.[148]

Many studies are available in literature, investigating the potential application of various polymeric nanoparticles such as micelles and liposomes, used for delivery of therapeutic agents to specifically targeted sites. Combination of polymeric system with nanostructured-based drug delivery system provides sustained drug release.

4. Polymeric micelles as nanocarrier for drug delivery

Block copolymer are systems consist of two or more distinct types of polymeric block covalently linked together, that recently have attracted considerable scientific interest owing

142 V. Lassalle, M. L. Ferreira, *PLA nano- and microparticles for drug delivery: an overview of the methods of preparation, Macromol. Biosci*., **2007**, *7*, 767-783

143 D. Garlotta, A litterature review of poly (lactic acid), J. Polym. Environ., 2001, 9, 63-84.

144 M. T. Martello, A. Burns and M. Hillmyer, *Bulk ring-opening transesterification polymerization of the renewable d-decalactone using an organocatalyst*, *ACS Macro Lett.*, **2012**, *1*(1), 131-135.

145 L. Glavas, P. Olsen, K. Odelius, A. C. Albertsson, *Achieving micelle control through core crystallinity, Biomacromolecules*, **2013**, *14*, 4150-4156.

146 P. Olsen, T. Borke, K. Odelius, A. C. Albertsson, *ε-decalactone: A thermoresilient and toughening comonomer to poly (L-lactide). Biomacromolecules,* **2013**, *14*(8), 2883-2890.

147 B. Ray, S. H. Teoh, D. W. Hutmacher, T. Cao, K. H. Ho, *Novel PCL-based honeycomb scaffolds as drug delivery systems for rhBMP-2, Biomaterials*, **2005**, *26*, 3739-3748.

148 M. S. Espuelas, P. Legrand, P. M. Loiseau, C. Bories, G. Barratt, J. M. Irache, *In vitro antileishmanial activity of Amphotericin B loaded in poly (epsilon-caprolactone) nanospheres, J. Drug Targe*t, **2002**, *10*(8), 593-599.

to their unique properties.[149] These systems consist of hydrophilic and hydrophobic segments and the self-assembly in solvent phase leads to formation of nano-sized particles with hydrophobic core and hydrophilic shell.[150,151] The core serves as reservoirs for hydrophobic drugs, whereas the exterior enhances the stability of carrier in an aqueous medium.[152] The self-assembly process is responsible for the formation of essential structures in nature, including lipid membranes and living cells.[153]

Micellization is a common self-assembly process, that usually occur in selective solvents, whereby amphiphilic molecules spontaneously aggregate into various nanostructures.[154] Polymeric micelles (PMs) are supramolecular self-assemblies formed when block copolymer concentration in solution exceeds a critical concentration, called critical micelle concentration (CMC).[155] The size of PMs are usually less than 100 nm and their hydrophilic surface is of crucial importance in overcoming the major obstacle of drug targeting the RES and MPS uptake.[156] For these reasons, they have been proposed as novel carrier systems in drug targeting due to their increased loading capacities, stability in physiological conditions and the possibility of engineering the core-shell architecture for different applications.[157]

In recent years, induced micellization of block copolymers has received considerable attention. The micellization process can be induced by several variations in the surrounding of the solubilized block copolymers, such as: temperature, pressure, pH, redox potential, metal salt formation, hydrogen bonding formation, covalent bond cross-linking, non-covalent bont formations, etc. In the literature are reported two most common micellization techniques: physically-induced micellization and chemically-induced micellization.[158] Physicallly-induced micellization depends on physical variable such as temperature, pressure volume, etc. as the driving force of block copolymer micellization. By their own nature, this technique leads to

149 A. Sousa-Herves, R. Novoa-Carballal, R. Riguera, E. Fernandez-Megia, Gatg dendrimers and pegylated block copolymers: from synthesis to bioapplications, J. AAPS, **2014**, *16*, 948-961.

150 R. Zana, *Dynamics of surfactant self-assemblies micelles, microemulsions, vesicles, and lyotropic phases, Surfactant sciences series, Taylor and Francis*, London, **2005**, *125*.

151 G. Srinivas, J. C. Shelley, S. O. Nielsen, D. E. Discher, M. L. Klein, *Simulation of di-block copolymer self-assembly, using a coarse-grain model, J. Phys. Chem. B*. **2004**, *108*(24), 8153-8160.

152 H. Liu, P. Hou, H. Zhang, J. Wu, *Synthesis of monosized core-shell Fe3O4/Au multifuctional nanoparticles by PVP-assisted nanoemulsion process, Colloid Surf.*, **2010**, *356*, 21-17.

153 K. Tanaka, J. M. M. Caaveiro, K. Morante, J. M. Gonzalez-Manas, K. Tsumoto, *Structural basis for self-assembly of a cytolytic pore lined by protein and lipid, Nature Comm.* **2015**, *6*(6337), 1-11.

154 G. Riess, *Micellization of block copolymers, Prog. Polym. Sci*., **2003**, *28*, 1107-1170.

155 K. Kataoka, A. Harada, Y. Nagasaky, *Block copolymer micelles for drug delivery: design, characterization and biological significance, Adv. Drug. Deliv. Rev*., **2001**, *47*(1), 113-131.

156 G. S. Kwon, S. Suwa, M. Yokoyama, T. Okano, Y. Sakurai, K. Kataoka, *Enhanced tumor accumulation and prolonged circulation times of micelle-forming poly (ethylene oxide-aspartate) block copolymer-adriamycin conjugates*, *J. Control. Release*, **1994**, *29*, 17-23.

157 G. S. Kwon, K. Kataoka, *Block copolymer micelles as long-circulating drug vehicles, Adv. Drug. Deliv. Rev*., **1995**, *16*(2-3), 295-309.

158 R. Bouchal, A. Hamel, P. Hesemann, M. In, B. Prelot, J. Zajac, *Micellization behavior of long-chain substituted alkylguadinium surfactants, Int. J. Mol. Sci.*, **2016**, *17*(2), 223.

reversible micellar nanoentities. Neradovic et coworkers, showed that block copolymers of poly (N-isopropyl acrylamide) (PNIPAM) with PEG, exhibit thermoresponsive solubility in aqueous solutions.[159] Instead, the chemically-induced micellization was reported as early as 1996 by Munk and co-workers. They showed that, depending on the reversibility of the chemical reaction used to induce the micellization the resulting micelles will be permanent or reversible nano-assemblies.[160]

Bader et al. were the first to consider polymeric micelles as drug nanocarriers due to their size, they have been often compared to natural carrier systems, such as viruses and lipoproteins.[161,162] Despite the pharmaceutical potential of PMs, these systems have several disadvantage that include poor drug-loading efficiency, poor physical stability in *vivo*, and insufficient cellular interaction on neutral micelles with malignant cells for uptake.[163] In this regard, different strategies have been employed to enhance micelles stability, also including core-shell crosslinking. For this reason, the next chapter focuses on the synthesis of highly-efficient methoxy poly(ethylene glycol)-block-poly(ε-caprolactone) crystalline cored micelle useful in anti-glaucoma treatment.

159 D. Neradovic, C. F. van Nostrum, W. E. Hennink, *Thermoresponsive polymeric micelles with controlled Instability based on hydrotycally sensitive N-isopropylacrylamide copolymers, Macromolecules*, **2001**, *34*(22), 7589-7591.

160 P. Munk, *Equilibrium and nonequilibrium polymer icelles, Solvents and Self-Organization of Polymers*, **1996**, *327*, 19-32.

161 H. Bader, H. Ringsdorf, B. Schmidt, *Water-soluble polymers in medicine, Angew Macromol. Chemie,* **1984**, *123*, 457-485.

162 M. Jones, J. Leroux, *Polymeric micelles - a new generation of colloidal drug carriers, Eur. J. Pharm. Biopharm*., **1999**, *48*, 101-111.

163 S. Kim, Y. Shi, J. Y. Kim, K. Park, J. X. Cheng, *Overcoming the barriers in micellar drug delivery: loading effiency, in vivo stability, and micelle-cell interaction, Expert Opin. Drug Deliv.*, **2010**, *7*(1), 49-62.

5. Exploring optimized methoxy poly(ethylene glycol)-block-poly(ε-caprolactone) crystalline cored micelles in anti-glaucoma pharmacotherapy

E. Enas, H. Gad, F. Biondo, L. Casettari and M. E. Soliman, International Journal of Pharmaceutics, ***2019****, 566, 573-584.*

Graphical Abstract

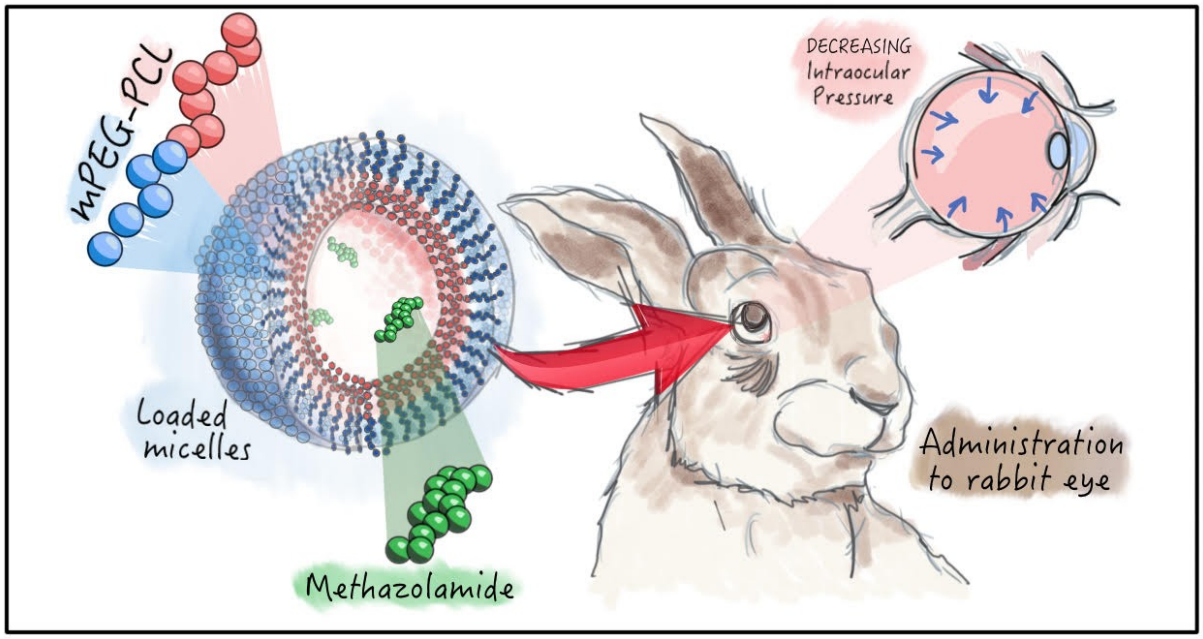

1. Introduction

The utilization of polymeric micellar structures has been gaining recognition in medical applications. Polymeric micelles (PMs) are nanoscopic carriers formed from the self-assembly of amphiphilic copolymers in aqueous media with their hydrophobic part forming the core of the micelles, while their hydrophilic part forming the outer shell.[164]

PMs type based on polyester-polyether deblock copolymers currently occupies a promising position in drug delivery. For instance, poly(lactic acid) (PLA), poly(ε-caprolactone) (PCL), and poly(lactide-co-glycolide) PLGA, mostly conjugated to the hydrophilic polyethylene glycol (PEG). These copolymers possess various merits of biodegradability, biocompatibility, amphiphilic property, hydrophilic surfaces, kinetic and thermodynamic stability and

164 R. S. Elezaby, H. A. Gad, A. A. Metwally, A. S. Geneidi, G. A. Awad, *Self-assembled amphiphilic core-shell nanocarriers in line with the modern strategies for brain delivery. J. Control. Release*, **2017**, *261*, 43–61.

nontoxicity.[165] Moreover, PEG is well-known to be a mucoadhesion promoter as well as mucosal permeability enhancer.[166,167]

From an efficacious ocular route delivery perspective, these nanoscale delivery carriers hold a great potential because of their small size, around 100 nm, that has led to well documented transcorneal penetration, intraocular absorption and decreased eye irritation and tearing.[168,169]Besides, PMs could present sustained drug release, minimized side effects and the ability to form clear aqueous solutions for hydrophobic drugs allowing administration as eye drops. They showed greater stability and transparency, avoiding blurring of vision when compared to surfactant micelles and dendrimers respectively.[170,171] Additionally, higher drug loading capacity was demonstrated relative to the commonly prepared liposomes.[172]

Self-assembled mPEG-PCL PMs seemed particularly useful in this respect based on previous literature that indicated their biocompatibility, affinity, and tolerability for ocular drug delivery.[173] PLC is FDA approved polymer, which demonstrated great corneal affinity when fabricated as nanoparticles.[174]

Most notably, De Campos and coworkers have verified that negatively charged PEG-coated PCL nanocapsules facilitated transcorneal transportation, reaching more depth in the intraocular area, compared to the positively charged chitosan coating that has been deposited in the superficial ocular mucosa.[175,176] Therefore, such outstanding findings have led to the

165 S. Zhou, X. Deng, H. Yang, *Biodegradable poly (ε-caprolactone)-poly (ethylene glycol) block copolymers: characterization and their use as drug carriers for a controlled delivery system, Biomaterials*, **2003**, *24*, 3563–3570.

166 R. D. Bachu, P. Chowdhury, Z. H. Al-Saedi, P. K. Karla, S. H. Boddu, *Ocular drug delivery barriers-role of nanocarriers in the treatment of anterior segment ocular diseases. Pharmaceutics*, **2018**, *10*, 28.

167 M. E. Soliman, E. Elmowafy, L. Casettari, C. Alexander, *Star-shaped poly (oligoethylene glycol) copolymer based gels: thermo-responsive behaviour and bioapplicability for risedronate intranasal delivery, Int. J. Pharm.,* **2018**, *543*, 224–233.

168 H. Gupta, M. Aqil, R. K. Khar, A. Ali, A. Bhatnagar, G. Mittal, *Sparfloxacin-loaded PLGA nanoparticles for sustained ocular drug delivery, Nanomed. Nanotechnol. Biol. Med*., **2010**, *6*, 324–333.

169 J. Li, S. Tian, Q. Tao, Y. Zhao, R. Gui, F. Yang, L. Zang, Y. Chen, Q. Ping, D. Hou, *Montmorillonite/chitosan nanoparticles as a novel controlled-release topical ophthalmic delivery system for the treatment of glaucoma, Int. J. Nanomed*., **2018**, *13*, 3975.

170 A. V. Kabanov, E. V. Batrakova, V. Y. Alakhov, *Pluronic® block copolymers as novel polymer therapeutics for drug and gene delivery, J. Control. Release,* **2002**, *82*, 189–212.

171 S. Wadhwa, R. Paliwal, S. R. Paliwal, S. Vyas, *Nanocarriers in ocular drug delivery: an update review, Curr. Pharm. Des.*, **2009**, *15*, 2724–2750.

172 S. Liu, L. Jones, F. X. Gu, *Nanomaterials for ocular drug delivery, Macromol. Biosci.*, **2012**, *12*, 608–620.

173 L. Xu, X. Xu, H. Chen, X. Li, *Ocular biocompatibility and tolerance study of biodegradable polymeric micelles in the rabbit eye, Colloids Surf.*, **2013**, *B112*, 30–34.

174 L. Marchal-Heussler, D. Sirbat, M. Hoffman, P. Maincent, *Poly (ε-caprolactone) nanocapsules in carteolol ophthalmic delivery, Pharm. Res.,* **1993**, *10*, 386–390.

175 A. M. De Campos, A. Sánchez, R. Gref, P. Calvo, M. A. J. Alonso, *The effect of a PEG versus a chitosan coating on the interaction of drug colloidal carriers with the ocular mucosa, Eur. J. Pharm. Sci.*, **2003**, *20*, 73–81.

176 C. Giannavola, C. Bucolo, A. Maltese, D. Paolino, M. A. Vandelli, G. Puglisi, V. H. Lee, M. Fresta, *Influence of preparation conditions on acyclovir-loaded poly-d, l-lactic acid nanospheres and effect of PEG coating on ocular drug bioavailability, Pharm. Res.*, **2003**, *20*, 584–590.

conclusion that PEG-coated nanocarriers, rather than chitosan coated ones could be beneficial in the intraocular distribution for the treatment of intraocular diseases like glaucoma.

Glaucoma is one of the most common vision-threatening public health issues worldwide, particularly within African and Asian people.[177] Early detection of the disease and appropriate treatment strategies could appear mandatory for disease management, preventing glaucoma-induced blindness.[178] Methazolamide (MTZ), being a member of carbonic anhydrase inhibitors (CAIs) has been widely used for the treatment of glaucoma.

CAIs treat glaucoma by decreasing the aqueous humor production resulting in lowering intraocular pressure (IOP).[179] Large MTZ doses administrated orally are needed to achieve the desired therapeutic effect; however, they result in unwanted systemic side effects mainly diuresis, vomiting, anorexia, renal failure, central nervous system depression and metabolic acidosis.[180,181] Topical ocular application of MTZ using traditional delivery systems (e.g. eye drops and ointments) faces many challenges owing to its poor aqueous solubility and low permeability across the cornea resulting in low bioavailability.[182,183]

Nanocarriers bearing MTZ for ocular delivery were previously reported using spanlastic vesicles, solid lipid nanoparticles, calcium phosphate nanoparticles and nanostructured lipid matrices.[184,185,186,187] However, in these fabricated nanocarriers, the in *vivo* pharmacodynamic study was performed on normotensive rabbits. Artificially induced glaucoma models in glaucomatous rabbits, mimicking glaucomatous human eyes, were proved to be a better

177 Y. C. Tham, X. Li, T. Y. Wong, H. A. Quigley, T. Aung, C. Y. Cheng, *Global prevalence of glaucoma and projections of glaucoma burden through 2040: a systematic review and meta-analysis, Ophthalmology*, **2014**, *121*, 2081–2090.

178 Y. B. Liang, Y. Zhang, D. C. Musch, N. Congdon, *Proposing new indicators for glaucoma healthcare service, Eye and Vision*, **2017**, *4*, 6.

179 Y. Qian, F. Wang, R. Li, Q. Zhang, Q. Xu, *Preparation and evaluation of in situ gelling ophthalmic drug delivery system for methazolamide, Drug Dev. Ind. Pharm.,* **2010**, *36*, 1340–1347.

180 S. Jiang, F. Wang, S. Zhu, X. Zhang, Z. Guo, R. Li, Q. Xu, *Preformulation study of methazolamide for topical ophthalmic delivery: physicochemical properties and degradation kinetics in aqueous solutions, Int. J. Pharm*., **2013**, *448*, 390–393.

181 Y. Qian, F. Wang, R. Li, Q. Zhang, Q. Xu, *Preparation and evaluation of in situ gelling ophthalmic drug delivery system for methazolamide, Drug Dev. Ind. Pharm*., **2010**, *36*, 1340–1347.

182 T. Maren, J. Haywood, S. Chapman, T. Zimmerman, *The pharmacology of methazolamide in relation to the treatment of glaucoma, Invest. Ophthalmol. Vis. Sci.,* **1977**, *16*, 730–742.

183 J. Youshia, A. O. Kamel, A. El Shamy, S. Mansour, *Design of cationic nanostructured heterolipid matrices for ocular delivery of methazolamide, Int. J. Nanomed.*, **2012**, *7*, 2483.

184 R. Chen, Y. Qian, R. Li, Q. Zhang, D. Liu, M. Wang, Q. Xu, *Methazolamide calcium phosphate nanoparticles in an ocular delivery system, Yakugaku Zasshi*, **2010**, *130*, 419–424.

185 R. Elazreg, M. Soliman, S. Mansour, A. El Shamy, *Preparation and evaluation of mucoadhesive gellan gum in-situ gels for the ocular delivery of carbonic anhydrase inhibitor nanovesicles, Int. J. Pharm. Sci. Res.,* **2015**, *6*, 3761–3774.

186 R. Li, S. Jiang, D. Liu, X. Bi, F. Wang, Q. Zhang, Q. Xu, *A potential new therapeutic system for glaucoma: solid lipid nanoparticles containing methazolamide, J. Microencapsul.*, **2011**, *28*, 134–141.

187 F. Wang, L. Chen, D. Zhang, S. Jiang, K. Shi, Y. Huang, R. Li, Q. Xu, *Methazolamide-loaded solid lipid nanoparticles modified with low-molecular weight chitosan for the treatment of glaucoma: vitro and vivo study, J. Drug Target.,* **2014**, *22*, 849–858.

meaningful investigative tool for the pharmacological response of the tested antiglaucoma agent than the normotensive ones.

Besides, the literature suggested that there is a difference in the underlying mechanisms of both models. The onset of antagonism of elevation of ocular pressure was reported to be earlier than that reduction of normal ocular pressure.[188]

Moreover, biopharmaceutical profile of such previous studies is not fully explored, lacking in vitro supporting data on ocular compatibility at the cellular level (cell viability test) or in *vivo* corneal toxicity (Draize test and histological assessment). In this light, the aim of the present study was to attain the optimal design of mPEG-PCL micelles of MTZ including colloidal size, reasonable optimum entrapment, sustained release pattern, and a promising safety profile. Design of experiment was employed to simultaneously handle the selected factors, understand the significant ones and extract the most appropriate information to optimize MTZ association within micelles. Assessment of *in vitro* release, *in vitro* and in *vivo* ocular tolerability in addition to in *vivo* investigation of the anti-glaucoma efficacy of MTZ from the fabricated micelles was performed as an indication of the in *vivo* scenario to ensure its topical effect in a sustained manner via the ocular route in comparison to MTZ solution.

2. Materials and methods

2.1. Materials

mPEG-PCL di-block copolymers with different molecular weight (Mw) (i.e. 3, 4 and 5.5 kDa) were synthesized in our lab using methoxy-PEG (mPEG) 1.9 kDa and ε-caprolactone, purchased from Polysciences (Germany) and Sigma-Aldrich (Italy), respectively. Methazolamide was purchased from Jiaxing Taixing Chemical and Pharm Co, (China). Sodium chloride, sodium bicarbonate, calcium chloride dihydrate, potassium chloride, and acetone were supplied from El-Nasr Pharmaceutical Co., (Egypt). Diprofos® a sterile aqueous solution containing 2 mg + 5 mg/mL of betamethasone in two different salt forms (i.e. dipropionate and disodium phosphate) was purchased from Medical Union Pharmaceuticals (Egypt) under license of Schering-Plough (New Jersey, USA). Benox® a sterile ophthalmic solution containing benoxinate hydrochloride (0.4%) was purchased from Egyptian International Pharmaceutical Industries (EIPICO) (Egypt). Primary human corneal epithelial cells (ATCC® PCS700-010™) were obtained from American Type Culture Collection, (Manassas, VA, USA). MTT (3-(4,5-dimethylthiazol-2-yl)-2,5-diphenyl-tetrazolium bromide)

188 R. Seidehamel, K. Dungan, *Characteristics and pharmacologic utility of an intraocular pressure (IOP) model in unanesthetized rabbits, Invest. Ophthalmol. Vis. Sci*., **1974**, *13*, 319–322

was purchased from Sigma-Aldrich Co. (St Louis, MO, USA). Spectra/Por dialysis membrane (molecular weight cutoff 12–14 kDa) was purchased from Spectrum Laboratories (Canada).

2.2. Synthesis and characterization of the copolymers

Synthesis and characterization of mPEG-PCL were performed by the ring opening polymerization (ROP) technique and ^{1}H-NMR and GPC analysis respectively as previously described by our group.[189,190] For more details, Synthesis and characterization of mPEG-PCL were described in Supplementary Materials section.

2.3. Preparation of mPEG-PCL micelles

MTZ loaded micelles (MTZ-PMs) were prepared using a modified thin film hydration method as stated by Shi and his colleagues.[191] mPEG-PCL copolymer and MTZ were co-dissolved in 5 mL of acetone. Then, the organic solvent was evaporated with the aid of vacuum and heat at 50 °C using a rotary evaporator (HB4-basic, IKA, Germany) until the formation of a dry thin film. The formed film was hydrated using 10 mL deionized water at 50 °C and introduced again into the rotary evaporator for 1 h. The formed micelles were then subjected to sonication at 50 °C for 1 h to produce a uniform particles size. According to previous literature, 0.15% w/v MTZ was used in the preparation of micelles.[192]

2.4. Determination of particle size, polydispersity index, and zeta potential of the formed micelles.

The particle size (PS), polydispersity index (PDI) and zeta potential (ZP) for the prepared micelles were determined at 25 °C using a laser diffraction particle size detector (Zetasizer; Malvern Instruments,Malvern, UK).

2.5. Determination of MTZ percentage entrapment efficiency

The percentage entrapment efficiency (% EE) of MTZ was estimated as previously reported. In brief, micelles were placed in simulated tear fluid (STF) (composed of 2 g NaHCO3, 6.7 g NaCl, 0.08 g CaCl2 dihydrate, and deionized water up to 1 L). The micelles were incubated in a mechanical shaker for 3 days to ensure complete drug liberation as manifested by

189 K. S. Shalaby, M. E. Soliman, G. Bonacucina, M. Cespi, G. F. Palmieri, O. A. Sammour, A. A. El Shamy, L. Illum, L. Casettari, *Nanoparticles based on linear and starshaped poly (ethylene glycol)-poly (ε-caprolactone) copolymers for the delivery of antitubulin drug, Pharm. Res.*, **2016**, *33*, 2010–2024.

190 K. S. Shalaby, M. E. Soliman, L. Casettari, G. Bonacucina, M. Cespi, G. F. Palmieri, O. A. Sammour, A. A. El Shamy, *Determination of factors controlling the particle size and entrapment efficiency of noscapine in PEG/PLA nanoparticles using artificial neural networks, Int. J. Nanomed*., **2014**, *9*, 4953.

191 S. Shi, Z. Zhang, Z. Luo, J. Yu, R. Liang, X. Li, H. Chen, *Chitosan grafted methoxy poly (ethylene glycol)-poly (ε-caprolactone) nanosuspension for ocular delivery of hydrophobic diclofenac, Sci. Rep.*, **2015**, *5*, 11337.

192 Op. cit. note 179

detectable constant drug concentrations following subsequent withdrawal of aliquots from STF medium. Aliquots were taken from STF medium, sonicated for 1 min and properly diluted. The drug was measured spectrophotometrically at 290 nm using a UV–Vis spectrophotometer (Shimadzu, model UV-1601 PC, Kyoto, Japan). The amount of MTZ was then determined according to a calibration curve of MTZ in STF. The % EE of MTZ was calculated using the following equation:

%EE = (amount of drug in PMs/total amount of drug used in formulation) x 100

2.6. Optimization of the formed micelles using a factorial design

The influence of two different formulation parameters on the MTZPMs EE% was evaluated using a 32 full factorial design composed of two factors each set at three levels. The two factors investigated were polymer molecular weight (Mw) "A" and drug to polymer ratio (D/ Pratio) "B" (transformed to polymer amount in mg to convert the categorical factor into a numerical factor), both at three levels: 3, 4 and 5.5 (kDa) for the first factor while 1:5, 1:7.5 and 1:10 for the second factor. For the selection of best PMs, desirability ratio (DR) was calculated and the formulation that shows the highest DR value to be selected for further investigation. DR was calculated by assigning that the best formulation should have the highest %EE.

2.7. Morphology of the formed micelles

Morphological examination of the selected PMs (NM3) was examined using a high-resolution transmission electron microscope (HRTEM) (Jeol Electron Microscope, JEM-1010, Japan). A droplet of the suspension was added to a carbon film-covered copper grid without staining. Excess liquid was drained with the aid of a filter paper. After sample dryness, PMs were visualized under an electron beam at a voltage of 200 kV and magnification X15,000 and X25,000.

2.8. In vitro release study and release kinetics

In vitro release study of MTZ from the selected PMs (NM3) and MTZ solution (0.15%, prepared using polyethylene glycol 400 (7%, v/v) and propylene glycol (53%, v/v) ,was carried out using a membrane diffusion technique.[193] An aliquot of PMs or drug solution equivalent to 1 mg of MTZ was placed in open-ended glass tubes having a diameter of 2.5 cm and covered from its lower end with a dialysis membrane. The glass tubes were then

193 A. S. Guinedi, N. D. Mortada, S. Mansour, R. M. Hathout, *Preparation and evaluation of reverse-phase evaporation and multilamellar niosomes as ophthalmic carriers of acetazolamide, Int. J. Pharm*., **2005**, *306*, 71–82.

suspended in USP dissolution apparatus (Pharma Test, Germany) and rotated at 50 rpm at 37 °C in 50 mL dissolution medium composed of simulated tear fluid (STF). At predetermined time intervals, 1 mL samples were withdrawn and immediately replenished with STF to keep the volume constant. The quantity of MTZ released was measured spectrophotometrically. The drug release data were fitted to first order, zero order, Higuchi and Peppas models for drug release to indicate MTZ release kinetics.

2.9. Differential scanning calorimetry (DSC)

The thermal properties of MTZ, mPEG-PCL copolymer, their physical mixture (1:1), selected lyophilized MTZ-PMs "lyophilization using Christ, alpha 1–2 LD plus, Germany", were studied using DSC (Shimadzu-DSC 60, Japan). Powdered samples (2–3 mg) were sealed in aluminum pans with lids and scanned at a temperature between 0 and 300 °C at a rate of 10 °C/min, using dry nitrogen as a carrier gas with a flow rate of 25 mL/min.

2.10. Ft-IR characterization

FT-IR spectra of MTZ, mPEG-PCL copolymer, their physical mixture (1:1) and selected lyophilized MTZ-PMs were recorded in the range of 4000–400 cm^{-1} on a Nicolet 6700 FTIR (Thermo Scientific, USA). Powdered samples were loaded on KBr discs without special treatment. All spectra were recorded at a resolution of 4 $cm^{-}1$ and 16 scans at ambient temperature.

2.11. Stability studies

The effect of aging on the selected MTZ-PMs (NM3) was studied. The selected MTZ-PMs were stored in the refrigerator at 4 °C and examined for the physical evaluation parameters (PS, PDI, ZP and EE%) at 1, 7, 14, 21 and 28 days. The *in vitro* stability of selected micelles was also evaluated in both STF and 0.1% bovine serum albumin (BSA) at 37 °C in a thermostatically controlled digital shaking water bath (Abbotta, 110X, USA).[194] At predetermined time intervals viz, 1, 2, 4, 6, 8 and 24 h, PS of the micelles was recorded.

2.12. Suitability of MTZ-PMs for ocular delivery

2.12.1. Determination of pH

The pH value of the selected MTZ-PMs (NM3) was measured using a pH meter (Model 3510, Jenway, UK).

194 H. R. Lin, P. C. Chang, *Novel pluronic-chitosan micelle as an ocular delivery system, J. Biomed. Mater. Res. B Appl. Biomater.*, **2013**, *101*, 689–699.

2.12.2. In vitro ocular cytocompatibility

MTT assay for monitoring the *in vitro* ocular cytotoxicity of selected micelles (NM3) against primary human corneal epithelial cells (ATCC® PCS700-010™) was carried out as previously stated.[195] Four aliquots of the selected micelles ranging in concentration from 3.9 to 250 µg/mL were tested and incubated with cells for 24 h. Both benzalkonium chloride and untreated cells were used as positive and negative controls respectively. Cell viability (%) was calculated using the equation:

Cell Viability = (Abs test/ Abs control) x 100

Where the Abs test is the absorbance of treated cells with the tested concentrations of the PMs. Instead, Abs control is the absorbance of untreated cells in the control wells. IC50 values were also calculated using the log (concentration) vs. % cell viability curve equation.[196]

2.12.3. In vitro hemocompatibility

The *in vitro* hemolysis activity of the selected micelles (NM3) was carried out according to the assay previously adapted with slight modifications. Briefly, rat blood was collected in EDTA-K3 containing sterile tubes and centrifuged at 4000 rpm for 15 min.[197,198] The obtained erythrocytes sediment was then washed three times with normal saline. 2% v/v erythrocytes suspension was prepared by dispersing the cells in normal saline. Different concentrations of the selected micelles were incubated with 900 µL erythrocytes at 37 °C for 1 h. The test samples were centrifuged at 4000 rpm for 15 min. The absorbances of the obtained supernatants were measured spectrophotometrically at 540 nm. Normal saline and triton X-100 (1% v/v) were taken as negative and positive controls, respectively. The hemolysis (%) was calculated using the following equation:

Hemolysis (%) = $(Abs_{test} - Abs_{negative\ control})/(Abs_{positive\ control} - Abs_{negative\ control})$ x100

Where the Abs_{test} is the absorbance of sample treated with the tested concentrations of the PMs; $Abs_{negative\ control}$ is the absorbance of sample treated with normal saline; and $Abs_{positive\ control}$ is the absorbance of sample treated with triton X-100.

195 H. Abdelkader, M. R. Longman, R. G. Alany, B. Pierscionek, *Phytosome-hyaluronic acid systems for ocular delivery of L-carnosine, Int. J. Nanomed.*, **2016**, *11*, 2815.

196 B. M. Ayesh, A. A. Abed, M. F. Doa'a, *In vitro inhibition of human leukemia THP-1 cells by L. Origanum syriacum and L. Thymus vulgaris extracts, BMC Res. Notes*, **2014**, *7*, 612.

197 D. Pooja, H. Kulhari, M. K. Singh, S. Mukherjee, S. S. Rachamalla, R. Sistla, *Dendrimer–TPGS mixed micelles for enhanced solubility and cellular toxicity of taxanes, Colloids Surf., B.*, **2014**, *121*, 461–468.

198 P. Zhang, L. Hu, Q. Yin, Z. Zhang, L. Feng, Y. Li, *Transferrin-conjugated polyphosphoester hybrid micelle loading paclitaxel for brain-targeting delivery: synthesis, preparation and in vivo evaluation, J. Control. Release,* **2012**, *159*, 429–434.

2.12.4. In vivo ocular tolerability

Assessment of ocular tolerability was carried out as a confirmatory test of *in vitro* cytocompatibility of MTZ-PMs. Gross ocular abnormalities and irritation and ocular toxicity on an *in vivo* ocular tissue level were examined using the Draize test and histopathological examination respectively. The experimental procedures were carried out following the ethical principles of the Egyptian Research Institute of Ophthalmology (Giza, Egypt) and the study protocol was approved by the Research Ethics Committee of the Faculty of Pharmacy, Ain Shams University. The New Zealand adult male rabbits, each weighing 3–3.5 kg were used in the *in vivo* study. The rabbits were kept in cages with free access to water and food and maintained on 12 h/12 h light/ dark cycle, at 20–24 °C. Before performing the *in vivo* study, all the experimental rabbits were observed and revealed to be free from any ocular abnormalities.

Ocular irritation caused by the selected micelles (NM3) was evaluated by the Draize technique. Three male albino rabbits, each weighing 3–3.5 kg, were used in the experiment. The selected formula was instilled directly into the lower conjunctival sac of the rabbit's right eye, with the left eye serving as normal control. Monitoring of ocular condition (redness, conjunctival congestion, swelling, discharge and iris, and corneal lesions) was carried out using a scoring system at 1, 6, 24, 48, 72 h and one-week post instillation as previously stated.[199,200]

The histopathological examination was carried out following the Draize test on day 7. The excised eyeballs, fixed in formalin solution 10% (v/v) for 24 h, were stained and examined under the light microscope (Axiostar plus, Zeiss, NY).[201]

2.13. In vivo pharmacodynamic study

The efficacy of the selected MTZ-PMs (NM3) in lowering the IOP following topical delivery was evaluated using hypertensive albino rabbits. The results were compared to the effect of 0.15% MTZ solution (prepared using polyethylene glycol 400 (7%, v/v) and propylene glycol (53%, v/v). Sterility of formulations was achieved by filtration through sterile 0.22 μm pore

199 O. Ashraf, M. Nasr, M. Nebsen, A. M. A. Said, O. Sammour, *In vitro stabilization and in vivo improvement of ocular pharmacokinetics of the multi-therapeutic agent baicalin: delineating the most suitable vesicular systems, Int. J. Pharm.,* **2018**, *539*, 83–94.

200 J. Kanoujia, P. S. Kushwaha, S. A. Saraf, *Evaluation of gatifloxacin pluronic micelles and development of its formulation for ocular delivery, Drug Deliv. Transl. Res*., **2014**, *4*, 334–343.

201 M. Shokry, R. M. Hathout, S. Mansour, *Exploring gelatin nanoparticles as novel nanocarriers for timolol maleate: augmented in-vivo efficacy and safe histological profile, Int. J. Pharm*., **2018**, *545*, 229–239.

size pyrogen-free cellulose filters (Bansal et al., 2018).[202] Rabbits were divided into two groups, each of four rabbits. Group I received MTZ solution (0.15% w/v), while Group II received MTZ-PMs (0.15% w/v).

2.13.1. Ocular hypertension model

All rabbits were subjected to the induction of ocular hypertension using steroids.[203] All rabbits received betamethasone injection (Diprofos® ampoules 14 mg/2 mL) in the sub-conjunctival sac in both eyes. The injection was repeated for three weeks based on a weekly administration to achieve an elevated IOP. The IOP of both eyes of each rabbit was measured using a standardized tonometer (Shiotz, Germany) before induction of glaucoma and twice per week to ensure the induction of glaucoma. IOP measurement was performed after instilling 1–2 drops of benoxinate hydrochloride (Benox® eye drops) to the eye as a local anesthetic.

2.13.2. Drug administration and evaluation of anti-glaucoma efficacy

For all rabbits, following induction of glaucoma, 50 µL dose of MTZ containing preparations (0.15% MTZ) was instilled onto the corneal surfaces of the right rabbit's eyes while the left eyes serve as controls with no treatment. IOP was measured immediately before instillation to serve as a baseline and everyone h after treatment for 8 h. ΔIOP (ocular antihypertensive activity) was expressed as the average difference of IOP between the treated and control eyes. The therapeutic profiles (ΔIOP versus time plots) of MTZ-PMs versus MTZ solution was used to calculate the following IOP response parameters, such as I_{max}, is the Maximal IOP response level (highest IOP reduction); T_{max} is the time required to achieve maximal IOP response level in hours; AUEC is the area under the effect versus time curve. (AUEC values from (t_0) to (t_{8h}) were calculated using the linear trapezoidal method).

2.14. Statistical analysis

All data were expressed as the mean of 3 replicates ± SD. The factorial design was analyzed using Design-Expert® v.8.0.7.1 (Stat-Ease, Inc., USA). The data obtained were compared using one-way analysis of variance (ANOVA) and the significance of the difference between formulations was calculated by Tukey-Kramer multiple comparisons using Graph Pad Instat® software (GraphPad Software, California). AUEC was calculated using GraphPad Prism (version 5.01; Graph Pad software Incorporated, California).

202 K. K. Bansal, J. Gupta, A. Rosling, J. M. Rosenholm, *Renewable poly (δ-decalactone) based block copolymer micelles as drug delivery vehicle: in vitro and in vivo evaluation, Saudi Pharm. J.,* **2018**, *26*, 358–368.

203 A. Zimmer, E. Mutschler, G. Lambrecht, D. Mayer, J. Kreuter, *Pharmacokinetic and pharmacodynamic aspects of an ophthalmic pilocarpine nanoparticle-deliverysystem, Pharm. Res.*, **1994**, *11*, 1435–1442.

3. Results and discussion

3.1. Preparation and characterization of MTZ-PMs

mPEG-PCL copolymers were successfully prepared and characterized, in order to obtain a well determined and specific structure as stated in our previous works.[204] The polymers used in the preparation of MTZ-PMs offer different molecular weights of 3, 4 and 5.5 kDa (**Table 1.**).

Polymer	NMR M_w (kDa)	GPC (Da)		
		Mn	M_w	PDI
A	3	3448	5182	1.5029
B	4	4742	8762	1.8478
C	5.5	5695	11096	1.9483

Table 1. Poymer Mw and PDI as estimated by nuclear magnetic resonance (NMR) and gel permeation chromatography (GPC).

Fig.S 1 and **Fig.S 2** show ^{1}H NMR spectrum of mPEG–PCL di-block copolymer in CDCL3, while illustrates GPC of mPEG–PCL di-block copolymers (refer to Supplementary Materials section). Considering their fabrication techniques, PMs were easily manufacturable using versatile procedures like solvent evaporation, film hydration, dialysis and direct dissolution.[205] Although all the aforementioned techniques avoid the use of surfactants and their toxicity-related issue, the drug loading efficiency of the micelles prepared by the two former methods is much higher compared to the two latter methods.[206] Therefore, in this study, thin film hydration technique was utilized for preparation of mPEG-PCL PMs.

mPEG-PCL PMs bearing the hydrophobic drug, MTZ, were formulated, owing to the self-assembling capability of the mPEG-PCL diblock copolymers. Optimization of the characteristics of the prepared PMs is depicted in Table 1. The impact of particle size (PS) in the nanorange on ocular tolerability and transmucosal permeation is well documented. Dynamic light scattering revealed that the average diameter of the PMs was maintained below 100 nm, ranging from 60.39 to 93.44 nm. The small obtained PS has attributed to the great aqueous solubility of the copolymer, resulting in decreasing the interfacial tension and the

204 D. R. Perinelli, G. Bonacucina, M. Cespi, A. Naylor, M. Whitaker, G. F. Palmieri, G. Giorgioni, L. Casettari, *Evaluation of P (L) LA-PEG-P (L) LA as processing aid for biodegradable particles from gas saturated solutions (PGSS) process, Int. J. Pharm.,* **2014**, *468*, 250–257.

205 R. D. Vaishya, V. Khurana, S. Patel, A. K. Mitra, *Controlled ocular drug delivery with nanomicelles. Wiley Interdiscip. Rev. Nanomed. Nanobiotechnol.,* **2014**, *6*, 422–437.

206 H. M. Aliabadi, A. Lavasanifar, *Polymeric micelles for drug delivery, Expert Opin. Drug Deliv*., **2006**, *3*, 139–162.

formation of small particles. The results revealed that increasing polymer Mw led to a positive significant increase in the produced particle diameters ($p < 0.0001$) with less contribution of D/P ratio factor (insignificant, p=0.3751). One possible explanation behind the increase in PS was the increase in PCL length that yielded simultaneously larger particles. Our results are in accordance with previous work reported by Shuai et al., and Ukawala et al.[207][208] Obviously, the maximum value of PS was obtained upon using mPEG-PCL copolymer of Mw 5.5 kDa and D/P ratio of 1:10 "PS value of NM9 = 93.44 nm" (**Table 2.**)

Formula code	Polymer (Mw)	D/P ratio	PS	PDI	EE%	ZP (m)V
NM1	3 kDa	1:5	72.53 ± 1.55	0.46 ± 0.08	64.43 ± 0.90	-2.42 ± 0.42
NM2	3 kDa	1:7:5	60.44 ± 5.02	0.55 ± 0.002	72.59 ± 1.72	-10.5 ± 1.73
NM3	3 kDa	1:10	60.39 ± 1.41	0.49 ± 0.011	93.91 ± 2.49	-9.27 ± 1.54
NM4	4 kDa	1:5	72.39 ± 12.80	0.18 ± 0.01	64. 34 ± 3.48	-7.87 ± 0.81
NM5	4 kDa	1:7:5	84.83 ± 1.74	0.28 ± 0.003	61.89 ± 1.64	-10.30 ± 0.89
NM6	4 kDa	1:10	79.68 ± 0.32	0.40 ± 0.032	77.35 ± 4.92	-10.30 ± 0.89
NM7	5.5 kDa	1:5	82.71 ± 11.05	0.36 ± 0.09	57. 05 ± 0.39	-8.26 ± 1.03
NM8	5.5 kDa	1:7:5	86.32 ± 11.05	0.27 ±0.01	65.08 ± 1.16	-13.00 ± 0.20
NM9	5.5 kDa	1:10	93.44 ± 2.47	0.37 ± 0.02	73.62 ± 2.36	-14.1 ± 1.10

Table 2. Effect of polymer molecular weight and drug to polymer ratio on the particle size, entrapment efficiency, and zeta potential of MTZ micelles.

Worthy to be stated that the micelles containing the lowest Mw copolymer (3 kDa) showed small variation in PS values with relatively lower values, ranged between 60.39 and 72.53 nm. It can be also noted that with exception of NM2 (PDI=0.55), the PDI values were acceptable (0.18–0.49).[209] Drug-loaded PMs possessed negative charge with ZP values fitted between −2.42 ± 0.42 and −14.1 ± 1.10 mV. The observed negative charge is contributed to ionized carboxyl groups of PCL segment, however, the low ZP values are assigned to the shielding effect offered by the neutral PEG shell.[210] Previous studies revealed that increasing the polymer Mw and D/P ratio was associated with increasing the negativity of ZP values, which may be attributed to the increase of hydrophobicity of the polymer as a function of the

207 X. Shuai, H. Ai, N. Nasongkla, S. Kim, J. Gao, *Micellar carriers based on block copolymers of poly (ε-caprolactone) and poly (ethylene glycol) for doxorubicin delivery, J. Control. Release*, **2004**, *98*, 415–426.

208 M. Ukawala, T. Rajyaguru, K. Chaudhari, A. Manjappa, S. Pimple, A. Babbar, R. Mathur, A. Mishra, R. Murthy, *Investigation on design of stable etoposide-loaded PEG-PCL micelles: effect of molecular weight of PEG-PCL diblock copolymer on the in vitro and in vivo performance of micelles, Drug Delivery*, **2012**, *19*, 155–167.

209 L. Wu, J. Zhang, W. Watanabe, *Physical and chemical stability of drug nanoparticles. Adv. Drug Deliv. Rev.,* **2011**, *63*, 456–469.

210 W. Xiong, L. Peng, H. Chen, Q. Li, *Surface modification of MPEG-b-PCL-based nanoparticles via oxidative self-polymerization of dopamine for malignant melanoma therapy, Int. J. Nanomed.*, **2015**, *10*, 2985.

molecular weight. The percent of MTZ entrapped within micelles was found to be in the range of 57.05–93.91%.

3.2. Factorial analysis and validation

The factorial design could be able to evaluate the importance of each factor with respect to the capability of micelles' to incorporate reasonable amounts of MTZ. Accordingly, the EE% response was optimized and chosen as response in the experimental design. Statistical analysis results are shown in **Table 3**.

Term	Coefficient	F-value
Intercept	63.39	-
A= Polymer Mw	-6.19	71.85*
B= D/P ratio	10.15	192.03*
AB	-2.96	11.08*
A^2	4.95	13.95*
B^2	4.65	13.52*
r^2	0.9356	
Adjusted r^2	0.9203	
Predicted r^2	0.8957	

Table 3. Statistical results for measures EE% response. *: significant.

The best-fitted model for the EE% was a quadratic model, being significant with a P value<0.0001. The combined influence of the independent variables on MTZ EE% exhibited fitting according to quadratic model according to the following equation:

E%= +122.90685 – 0.024788 * polymer Mw – 0.202523 * Polymer amount – 6.30573 E – 005 * polymer Mw * Polymer amount +3.16859 E – 006 * polymer Mw^2 + 3.30588 E – 003 * Polymer $amount^2$

The obtained desirable adequate precision (>4; 22.980) evidenced the capability of the high accuracy model for the EE% response to navigate the design space. The model was internally validated as reflected by the Box-Cox evaluation test (**Figure 2.**).

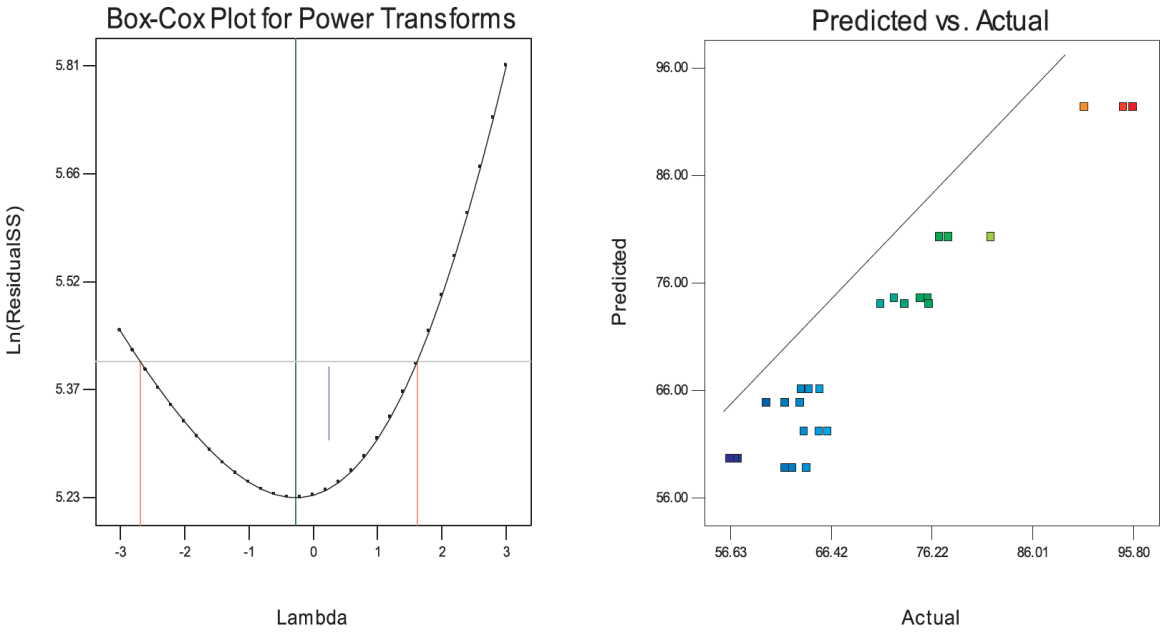

Figure 2. Box-Cox plots (left panel) and predicred vs. actual (right panel) for the entrapment efficiency response.

The Box-Cox plot for power transformation indicates that the model did not require any further transformation and was sufficient, showing the lambda value=1. Additionally, comparing quantitatively the experimental values of the EE% response with the predicted ones revealed the high correlation and fit between them, as shown in predicted versus actual values plot, confirming high predicted r2 values (**Table 3.**).

3.3. Dependence of MTZ entrapment efficiency on the independent variables

Concerning EE%, **Figure 3.**, D/P ratio factor exhibited the most powerful positive effect ($p < 0.0001$), where increasing drug to polymer ratio caused a significant increase in the percent drug entrapped within the micelles.

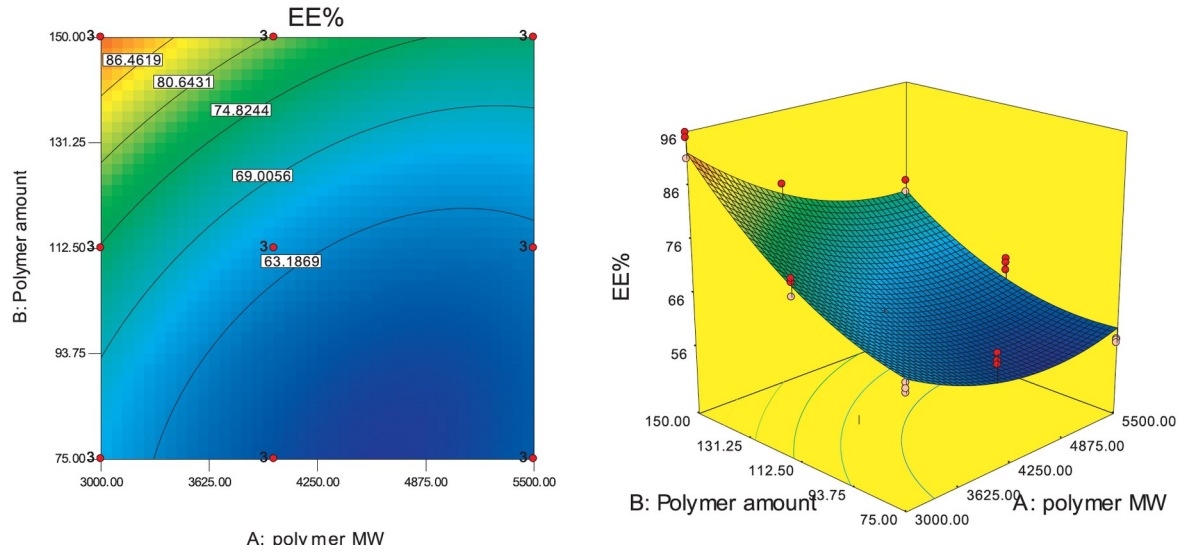

Figure 3. Contour plot and 3D response surface plot demonstrating the effect of variables. A) Polymer molecular weight; B) Drug to polymer ratio on MTZ EE%.

The rank order for EE% with respect to D/P ratio was revealed in this order 1:10 > 1:7.5 > 1:5. This could be attributed to the greater amount of copolymer available to accommodate more drug during micelles' formation and reduced drug distribution to the aqueous phase. Besides, the hydrophobic interactions between the drug and hydrophobic chains of the copolymer could be at the base of enhanced drug encapsulation as previously demonstrated by Shuai et al. Moreover, possible formation of hydrogen bonding between MTZ and mPEG-PCL copolymer might contribute to an increased percentage of drug entrapment "this will be addressed under FT-IR section".

Contrary, the polymer Mw and EE% of MTZ were negatively correlated ($p < 0.0001$). As depicted, increasing polymer Mw resulted in a significant reduction in %EE. Minimum EE% was achieved at the highest polymer Mw "5.5 kDa" using 1:5 D/P ratio (EE% value=57.05%). Increasing the polymer molecular weight is accompanied by two main effects; namely increasing the polymer chain length and the polymer crystallinity.[211] This could be explained as follows: increasing the PCL chains length results in the formation of a greater number of micelles with greater core and larger size accommodating more drug amounts, which permits higher drug encapsulation within nanoparticles matrices. Controversy, increasing the polymer crystallinity is associated with decreasing drug encapsulation as only the amorphous phase of PCL polymer is responsible for drug accommodation. In this work, increasing polymer crystallinity would have created the pronounced unfavorable condition or MTZ encapsulation.

211 S. M. D'addio, W. Saad, S. M. Ansell, J. J. Squiers, D. H. Adamson, M. Herrera-Alonso, A. R. Wohl, T. R. Hoye, C. W. Macosko, L. D. Mayer, *Effects of block copolymer properties on nanocarrier protection from in vivo clearance, J. Controlled Release*, **2012**, *162*, 208–217.

Most notably, the interaction between polymer Mw and D/P ratio exhibited a significant antagonistic effect on EE% (p=0.0032). A2 and B2 model terms were revealed to favor significantly EE% optimization (p=0012 and p=0.0014 respectively). Based on the previous findings, NM3 of optimum maximum EE% (93.91%) and lowest PS (60.39 nm) and the highest desirability ratio (DR=0.832) was selected for further investigations.

3.4. Morphology of the micelles

Figure 4 shows the TEM images of MTZ-PMs (NM3).

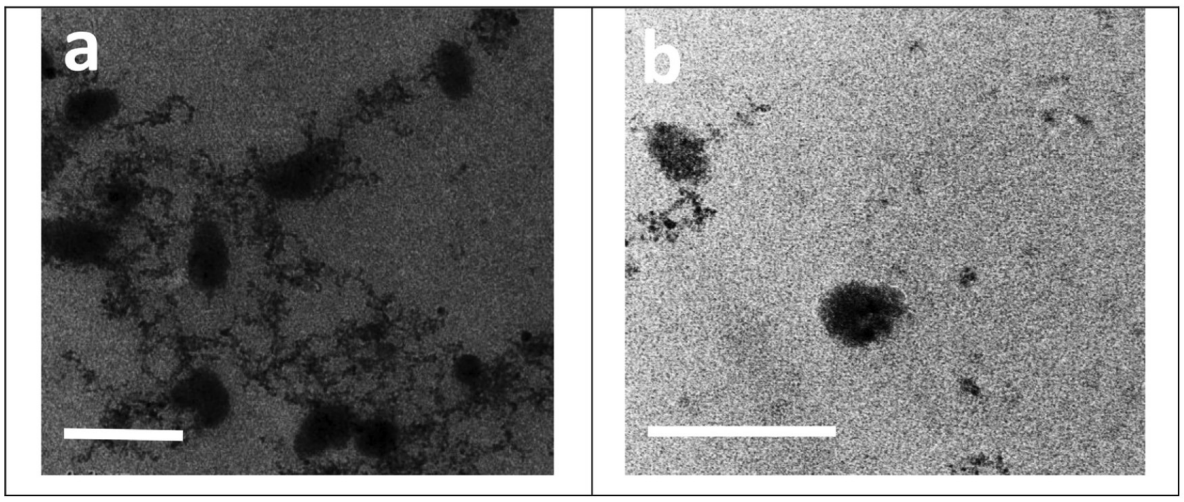

Figure 4. Trasmissin electron microscopy imaging of MTZ-PMs (NM3). Visualized under a voltage of 200 kV andmagnification X15000 (a) and X25000 (b) white bar 200 nm.

As revealed, PMs were spherical with a size of less than 100 nm as confirmed by particle size measurement using the dynamic light scattering technique. Previous studies have demonstrated the effectiveness of this nanoscopic particle size on improving the ocular bioavailability of drug loaded micelles.[212,213]

3.5. In vitro release study and release kinetics

Figure 5 shows the *in vitro* release study of MTZ from selected PMs (NM3).

212 S. Liu, L. Jones, F. X. Gu, *Nanomaterials for ocular drug delivery, Macromol. Biosci*., **2012**, *12*, 608–620.
213 A. K. Gupta, S. Madan, D. Majumdar, A. Maitra, *Ketorolac entrapped in polymeric micelles: preparation, characterisation and ocular anti-inflammatory studies, Int. J. Pharm*., **2000**, *209*, 1–14.

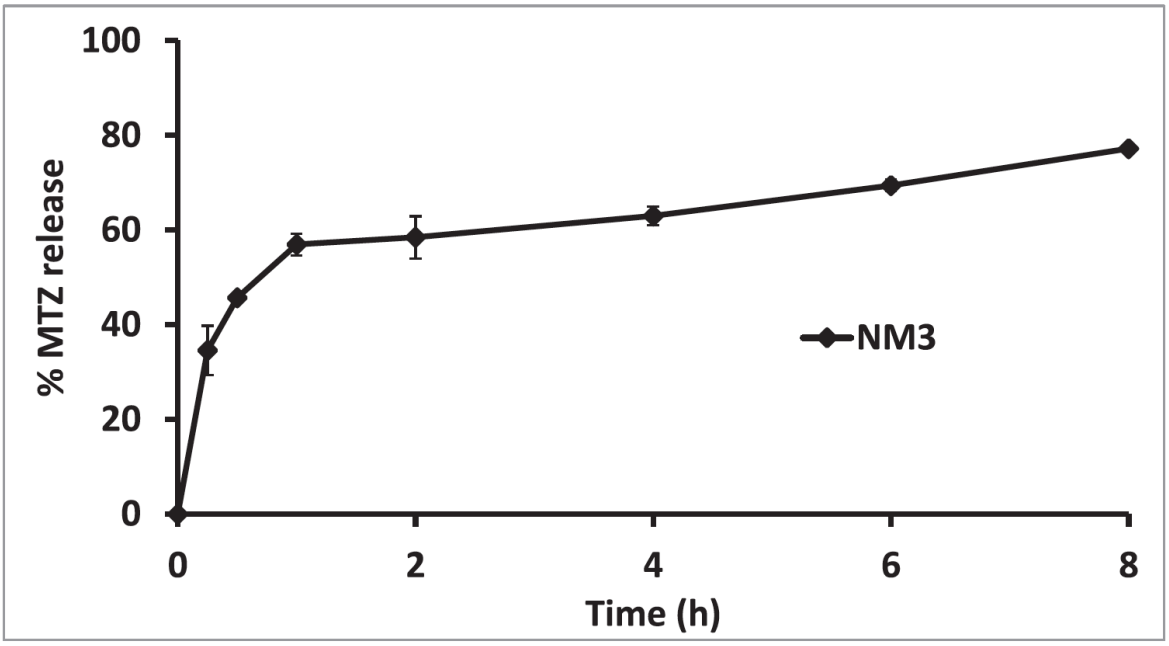

Figure 5. *In-vitro* release of MTZ-PMs (NM3) in simulated tear fluid at 37 °C.

As revealed, MTZ-PMs shows a biphasic release profile with an initial burst effect of more than 50% MTZ followed by a sustained drug release for 8 h. The initial burst effect is attributed to the easily desorbed drug from the surface of the particles.[214] Whereas, the slower drug release was guarded by drug diffusion from the core of the matrix and by the polymer degradation.[215,216] Such a two-stage release of PMs was previously well described.[217] In contrast, MTZ solution was completely released within 4 h (data not shown), indicating the capability of polymeric micelles of significantly sustaining MTZ release. Interestingly, previous studies investigated the importance of the initial rapid drug release to achieve a therapeutic effect in a short time followed by a sustained effect to maintain the effective drug concentration.[218] MTZ release from selected micelles (NM3) was best fitted by the Higuchi model with the highest linearity (r2=0.973). Similarly, fitting to Peppas model exhibited good linearity (r2=0.929) with values of 0.20 (Fickian), indicating diffusion controlled MTZ release.

3.6. DSC

214 C. Giovino, I. Ayensu, J. Tetteh, J. S. Boateng, *Development and characterisation of chitosan films impregnated with insulin loaded PEG-b-PLA nanoparticles (NPs): a potential approach for buccal delivery of macromolecules, Int. J. Pharm.,* **2012**, *428*, 143–151.

215 F. Danhier, N. Lecouturier, B. Vroman, C. Jérôme, J. Marchand-Brynaert, O. Feron, V. Préat, *Paclitaxel-loaded PEGylated PLGA-based nanoparticles: in vitro and in vivo evaluation, J. Control. Release*, **2009**, *133*, 11–17.

216 A. U. Shinde, P. N. Joshi, D. D. Jain, K. Singh, *Preparation and evaluation of N trimethyl chitosan nanoparticles of flurbiprofen for ocular delivery, Curr. Eye Res.,* **2019**.

217 A. K. Mohanty, U. Jana, U., P. K. Manna, G. P. Mohanta, Synthesis and evaluation of MePEG-PCL diblock copolymers: surface properties and controlled release behavior, Prog. Biomater., 2015, 4, 89–100.

218 X. Li, Z. Zhang, H. Chen, *Development and evaluation of fast forming nanocomposite hydrogel for ocular delivery of diclofenac, Int. J. Pharm*., **2013**, *448*, 96–100.

The thermal properties of the prepared lyophilized NM3, MTZ, mPEG-PCL copolymer and their physical mixture were studied using DSC as revealed in **Figure 6**.

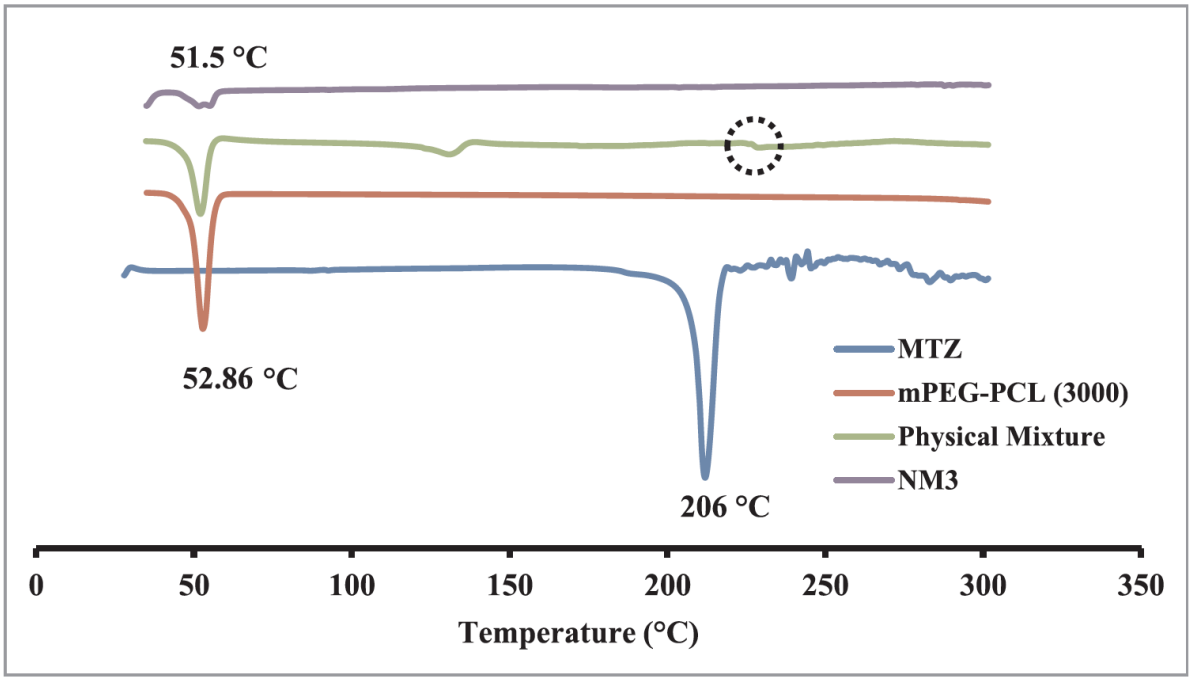

Figure 6. DSC thermograms of MTZ, mPEG-PCL copolymer mixture and MTZ-PMs (NM3).

MTZ shows a sharp endothermic peak at 206 °C corresponding to its melting point, while mPEG-PCL polymer shows an endothermic melting peak at 52.86 °C, indicating the crystalline nature of PCL (Mohanty et al., 2015). The physical mixture formed of the drug and the copolymer shows the same sharp peak of the copolymer and small drug peak. MTZ-PMs shows only a broad peak at 51.5 °C of the mPEG-PCL copolymer with the complete vanishing of MTZ peak, reflecting the possible interaction between the drug and the copolymer during PMs formation.

3.7. FT-IR

In order to reveal the possible interaction between MTZ and mPEG-PCL copolymer, FT-IR spectra were employed as shown in Fig. 6.

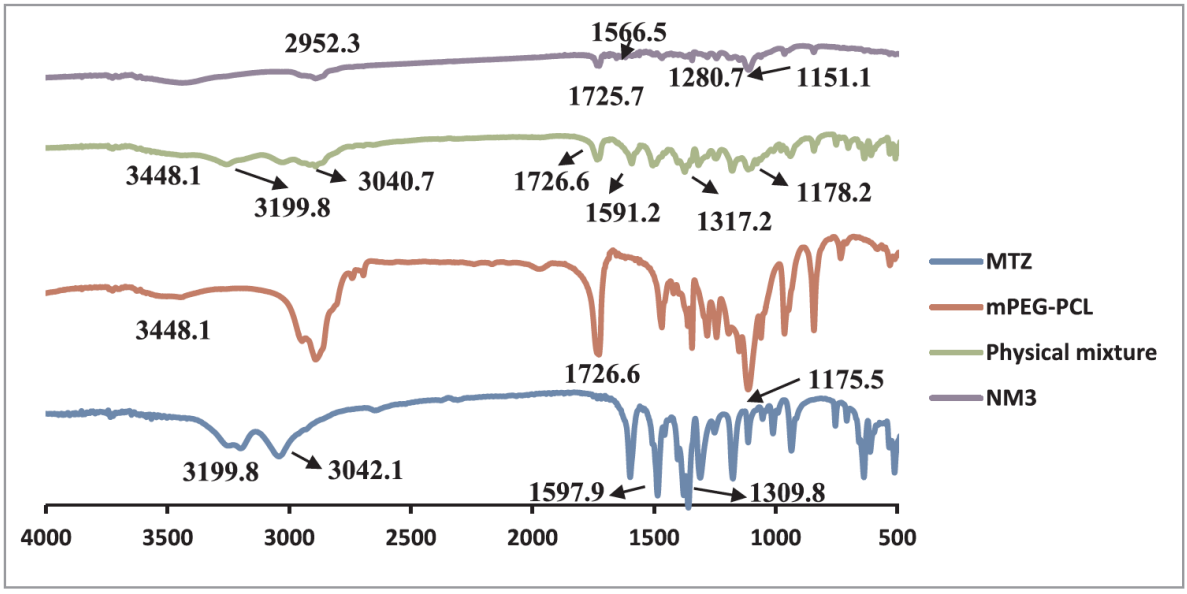

Figure 7. FT-IR spectra of MTZ, mPEG-PCL copolymer, physical mixture, and MTZ-PMs (NM3).

In generated spectrum for MTZ, the wide bands of 3199.89 and 3042.18 cm^{-1} were assigned to the N–H and C–H stretching vibrations respectively, the sharp bands around 1597.93 cm^{-1} to the C=O stretching vibration and the bands of both 1309.83 and 1175.57 cm^{-1} to the S=O stretching of the sulfonyl groups. Characteristic mPEG-PCL copolymer high-intensity signals at 1726.64 cm^{-1} for C=O vibrations, indicating the crystalline nature of the micelle core, and weak bands at 3448.17 cm^{-1} for O–H stretching vibrations. No recognizable changes were detected in the physical mixture between MTZ and mPEG-PCL copolymer that showed the superposition of N–H stretching vibration of MTZ and O–H stretching vibration of the mPEG-PCL copolymer. However, in the spectrum of MTZ-PMs, noticeable weak characteristic peaks of C=O and S=O stretching of MTZ as well hydrogen-bonded C=O vibrations of mPEG-PCL copolymer were observed with slight shifting. Such findings could indicate that, added to the hydrophobic interactions between MTZ and PCL block of the copolymer, the lower crystallinity of the copolymer and augmented hydrogen-bonding with MTZ in the formed micelles might have high implications on MTZ EE%.

3.8. Stability studies

A major concern with clinical ocular administration of colloidal dispersions was their physical stability, by virtue of their ability to retain their size and structure integrity. In this regard, the effect of short-term storage on the selected MTZ-PMs was monitored for 28 days at 4 °C. As observed in **Figure 8** (a), negligible variations in PS were recognized over 21 days compared to the initial results (0 day) ($p > 0.05$).

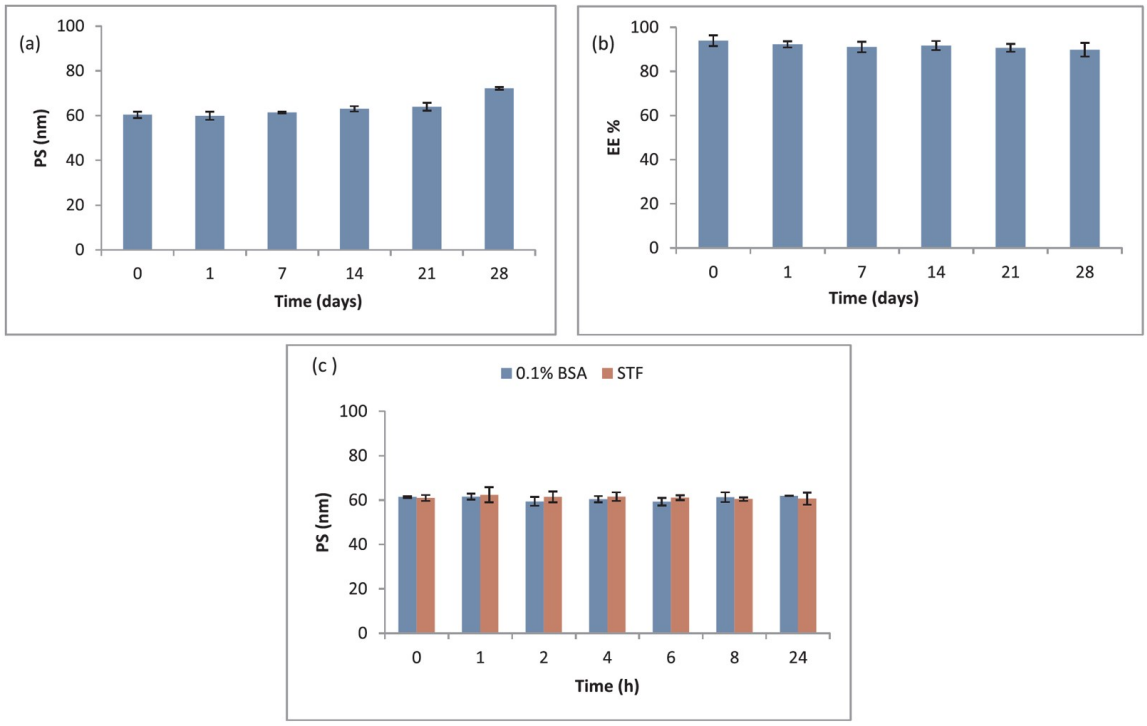

Figure 8. Variation in (a) PS, (b) EE% of the selected MTZ-PMs (NM3) as a fuction of incubation time (28 days) at 4 °C and (c) PS in the presence of 0.1% BSA and STF over 24 h at 37 °C.

However, a slight increase in PS, yet non-significant, was revealed at the end of storage period "28 days" ($p > 0.05$). This phenomenon could be due to the possible hydration with subsequent swelling of PEG chains.[219,220] Similarly, a slight non-significant decrease in EE% was observed ($p > 0.05$), reaching 89.82% at the end of the measurement period (**Figure 8** (b)). It is worthy to note that values of PDI (0.49–0.54) and ZP (-8.99-−9.63) exhibited no significant changes over 28 days ($p > 0.05$). The steric hindrance, imparted by the hydrophilic PEG coronal shell, could impede the aggregation of the micelles. This came in line with the previous literature.[221] Furthermore, to mimic the physiological protein containing eye environment, *in vitro* stability study of the selected micelles in the presence of 0.1% BSA and STF was conducted at 37 °C. The PS of micellar dispersions remained nearly unchanged after 24 h incubation ($p > 0.05$) (**Figure 8** (c)). These results confirmed the non-adherence of the micelles to the eye proteins, avoidance of removal by lacrimal fluids and extended corneal retention. This was consistent with previous findings.[222,223]

219 H. Danafar, A. Sharafi, H. Kheiri Manjili, S. Andalib, *Sulforaphane delivery using mPEG–PCL co-polymer nanoparticles to breast cancer cells, Pharm. Dev. Technol.*, **2017**, *22*, 642–651.

220 M. Zamani, A. Shirinzadeh, M. Aghajanzadeh, S. Andalib, H. Danafar, *In vivo study of mPEG–PCL as a nanocarriers for anti-inflammatory drug delivery of simvastatin, Pharm. Dev. Technol*., **2019**, 1–8.

221 D. Liu, Q. Wu, W. Chen, H. Lin, Y. Zhu, Y. Liu, H. F. Liang, F. Zhu, *A novel FK506 loaded nanomicelles consisting of amino-terminated poly (ethylene glycol)-blockpoly (D, L)-lactic acid and hydroxypropyl methylcellulose for ocular drug delivery,* **2019**.

222 Op. cit. *179*.

223 Op. cit. 208.

3.9. Suitability of MTZ-PMs for ocular delivery

3.9.1. Determination of pH

pH of formulations intended for ophthalmic delivery should be ranged from 5 to 7.4 in order to be tolerated by ocular surface.[224] The pH of the prepared MTZ-PMs was around the pH value of 5.52, depicting the non-irritancy, ocular comfort and subsequent therapeutic compliance of MTZ PMs following ocular instillation.

3.9.2. In vitro ocular cytocompatibility

MTT assay was employed to measure the viability of PCS700-010 cells after 24 h incubation of different concentrations of MTZ and NM3. As evident in **Figure 9**, benzalkonium chloride, the most commonly used preservative in eye drops, showed a highly pronounced cytotoxicity.

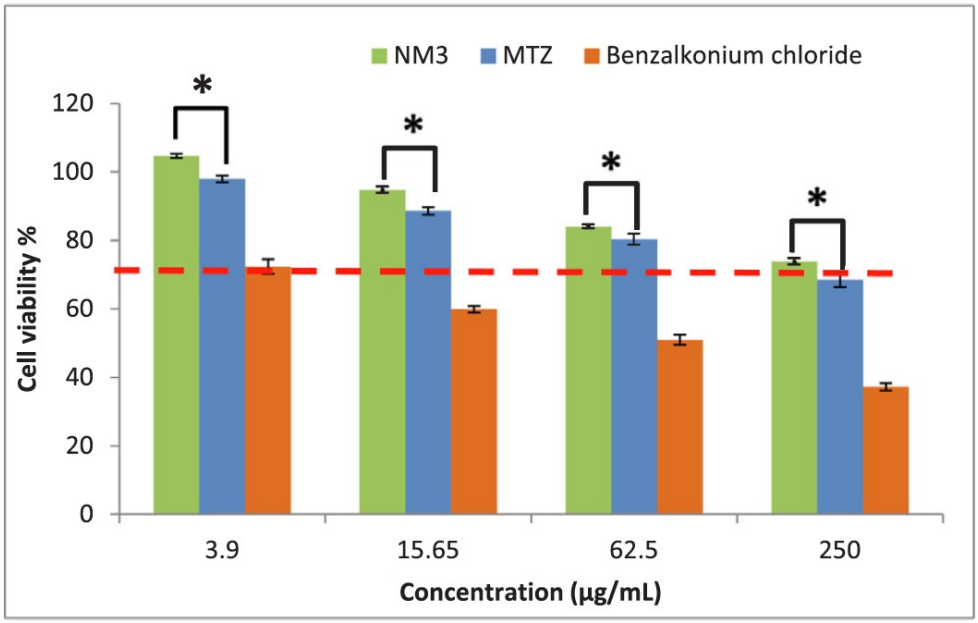

Figure 9. Percent cell viability of PCS700-010 after 24 h incubation with benzalkonium chloride, MTZ, and MTZ-PMs (NM3). The dashed line indicates 70% cell viability (* significant at $p < 0.05$).

Benzalkonium chloride was reported to be cytotoxic, causing considerable mitochondrial dysfunction in human corneal epithelial cells.[225;226] Furthermore, statistical difference in cell viability was noticed between MTZ-PMs (NM3) and MTZ at all the tested concentrations ($p <$

224 V. S. Panchal, R. N. Chilkwar, J. K. Saboji, S. M. Patil, B. K. Nanjwade, *Development and evaluation ophthalmic in situ gel of betaxolol HCl by temperature dependent method for treatment of glaucoma, J. Pharm. Sci. Pharmacol.,* **2015**, *2*, 21–25.

225 S. Datta, C. Baudouin, F. Brignole-Baudouin, A. Denoyer, G. A. Cortopassi, *The eye drop preservative benzalkonium chloride potently induces mitochondrial dysfunction and preferentially affects LHON mutant cells, Invest. Ophthalmol. Vis. Sci.,* **2017**, *58*, 2406–2412.

226 T. Y. Tsai, T. C. Chen, I. J. Wang, C. Y. Yeh, M. J. Su, R. H. Chen, T. H. Tsai, F. R. Hu, *The effect of resveratrol on protecting corneal epithelial cells from cytotoxicity caused by moxifloxacin and benzalkonium chloride, Invest. Ophthalmol. Vis. Sci.*, **2015**, *56*, 1575–1584.

0.05). Despite the dose-dependent reduction in cell viability up to 250 µg/mL (73.89% cell viability) noticed with MTZ-PMs (NM3), such values were above the acceptable minimum threshold for ocular cytotoxicity (70% cell viability), stated by the Occupational Safety and Health Administration (OSHA).[227,228] Worthy to note that MTZ showed slightly lower percentage cell viability, reaching 68.47% at the highest concentration (250 µg/mL). IC50% of the selected formula NM3 and MTZ was found to be 6513 and 3635.3 µg/mL respectively. This indicates that selected NM3 was physiologically tolerated and do not cause ocular cytotoxicity *in vivo* (IC50 > 100 µg/mL) (Ismail et al., 2006) when compared to the benzalkonium chloride which showed moderate cytotoxicity (IC_{50}=60.76 µg/mL).

3.9.3. In vitro hemocompatibility

The erythrocytes hemolysis assay has been utilized as a powerful predictive pre-screen test for the assessment of ocular irritancy of water soluble or water dispersible materials (e.g. surfactants).[229;230] Therefore, the hemolysis toxicity was investigated for the selected MTZ-PMs and the percent hemolysis induced by different concentrations of the tested micellar dispersion was compared as illustrated by Figure 10.

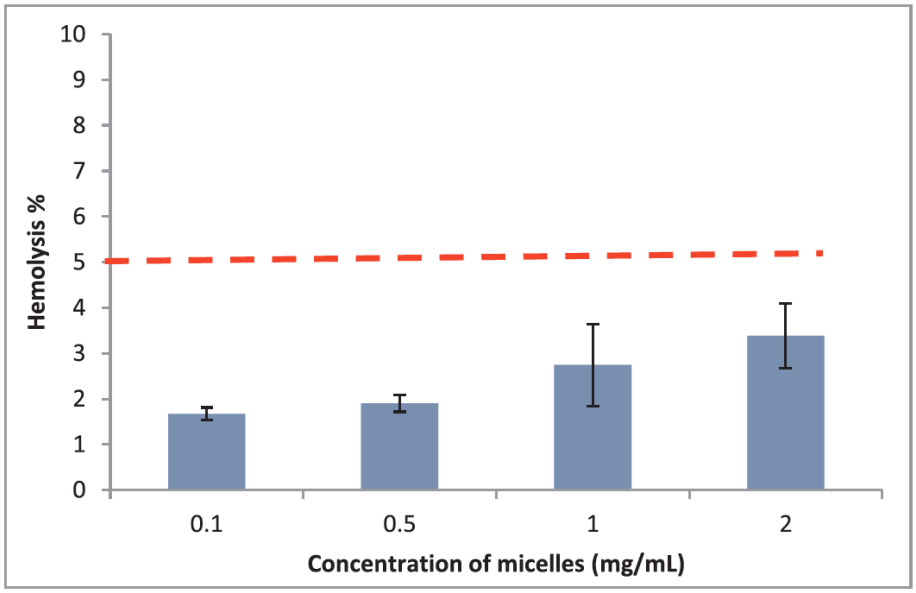

Figure 10. Percent hemolysis of MTZ-PMs (NM3) after 1 h incubation with erythrocyte. The dashed line indicates 5% hemolysis.

227 M. V. Fedorchak, I. P. Conner, J. S. Schuman, A. Cugini, S. R. Little, *Long term glaucoma drug delivery using a topically retained gel/microsphere eye drop, Sci. Rep.*, **2017**, *7*, 8639.

228 S. L. Wilson, M. Ahearne, A. Hopkinson, *An overview of current techniques for ocular toxicity testing, Toxicology* **2015**, *327*, 32–46.

229 R. Lewis, J. McCall, P. Botham, *A comparison of two cytotoxicity tests for predicting the ocular irritancy of surfactants, Toxicol. In Vitro,* **1993**, *7*, 155–158.

230 C. Lotz, F. F. Schmid, A. Rossi, S. Kurdyn, D. Kampik, B. De Wever, H. Walles, F. K. Groeber, *Alternative methods for the replacement of eye irritation testing, ALTEX-Alternat, Animal Experim.,* **2016**, *33*, 55–67.

The percent hemolysis was heightened as a function of increasing the micellar dispersion concentrations (0.1–2 mg/mL) in blood. However, the percent hemolysis was considered negligible, not exceeding the permissible reported threshold; 5% in all tested concentrations. These results proved the biocompatibility of the selected MTZ-PMs and lack of their eye irritant effect. These findings were similar to those previously reported for mPEG-PCL co-polymers and micelles.[231]

3.9.4. In vivo ocular tolerability

In vivo ocular irritation – The results of Draize test displayed good ocular tolerability of MTZ-PMs. Temporary mild conjunctival redness and swelling (+1) was noticed in the treated eye after 1 h. This transient ocular alteration might be due to the localization of high drug concentration on the ocular surface following instillation as previously reported.[232] No other signs of ocular damage or clinical abnormalities were detected in the cornea, iris, conjunctiva or pupil region.

Histopathological assessment of treated ocular tissues – There were no histopathological alterations and the normal histological structure of the covering epithelium of the cornea with the underlying lamellar stroma and the inner surface of the thin endothelium were recorded. No histopathological changes were also revealed in the other investigated ocular tissues (iris, retina or sclera) of the selected PMs (NM3) as shown in **Figure 11** when compared to the normal control.

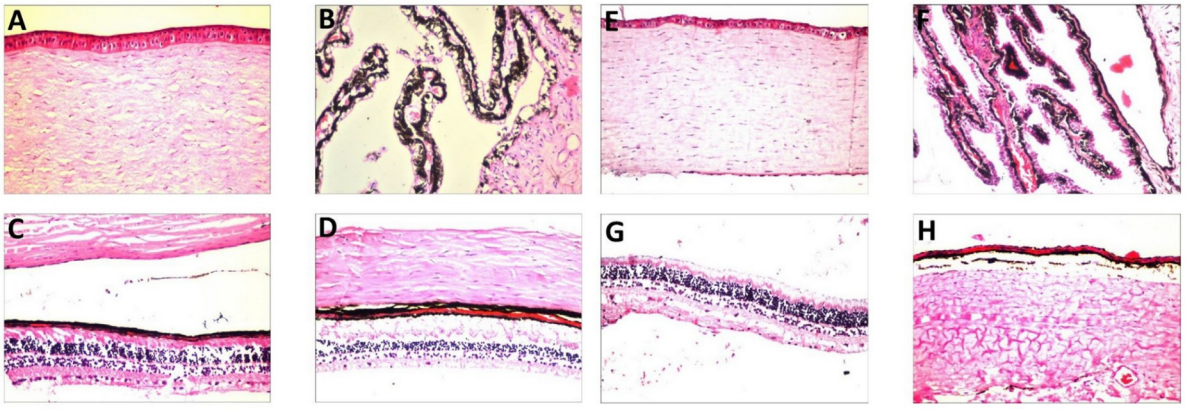

Figure 11. Histological examination of rabbit (A) Cornea, (B) Iris, (C) Retina and (D) Sclera of untreated control group and (E) Cornea, (F) Iris, (G) Retina and (H) Sclera of MTZ-PMs (NM3) treated group.

231 Q. Hu, Y. Zhang, C. Wang, J. Xu, J. Wu, Z. Liu, W. Xue, *Hemocompatibility evaluation in vitro of methoxy polyethyleneglycol–polycaprolactone copolymer solutions, J. Biomed. Mater. Res. Part A,* **2016**, *104*, 802–812.

232 M. M. Ibrahim, A. E. H. Abd-Elgawad, O. A. Soliman, M. M. Jablonski, *Novel topical ophthalmic formulations for management of glaucoma, Pharm. Res.*, **2013**, *30*, 2818–2831.

No edema, bleeding or inflammations were detected. This delineated the compatibility of the proposed PMs and confirmed the findings of MTT assay and Draize test.

In vivo pharmacodynamic study – Sub-conjunctival injection of betamethasone has successfully resulted in an artificial elevation of IOP in the glaucomatous eyes before treatment. **Figure 12** shows the reduction in the IOP of glaucomatous eyes upon instillation of selected formulation compared to that of MTZ solution while **Table 4** shows the IOP response parameters.

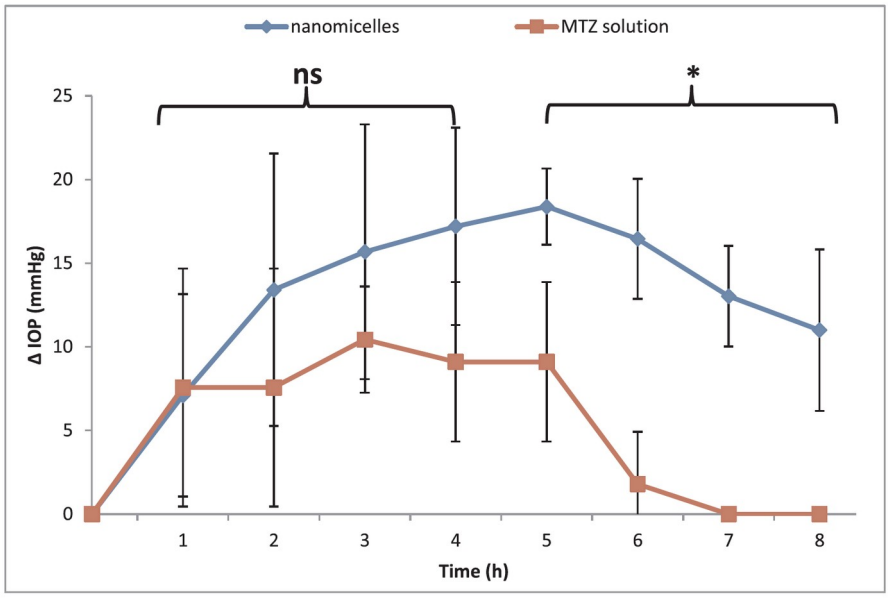

Figure 12. IOP Lowering effect of topical MTZ-Pms (NM3) compared to MTZ solution. (ns denotes points which are non-significant at p> 0.05 and * denotes data points which are significant at p< 0.05).

Formula	I_{max} (mmHg)	T_{max}	AUEC (mmHg.h)
MTZ solution	10.43 ± 3.17	3	
MTZ-PMs (NM3)	18.37 ± 2.27	5	106.7 ± 29.09

Table 4. IOP response parameters after ocular instillation of MTZ solution and MTZ-PMs (mean ± SD, n= 4).

A pronounced reduction in IOP was provoked for MTZ-PMs in contrast to the aqueous reference solution ($p < 0.05$). However, statistical insignificance in Δ IOP values was recognized at the first 4 h for both MTZ-PMs and MTZ solution ($p > 0.05$). This fast-initial pharmacological response of both MTZPMs and MTZ solution came in line with the *in vitro* release results that revealed complete drug release of MTZ solution and more than 50% release of MTZ-PMs within the first 4 h as mentioned above. After that, statistically higher lowering in IOP was observed for MTZ-PMS than for MTZ solution till the end of experiment

period ($p < 0.05$). The maximal response of MTZ solution (I_{max}=10.43 mmHg) occurred 3 h after instillation and lasted only for 6 h. On the other hand, the decrease in IOP of MTZ-PMs reached its peak (I_{max}=18.37 mmHg) at 5 h and continued over 8 h. These findings were confirmed by the statistically significant higher value of the area under the effect (decrease in IOP) time curve ($AUEC_{0–8h}$) parameter of MTZ-PMs compared to that of MTZ solution ($p < 0.05$). The enhanced IOP lowering effect and prolonged duration of action of MTZ entrapped in PMs could be ascribed to improved ocular penetration of the small-sized nanoparticulates and sustained release manner.[233] Nanoparticles were revealed to form a pre-corneal depot, provoking direct transport of drug from this depot to the site of action. Furthermore, previous studies demonstrated that the presence of PEG on micelles surface might exert augmented transport and permeation across the whole epithelium.

4. Conclusion

We suggest that the developed PMs can contribute to the ocular delivery of MTZ. The characterization of the prepared PMs and the results of release, *in vitro* MTT assay, hemocompatibility, Draize test, and *in vivo* histology experiments showed favorable nanosize, reasonable entrapment efficiency, sustained drug release, and superior ocular tolerability. Moreover, better *in vivo* inhibitory effect of MTZ-PMs was achieved compared to MTZ solution on glaucoma induction in experimental rabbits. Hence, these newly developed nanoformulations have characteristics which are appropriate for ocular nanodelivery.

233 J. Li, S. Tian, Q. Tao, Y. Zhao, R. Gui, F. Yang, L. Zang, Y. Chen, Q. Ping, D. Hou, *Montmorillonite/chitosan nanoparticles as a novel controlled-release topical ophthalmic delivery system for the treatment of glaucoma, Int. J. Nanomed.*, **2018**, *13*, 3975.

Supporting Information

Synthesis of block copolymers:

The mPEG-PCL di-block copolymers with different molecular weight (M_w) were synthesized using ring opening polymerization technique as previously described by our group. Briefly, in a magnetically stirred three-neck round bottom flask, mPEG 1.9 kDa was melted at 150°C under nitrogen atmosphere. The reaction was then carried out by adding accurately weighed amounts of PCL, and catalyst; stannous-2-ethyl-hexanoate, to the reaction flask at 150°C for specified time intervals. The resultant copolymers were dissolved using dichloromethane and collected by precipitation in cold diethyl ether. The obtained white powders were stored at 2-8˚C for further studies.

Characterization of block copolymers:

The chemical structure, M_w and PDI of the obtained mPEG-PCL di-block copolymers were elucidated using Proton nuclear magnetic resonance (^{1}H-NMR) and Gel permeation chromatography (GPC) (**Table 1**).

Proton nuclear magnetic resonance (^{1}H-NMR)

The ^{1}H-NMR spectra of the mPEG-PCL di-block copolymers were recorded, to elucidate the structure of the copolymers, using deuterated chloroform CDCl3 as solvent (Bruker AC 200 MHz spectrometer). Chemical shifts were reported in ppm using the internal reference; tetramethylsilane (Me_4Si). The chemical shift signals at 1.40, 1.64, 2.28 and 4.04 ppm were assigned to the β-methine (CH) proton, γ and δ-methine (CH) proton, α- methine (CH) proton, and ε-methine (CH) proton in PCL blocks respectively. The sharp characteristic peak of PEG was observed at 3.65 ppm (**Fig.S 1** and **Fig.S 2**).

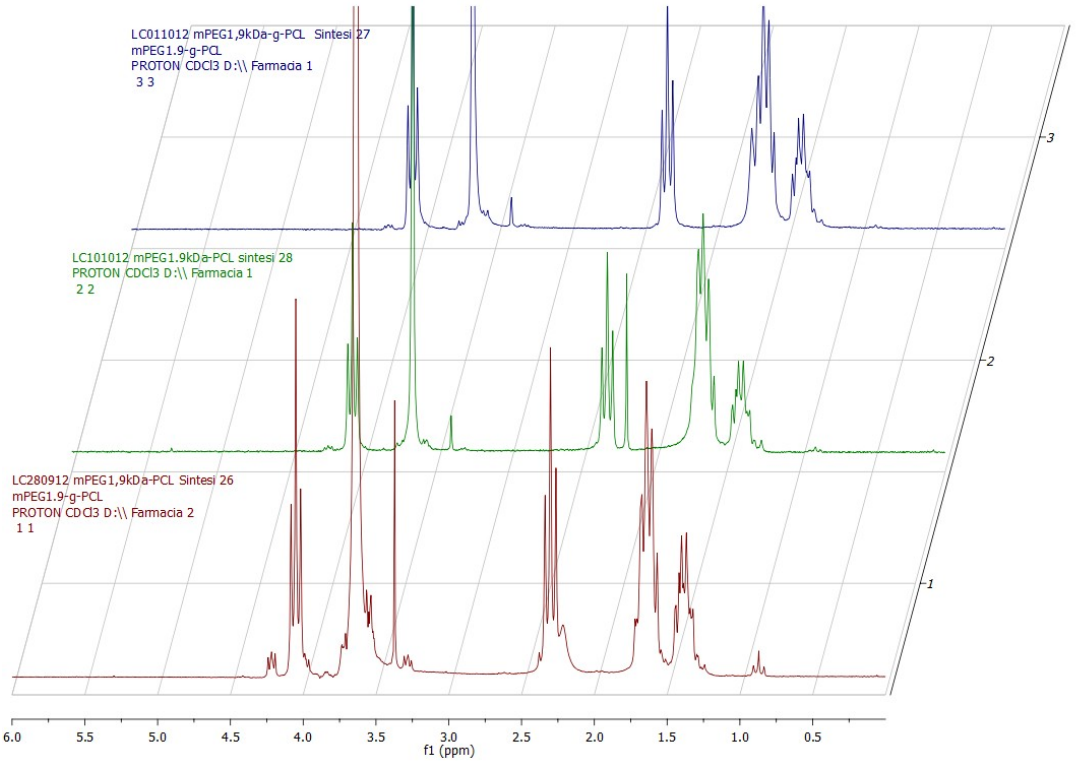

Fig.S 1. ^{1}H-NMR spectra of different diblock copolymers

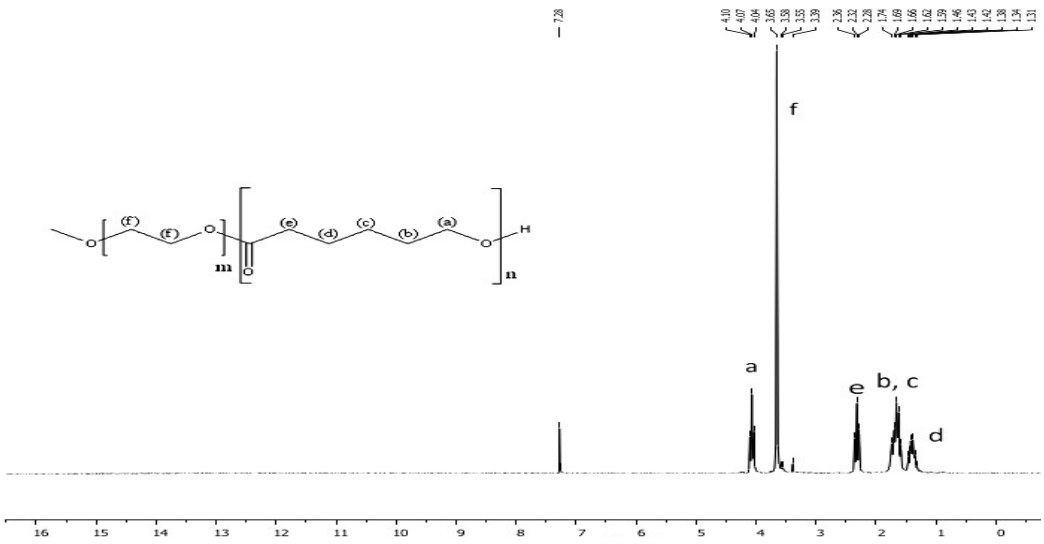

Fig.S 2 ^{1}H-NMR spectra of mPEG_PCL di-block copolymer in $CDCl_3$

Gel permeation chromatography (GPC)

7.5 mgs of the polymer was dissolved into 1.5 mL chloroform (HPLC grade). The solution was then filtered through 0.45 µm pore size syringe filter (regenerated cellulose) then 7.5 µL of acetonitrile were added to different samples as flow marker. GPC analysis was carried out utilizing HP HPLC system using tetrahydrofuran (THF) as an eluent and gel permeation

column (G2500HHR from Tosoh Bioscience, Tokyo, Japan) at 35°C at flow rate of 1 mL/min. A standard calibration curve was constructed using a Polyethylene Glycol standards with molecular weight ranging from 106 to 21,300 then data were analyzed utilizing Clarity software (DataApex).

As observed in , the symmetric GPC curves indicated the low PDI of the mPEG-PCL di-block copolymers.

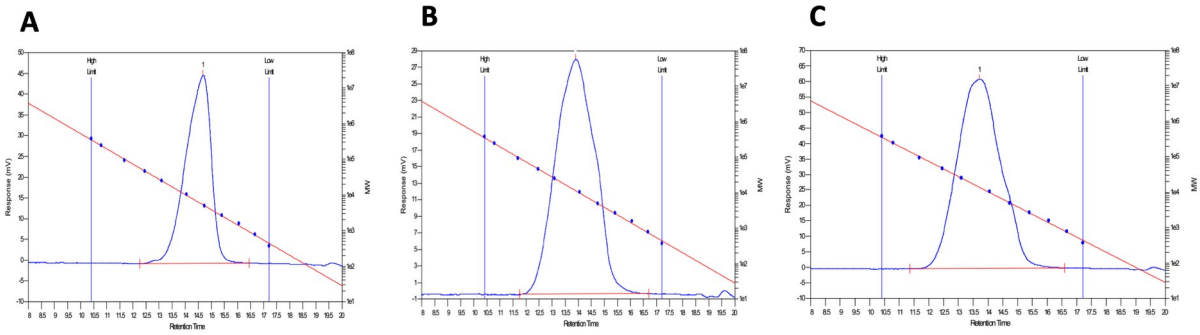

Fig.S 3. GPC of mPEG-PCL di-block copolymers. A)3 kDa, B) 4kDa, and c) 5.5 kDa

SECTION II

PHOSPHOLIPID NANOPARTICLE IN DRUG DELIVERY

1. Introduction

The development of highly selective and effective nanoparticles for drug delivery has brought new hope for the treatment of various diseases such as cancer, cardiovascular diseases, diabetes, bacterial infection and so on.[234,235] Previously, we discuss the importance of nanoparticle in drug delivery. In particular, therapeutic nanoparticle can improve the solubility of poorly water-soluble drugs, prolong half-life of drugs in the systemic circulation by reducing immunogenicity, release drugs at a sustained rate and thus lower the frequency of administration, deliver drugs in a targeted manner to minimize systemic side effect and deliver two or more active agents simultaneously for combination therapy to generate synergistic effects.[236] Based on this, nanosize drug delivery systems generally focus on formulating bioactive molecules in biocompatible nanosystems, such as nanocristals, solid lipid nanoparticles, polymeric NPs, nanostructure lipid carriers, lipid drug conjugates, liposomes and so forth.[237]

Bangham and co-workers, in the early 60s, were the first to describe liposomes as spherical vesicles consisting of one or more phospholipid bilayers. These lipid vesicles were, at the beginning, called "*smectic mesophases*".[238] Later, a colleague of Bangham, termed them "liposomes".[239] Since the 1990s, liposome formulation has been largely developed for pharmaceutical purposes and they were recognized as promising candidates for Drug Delivery.[240,241] In general, liposomes are self-assembled spherical vesicles, that consist of an aqueous core domain entrapped by one or more lipid bilayers.[242] The hydrophilic/hydrophobic

234 L. Brannon-Peppas, J. O. Blanchette, *Nanoparticle and targeted systems for cancer therapy, Adv. Drug Deliv. Rev*., **2004**, *56*(11), 1649-1659.
235 D. Peer, J. M. Karp, S. Hong, O. C. Farokhzad, R. Margalit, R. Langer, *Nanocarriers as an emerging platform for cancer therapy, Nat. Nanotechnol*., **2007**, *2*, 751-760.
236 S. Ji, J. Y. Walz, *Synergistic effects of nanoparticles and polymers on depletion and structural interaction, Langmuir*, **2013**, *29*(49), 15159-15167.
237 B. Mukherjee, *Nanosize drug delivery system, Curr. Pharm. Biotechnol*., **2013**, *14*(15), 1221.
238 A. D. Bangham, *Lipid bilayers and biomembranes, Annual Rev. of Biochem*., **1972**, *41*, 753-776.
239 G. Sessa, G. Weissmann, *Phospholipid spherules (liposomes) as a model for biological membranes, J. of Lipid Research*, **1968**, *9*(3), 310-318.
240 G. Gregoriadis, P. D. Leathwood, B. E. Ryman, *Enzyme entrapment in liposomes, FEBS Letters*, **1971**, *14*(2), 95-99.
241 Y. E. Rahman, M. W. Rosenthal, E. A. Cerny, E. S. Moretti, *Preparation and prolonged tissue retention of liposome encapsulated chelating agents, J. of Laboratory and Clinical Medicine*, **1974**, *83*(4), 640-647.
242 A. Sharma, U. S. Sharma, *Liposomes in drug delivery: progress and limitations*, *Int. J. Pharm.*, **1997**, *154*, 123-140.

interaction between lipid/lipid and lipid/water molecules, results in the formation of liposomes.[243]

In particular, in the aqueous medium, lipids arrange themselves as a bilayer sheets, with the hydrophilic headgroup of the lipid facing the water phase, while the hydrophobic hydrocarbon chains are forced to face each other. In this system, the liposomes formation occurs.[244] Liposomes have been widely studied and used to deliver both hydrophilic and hydrophobic drugs in the past decades.[245] Doxil was the first liposome drug formulation approved by Food and Drug Administration (FDA) for the treatment of AIDS associated with Kaposi's sarcoma in 1995.[246] Other liposomal drug formulation that are also commercially available include daunorubicin liposomes, morphine liposomes, verteporfin liposomes, cytarabine in liposomes and amphotericine B liposome.[247,248]

To understand the importance of liposome formulation in this ***Section II*** we analyse how the efficacy of liposomes depends on the nature of their components and their size, surface charge and lipidic organization. Moreover, we describe some strategies to develop these phospholipid-nanoparticles. Besides, in the previous section we discussed how biodegradable polymeric nanocarriers have shown great therapeutic potential as a drug delivery nanocarrier. Based on this, the ultimate goal is to obtain an hybrid/mixed/chimeric liposome formulations which exhibits the best properties of polymeric nanoparticles and liposome formulation. In the present study, the synthetic block copolymer polyethylene glycol-co-poly(delta-decalactone) ($mPEG_x$-PDL_y) was incorporated into 1,2-dipalmitoil-sn-glycore-3-phosphocholine (DPPC) and 1,2-diasteroyl-sn-glycero-3-phosphocholine (DSPC) lipid bilayers. These systems were fully characterized, and the experimental methods of their *in vitro* behaviours have been extensively analysed.

2. Synthesis and physico-chemical characteristics of liposome formulation

Since their discovery, liposomes have been subject to extensive evolution, in terms of composition, manufacturing and application, which led to several openings in several cosmetics, food and pharmaceutical fields. Prior work involved liposomes made from certain

243 A. Jesorka, O. Owark, *Liposomes: technologies and analytical applications, Annu. Rev. Anal. Chem*., **2008**, *1*, 801-832.
244 M. R. Mozafari, *Liposomes: an overview of manufacturing techniques, Cell. Mol. Biol. Lett.*, **2005**, *10*, 711-719.
245 V. P. Torchilin, *Recent advances with liposomes as pharmaceutical carriers, Nat. Rev. Drug Discov.*, **2005**, *4*, 145-160.
246 D. Wagner, W. V. Kern, P. Kern, *Liposomal doxorubicin in AIDS-related Kaposi's sarcoma: long term experiences, Clin. Invest*., **1994**, *72*, 417-423.
247 L. Zhang, F. X. Gu, J. M. Chan, A. Z. Wang, R. S. Langer, O. C. Farokhazad, *Nanoparticles in medicine: therapeutic application and developments, Cli. Pharmacol. Ther.*, **2008**, *83*, 761-769.
248 M. Ferrari, *Cancer nanotechnology: opportunities and challenges, Nat. Rev. Cancer,* **2005**, *5*, 161-171

phospholipids in the context of understanding biomembrane functions of human cell.[249] Based on this, liposomes are made of natural or synthetic phospholipids.[250]

Various kind of phospholipids whit different chemical structures are found in the natural word.[251] Phospholipids play a fundamental role with their unique properties of being amphiphilic and their self-assembly to encapsulate therapeutic agents which can then be targeted to specific site. These molecules consist of a diglycerides, a phosphate group and an organic molecule, such as choline. A diglyceride is composed of two fatty acid chains that are covalently bound to a single glycerol molecule via an ester linkage. Glycerol is responsible for the solubility of phospholipids in water and acts as a backbone by its attachment to both fatty acids chains and a phosphate group.[252] Fatty acid molecules are either saturated or unsaturated and are insoluble in water.[253] Thus, phospholipids is composed of hydrophobic moiety comprising two fatty acid chains and a hydrophilic head made of glycerol and phosphate. The bilayer structure is formed when the fatty acid moiety of the one layer faces the fatty acid moiety of another layer and the head groups face the water.

Phospholipids are either natural or synthetic. Naturally occurring phospholipids include phosphatidylcholine (PC), soya phosphatidylcholine (SPC) and egg phosphatidylcholine (EPC), etc. The synthetic phospholipids include dipalmitoyl phosphatidylcholine (DPPC), dimyrestoyl phosphatidylcholine (DMPC), 1,2-dioleoylphosphatidylcholine (DOPC), 1,2-disteroylphosphatidylcholine (DSPC) and so forth.[254] Because of their peculiar characteristics, phospholipids are used as emulsifier, wetting agent, solubilizer and liposome former.[255,256] The relative ease in incorporating hydrophilic (in the aqueous core) and lipophilic (in the lipid bylayer) therapeutic agents in liposomes; the properties of liposomes to protect therapeutic agents from inactivation and enzymatic degradation; the possibility of directly delivering liposomes to a specific and an accessible body site, and the relative non-immunogenicity and low toxicity of liposomes, and their capability to increase the pharmacological activity of

249 R. Pignatello, T. Musumeci, L. Basile, C. Carbone, G. Puglisi, *Biomembrane models and drug-biomembrane interaction studies: Involvement in drug design and development, J. Pharm. Bioallied. Sci*., **2011**, *3*(1), 4-14.

250 J. Li, X. Wang, T. Zhang, C. Wang, Z. Huang, X. Luo, Y. Deng, *A review on phospholipids and their main application in drug delivery systems, Asian Journal of Pharmaceutical Sciences*, **2014**, *10*(2), 81-98.

251 S. Mashaghi, T. Jadidi, G. Koenderink, A. Mashaghi, Lipid nanotechnology, *Int. J. Mol. Sci*., **2013**, *14*(2), 4242-4282.

252 S. Vemuri, C. T. Rhodes, *Preparation and characterization of liposomes as a therapeutic delivery systems: a review, Pharmaceutica Acta Helvetiae*, **1995**, *70*, 95-111.

253 L.Zelles, *Fatty acid patterns of phospholipids and lipopolysaccharides in the characterisation of microbial communities in soil: a review, Biology and fertility of soils*, **1999**, *29*(2), 111-129.

254 P. Van Hoogevest, A. Wendel, *The use of natural and synthetic phospholipids as pharmaceutical excipients, Eur. J. Lipid Sci. Technol.*, **2014**, *116*(9), 1088-1107.

255 G. Fricker, T. Kromp, A. Wendel, A. Blume, et al., *Phospholipids and lipid-based formulations in oral. Drug delivery, Pharm. Res.*, **2010**, *27*, 1469-1486.

256 P. van Hoogevest, X. Liu, A. Fahr, M. L. S. Leigh, *Role of phospholipids in the poral and parenteral delivery of poorly water soluble drugs, J. Drug Deliv. Sci. Technol*., **2011**, *21*, 5-33.

drugs which subsequently decrease the dosage of drugs, have rendered the liposomal system highly attractive for drug delivery.[257,258,259,260]

Liposomes have particle size ranging from 30 nm to several micrometers, and they can be classified according to their number of bilayer membranes. We find small unilamellar vesicle (SUVs) with size range 0.02 μm to 0.2 μm, large unilamellar vesicles (LUVs) (0.2 μm to 1 μm), giant unilamellar vesicles (GUVs) (>1μm), multilamellar vesicles (MLVs) (>0.1 μm), and oligolamellar vesicles (OLV) (100-1000 nm). In literature, there are several techniques that can be used in the liposome's preparation. These are divided into three categories: mechanical procedures, methods based on replacement of organic solvents by aqueous media, and procedures based on detergent removal.[261]

Mechanical methods include 1) vortex or hand shaking of phospholipid dispersions;[262] 2) extrusion through polycarbonate filters at low or medium pressure or through a French press cell, called microfluidizer technique;[263,264] 3) high-pressure homogenization (HPH) that offers rapid reduction of vesicle size and lamellarity to achieve SUVs whilst narrowing the distribution;[265] 4) sonication, or exposure to ultrasounds, is used to manufacture SUVs of minimal size;[266] and 5) Bubbling of gas to obtain bubblesomesa (BSV).[267]

The procedures, to obtain liposomes, based on replacement of organic solvents by aqueous media are 1) thin-film hydration method, where a dried film is hydrated in an aqueous buffer solution, at a temperature above the transition temperature of the lipids. With this technique originates MLVs eith high heterogeneity in size, size distribution and lamellarity;[268] 2) use of water-immiscible solvents such as ether and petroleum, which allows to obtain MLVs, OLVs

257 A. A. Date, M. D. Joshi, V. B. Patravale, *Parasitic disease: liposomes and polymeric nanoparticles versus lipid nanoparticles, Adv. Drug Deliv. Rev*., **2007**, *59*, 505-521.

258 T. M. Allen, *Liposomal drug formulations. Rationale for development and what can we expect for the future, Drugs,* **1998**, *56*, 747-756.

259 G. Gregoriadis, *Overview of liposomes, J. Antimicrob. Chemother*., 1991, *28*, 39-48.

260 G. Gregoriadis, *Engineering liposomes for drug delivery: progress and problems, Trends Biotechnol*., **1995**, *13*, 527-537.

261 D. Lasic, Y. Barenholz, Handbook of Nonmedical Applications of Liposomes, CRC-Press, New York, NY, USA, **1996**, *3*, chap. 3.

262 C. Dwivedi, S. Verma, *Review on preparation and characterization of liposomes with application, J. of Sci. and Innov. Res*., **2013**, *2*(2), 486-508.

263 L. D. Mayer, M. J. Hope, P. R. Cullis, *Vesicles of variable size produced by a rapid extrusion procedure, Biochimica et Biophysica Acta*. **1986**, *858*, 161-168.

264 G. J. Vanderheiden, A. C. Fairchild, G. R. Jago, *Constrution of a laboratory press for use with the French pressure cell, Appl. Microbiol*., **1970**, *19*(5), 875-877.

265 A. K. Kundu, S. Hazari, D. D. Chinta, Y. V. Pramar, S. Dash, T. K. Mandal, *Development of nanosomes using high-pressure homogenization for gene therapy*, **2010**, *62*(9), 1103-1111.

266 D. D. Lasic, Application of Liposomes, *B. V. Handbook of Biological Physics, Elsevier*, **1995**, *1*.

267 Md. M. Hasan, M. Hasan, J. C. Mondal, M. A. Hasan, S. Talukder, H. A. Rashid, *Liposomes: an advance tools for drug delivery system, The Pharma Innovation Journal,* **2017**, *6*(11), 304-311.

268 A. D. Bangham, M. M. Standish, J. C. Watkins, *Diffusion of univalent ions across the lamellae of swollen phospholipids, J. of Molecular Biol*ogy, **1965**, *13*(1), 238-252.

and LUVs; 3) Ethanol injection method, its main relevance resides in the observation that a narrow distribution of small liposomes, with size under 100 nm, can be obtained by simply injecting an ethanolic lipid solution in water, in one step, without extrusion or sonication;[269] 4) Infusion methods, called also solvent vaporization, the lipid dissolved in the immiscible organic solvent, such as ether, which is injected very slow into an aqueous solution at a temperature high enough for rapid evaporation of the solvent. The ether vaporizes upon contacting the aqueous phase, and the dispersed lipid forms primarily unilamellar liposomes.[270]

Another procedure, based on replacement of organic solvents for the liposome preparation, is the 5) reverse-phase evaporation. In this technique a lipidic film is prepared by evaporating organic solvent under reduced pressure. The system is purged with nitrogen and the lipids are re-dissolved in a second organic phase which is usually constituted by diethy ether and/or isopropyl ether. Large unilamellar and OLVs are formed when an aqueous buffer is introduced into this mixture. Then the organic solvent is subsequently removed, and the system is maintained under continuous nitrogen flow.[271] At the end the procedures based detergent removal to manufacture liposomes are, for example, gel-exclusion chromatography for investigation of encapsulation, insertion/interaction of substances from small solutes, such as ions, surfactants and drug, up to large molecules, as well as proteins, peptides and nucleic acids, in liposomes. This method involves the use of beads that have tiny tunnels in them that each have a precise size. The size is referred to as an exclusion limit, which that molecules above a certain molecular weight will not fit into the tunnels.

Molecules with sizes larger than the exclusion limit do not enter the tunnels and pass through the column relatively quickly by making their way between the beads. Smaller molecules, which can enter the tunnels, do so, and thus, have a longer path that they take in passing through the column. Because of this, molecules larger than the exclusion limit will leave the column earlier, while those that pass through the beads will elute from the column later. This method allows separation of molecules by their size and can be obtained SUVs liposomes.[272] Detergent dialysis, is another technique, where liposomes in the size range of 40-80 nm, are

269 P. Stano, S. Bufali, C. Pisano, F. Bucci, M. Barbarino, M. Santaniello, P. Carminanti, P. L. Luisi, *Novel camptothecin analogue (gimatecan)-containing liposomes prepared by ethanol injection method, J. Liposome Res*. **2004**, *14*(1-2). 87-109.

270 D. Deamer, A. D. Bangham, *Large volume liposomes by an ether vaporization method, Biochim. Biophys. Acta*., **1976**, *443*(3), 629-634.

271 R. Cortesi, *Preparation of liposomes by reverse-phase evaporation using alternative organic solvents, J. of Microencapsulation, Micro and Nano Carriers*, **1999**, *16*(2), 251-256.

272 G. C. Madelmont, S. Lesieur, M. Ollivon, *Characterization of loaded liposomes by size exclusion chromatography, J. Biochem. Biophys. Methods*, **2003**, *56*(1-3), 180-217.

formed when lipids are solubilized with detergent, yielding defined micelles. Subsequently, the detergent is removed by controlled membrane dialysis, phospholipids from homogeneous unilamellar vesicles with usefully large encapsulated volume.[273]

Furthermore, since industrial scale production of liposomes has become reality, the range of liposome preparation methods has been extended by an high number of techniques, such as heating method, spray drying, freeze drying, super critical reverse phase evaporation (SCRPE) and several modified ethanol injection procedures which are increasingly attractive in the field of nanotechnology.[274,275,276] The choice of liposome preparation method depends on the physicochemical characteristics of the material to be entrapped and those of the liposomal ingredients; the nature of the medium in which the lipid vesicles are dispersed; the effective concentration of the encapsulated substance and its potential toxicity; additional process involved during application/delivery of the liposomes. Furthermore, they should have an optimum size, polydispersity index and shelf-life for the intended application and batch-to-batch reproducibility and possibility of large-scale production of safe and efficient liposomal products.[277,278]

Although liposomes have shown some success in drug product development, the most common disadvantages of these nanocarriers arise partly from poor stability oxidation and hydrolysis, leakage and loss of hydrophilic cargoes, as well as a rapid elimination from blood by RES. Mozafari et al., discussed in their work, that these kinds of systems may have drawbacks due to toxicities related to product development procedures. Moreover, low pH conditions and the presence of digestive enzymes, such as lipases, these lipidic carriers cannot generally pass intact to the lower gastrointestinal tract.[279] In relation to these issues, to overcome these problems, some strategies have been explored to improve the use of liposomes for drug delivery. For example, antibodies, generally of the IgG class, can be attached by covalent binding to phospholipids, in order to increase a desired bioaccumulation

273 K. Adamala, A. E. Engelhart, N. P. Kamat, L. Jin, J. W. Szastak, *Construction of liposome dialyzer for preparation of high value, small-volume liposome formulations, Nat. Protoc*., **2015**, *10*(6), 927-938.

274 N. Skalko-Basnet, Z. Pavelic, M. Becirevic-Lacan, *Liposomes containing drug and cyclodextrin prepared by one-step spray-drying method, Drug. Dev. Ind. Pharm.*, **2000**, *26*(12), 1279-1284.

275 K. Otake, T. Imura, H. Sakai, M. Abe, *Development of a new preparation method of liposomes using supercritical carbon dioxide, Langmuir*, **2001**, *17*, 3898-3901.

276 A. Wagner, K. Vorauer-Uhl, H. Katinger, *Liposomes produced in a pilot scale: production, purification and efficiency aspects, Eur. J. Pharm. Biopharm*., **2002**, *54*(2), 213-219.

277 A. Gomezhens, J. Fernandezromero, *Analytical methods for the control of liposomal delivery systems, Trends in Analytical Chem*., **2006**, *25*(2), 167-178.

278 M. R. Mozafari, C. Johnson, S. Hatziantoniu, C. Demetzos, *Nanoliposomes and their applications in food nanotechnology, J. of Liposome Res*., **2008**, *18*(4), 309-327.

279 M. R. Mozafari, E. T. Baran, S. Yurdugul, A. Omri, *Liposome-based carrier systems, Nanoliposomes: From Foundamentals to Recent Development*, Trafford Pub, Ltd, UK, **2005**, 67-76.

of liposomes on the targeted tissue.[280,281] Another approach is to use pH-sensitive liposomes, whose lipid bilayer becomes unstable below certain pH values. This allows for releasing the active compound only after aggregate internalization by cells via the endosomal pathway.[282] In addition, to provide long circulation and increased bioavailability, polymers like PEG and derivates, can be attached to the phospholipids increasing their flexibility. PEG forms a protective layer over the liposomes, that delays and avoid they recognition by opsonins, and the subsequent clearance.[283] These selected examples, show the potential of manipulating liposome formulation properties, in order to obtain a customized structure for particular task.

3. Hybrid nanosystem for drug delivery

Liposomes and biodegradable polymeric nanoparticles represent the two of most successful classes of drug delivery nanocarriers. The benefits of liposomal formulations include ability to carry hydrophilic and hydrophobic drugs, high biocompatibility that provides perfect shield to protect the therapeutic agent from external and internal environment, and easy surface modification with other molecules such as PEG, and other synthetic derivates, and targeting ligand to achieve prolonged systemic circulation lifetime and targeted drug delivery, respectively. The application of liposome formulations are typically limited by some drawbacks such as relatively complicated fabrication steps associated with liposome manufacture steps and purification, low encapsulation efficiency for lipophilic drugs, and instability during storage leading to short shelf-life.

On the other hand, biodegradable polymeric nanoparticles have shown great therapeutic potential as a drug delivery nanocarrier. These PNs can carry hydrophobic active agents with higher loading capacity than liposomes. Besides, drug release from these nanocarriers is usually dominated by polymer degradation and drug diffusion, which can be controlled by choosing proper polymers. Despite all these appealing features, polymeric nanoparticles have not gained as much success as liposomes, maybe is due to their moderate circulation life-time and potential biocompatibility issues. In order to improve the efficiency of a specific nanosystems useful in drug delivery, efforts have been made to combine the positive

280 E. Markoutsa, G. Pampalakis, A. Niarakis, I. A. Romero, B. Weksler, P. O. Couraud, S. G. Antimisiaris, *Uptake and permeability studies of BBB-targeting immunoliposomes using the hCMEC/D3 cell line*, *Eur. J. Pharm. Biopharm*., **2011**, *77*, 265-274.

281 O. V. Gerasimov J. A. Boomer, M. M. Qualls, D. H. Thompson, *Cytosolic drug delivery using pH- and light sensitive liposomes, Adv. Drug Deliv. Rev*., **1999**, *38*, 317-338.

282 S. General, A. F. Thunemann, *pH-sensitive nanoparticles of poly(amino acid) dodecenoate complexes, Int. J. Pharmaceut.*, **2001**, *230*, 11-24.

283 M. L. Immordino, F. Dosio, L. Cattel, *Stealth liposomes: review of the basic science, rationale, and clinical applications, existing and potential, Int. J. Nanomedicine*, **2006**, *1*, 297-315.

properties of both liposomes and polymeric nanoparticles into a single delivery system, called "hybrid nanosystems".[284]

The structural components of the hybrid nanoparticles are mainly classified based on the therapeutic function they deliver. Structural nanocomponents, such as liposomes, a micelle, mesoporous silica, a polymer, or a virus can mainly carry a drug cargo, while structural nanocomponents such as gold nanoparticles or a carbon nanotube enable photoablation therapy.[285] In literature, various methods have been reported for the preparation of this novel hybrid nanosystem.[286] For example, hybrid chitosan-cyclodextrin nanoparticles have also demonstrated their potential for enhancing the transport of complex molecules across the nasal barrier.[287] Furthermore, Mehdipoor et al., in 2011, deposited γ-Fe_2O_3 nanoparticles onto the surface of carbon nanotubes to produce magnetic hybrid nanomaterials with potential application in cancer therapy.[288] Jain and co-workers in their work, discussed about a polymer lipid hybrid nanoparticles of amphotericin B which were prepared using lecithin and gelatine by two step desolvation and characterized for size, entrapment efficiency, release, confocal laser scanning electron microscopy, and fluorescent resonance energy transfer analysis. Highly permeable, sustained release nanoparticles, more oral bioavailability and significantly lesser haemolytic and nephrotoxicity was observed.[289]

In 2013, Zohri et al., developed a hybrid nanoparticle made of alginate and chitosan, which was complexed with nisin for application in feta cheese conservation. The efficiency of the nanoparticles in inhibiting the growth of L. monocytogenes and Staphylococcus was five times higher than free nisin, showing an increased preservation potential of this formulation.[290] Another example of hybrid nanosystem, was proposed in 2015 by Gajra et al. They developed polymeric lipid hybrid nanoparticles loaded with itraconazole and explored strategies to optimize the intestinal permeability of the hybrid. The nanoparticles were prepared with biodegradable polycaprolactone, soya lecithin and poly vinyl alcohol. No initial burst release was observed during the *in vitro* assays, suggesting its safety. In an *ex vivo* tissue

284 M. J. Sailor, *Hybrid nanoparticles for detection and treatment of cancer, Adv. Mater*., **2012**, *24*(28), 3779-3802.
285 Y. Feng, N. Panwar, D. J. Hang Tng, S. C. Tjin, K. Wang, K. T. Yong, *The application of mesoporous silica nanoparticle family in cancer theranostics, Coordination Chem. Rev*., **2016**, *319*, 86-109.
286 K. Hadinoto, A. Sundaresan, W. S. Cheow, *Lipid-polymer hybrid nanoparticles as a new generation therapeutic delivery platform: a review, European J. of Pharmaceutics and Biopharmac*., **2013**, *85*(3), 427-223.
287 D. Teijeiro-Osorio, C. Remunan-Lopez, M. J. Alonso, *New generation of hybrid poly/Oligosaccharide nanoparticles as carriers for the nasal delivery of macromolecules, Biomacromolecules*, **2009**, *10*, 243-249.
288 E. Mehdipoor, M. Adeli, M. Bavadi, P. Sasanpour, B. A. Rashidian, *A possible anticancer drug delivery system-based on carbon nanotube-dendrimer hybrid nanomaterials, J. Chem*., **2011**, *21*, 15456-15463.
289 S. Jain, P. U. Valvi, N. K. Swarnakar, K. Thanki, *Gelatin coated hybrid lipid nanoparticles for oral delivery of amphotericin B, Mol. Pharm.*, **2012**, *9*, 2542-2553.
290 M. Zohri, M. S. Alavidjeh, S. S. Mirdamadi, H. Behamadi, S. M. H. Nasr, S. E. Gonbaki, M. S. Ardestani, A. J. Arabzadeh*, Nisin-loaded chitosan/alginate nanoparticles a hopeful hybrid biopreservative, J. Food Safety*, **2013**, *33*, 40-49.

penetration model, the nanoparticles reached about 30% of permeability after 4 h of exposure.[291] The behaviour of hybrid nanoparticles as drug carriers includes receiving external physica or chemical signals, chemical reaction or the material properties change and transfer of those changes, resulting in the drug release at the target site. Receiving a chemical and biochemical signal is based on physical or chemical interaction between the material used and signalling factors.[292]

According to this information, the central goal of this study was to create novel self-assembled and functional hybrid synthetic/biological macromolecular nanostructures and enrich basic understanding on behavioural motifs, as well as widen the application potential of nanostructured polymeric colloidal systems. In particular, a synthetic block copolymer polyethylene glycol-co-poly(delta-decalactone) ($mPEG_x$-PDL_y) was incorporated into 1,2-dipalmitoil-sn-glycore-3-phosphocholine (DPPC) and 1,2-diasteroyl-sn-glycero-3-phosphocholine (DSPC) lipid bilayers. This nanosystem shown combined advantage of biodegradable polymeric nanoparticles and liposomes and was synthesized in order to control particle size, surface functionality with various ligands, and to achieve more efficient drug-loaded nanoparticles for several diseases treatment.

4. Incorporation of PEGylated δ-decalactone into lipid bilayers thermodynamic study and chimeric liposomes development

N. Pippa, A. Skouras, N. Naziris, F. Biondo, M. Tiboni, H. Katifelis, M. Gazouli, C. Demetzos, L. Casettari, Journal of Liposome Research, ***2019****.*

1. Introduction

Over the last few years, polymer-grafted/hybrid liposomes have gained ground compared to all other nanoparticles. Most of these systems exhibit several advantages in cancer chemotherapy, such as biocompatibility and stealthiness, due to lipids and PEG-chains that make them ideal nanocarriers for therapeutics. The combination of lipids with polymers in a new carrier has led to a new class of nanocarriers, appear-ing in the literature as hybrid/mixed/chimeric liposomes. These systems are unique for their physicochemical charac-teristics, morphologies, *in vitro* and *in vivo* behavior and drug loading and release

291 B. Gajra, C. Dalwadi, R. Patel, *Formulation and optimization of itraconazole polymeric lipid hybrid nanoparticles (Lipomer) using Box Behnken design, Daru. J. Pharm. Sci*., **2015**, *23*, 3.

292 M. Adeli, R. S. Sarabi, F. R. Yadollahi, M. Mahmoudi, M. Kalantari, *Polyroxane/gold nanoparticle hybrid nanomaterials as anticancer drug delivery systems, J. Mater. Chem*., **2011**, *21*, 18686-18695.

properties.[293,294,295,296] According to Bose et al., lipid-polymer hybrid nanoparticles (LPHNPs) have emerged as promising nanocarriers for several biological applications, including the delivery of therapeutics (drugs and proteins) and diagnosis of diseases, while their clinical translation has progressed incrementally.

Differential scanning calorimetry (DSC), which belongs to thermal analysis techniques, is widely used for studying the physical properties of materials (i.e. melting point, main transition temperature, enthalpy, etc.) and the interactions between different materials. It also represents a useful tool for pre-formulation studies. More specifically, when designing and developing a new drug nanocarrier, DSC studies are used for the characterization of the types of interactions and the ideal molar ratio between the active pharmaceutical ingredient and the excipients.[297,298] According to the literature, DSC has also several appli-cations in biology and nanoscience.[299] Namely, the thermal stability of plasmid DNA complexed with cat-ionic lipids and polymers is investigated by DSC.

The first step for the design and the development of polymer-grafted liposomes is to investigate the interactions between lipids and polymers. More specifically, the ideal molar ratio between the lipid and the polymer used in the system can be identified by DSC, in order to prepare chimeric/mixed liposomes with controlled-release and stimuli-responsive properties.[300,301]

δ-Decalactone is a natural aliphatic product of *Cryptocaryamassoia* (the flowering plant *Lauraceae*) approved by the FDA as a flavouring agent and the ring opening of this monomer leads to the synthesis of the corresponding polymer poly(δ-decalactone) (PDL).[302] PDL is a biodegradable polymer that has a flexible main chain, which results in an amorphous state and

293 K. Hadinoto, A. Sundaresan, W. S. and Cheow, *Lipid–polymer hybrid nanoparticles as a new generation therapeutic delivery plat-form: a review, European journal of pharmaceutics and biopharmaceutics*, **2013**, *85*(3), 427–443.

294 R. J. C. Bose, et al., *Lipid–polymer hybrid nanoparticle-mediated therapeutics delivery: advances and challenges, Drug discovery today*, **2017**, *22*(8), 1258–1265.

295 T. P. T. Dao, et al., *Mixing block copolymers with phospholipids at the nanoscale: from hybrid polymer/lipid wormlike micelles to vesicles presenting lipid nanodomains, Langmuir*, **2017**, *33*(7), 1705–1715.

296 N. K. Garg, et al., *Lipid–polymer hybrid nanocarrier-mediated cancer therapeutics: current status and future directions, Drug discovery today*, **2018**, *23*(9), 1610–1621.

297 B. A. Lobo, et al., *Differential scanning calorimetric studies of the thermal stability of plasmid DNA complexed with cationic lipids and polymers, Journal of pharmaceutical sciences*, **2002**, *91*(2), 454–466.

298 F. Castelli, et al., *Characterization of indomethacin-loaded lipid nanoparticles by differential scanning calorimetry, International journal of pharmaceutics,* **2005**, *304*(1–2), 231–238.

299 P. Gill, T. T. Moghadam, B. Ranjbar, *Differential scanning cal-orimetry techniques: applications in biology and nanoscience, Journal of biomolecular techniques*, **2010**, *21*, 167–193.

300 Pippa, N., et al., *Calorimetric study on pH-responsive block copoly-mer grafted lipid bilayers: rational design and development of lipo-somes, Journal of liposome research*, **2016**, *26*(3), 211–220.

301 Kyrili, A., et al., *Design and development of pH-sensitive liposomes by evaluating the thermotropic behavior of their chimeric bilayers, Journal of thermal analysis and calorimetry*, **2017**, *127*(2), 1381–1392.

302 M. T. Martello, A. Burns, M. Hillmyer, *Bulk ring-opening trans-esterification polymerization of the renewable δ-decalactone using an organocatalyst, ACS macro letters*, **2012**, *1*(1), 131–135.

a low glass transition temperature. Furthermore, the presence of the alkyl side chain increases the lipophilicity of the polymer, without affecting its degradation rate. The latter depends on the ester groups' distance and is considered to be important in drug delivery applications, increasing drug loading efficiency, whereas it may also provide a structural advantage, disrupt-ng condensed packing. PDL-derived amphiphilic block copolymers have been reported to have great potential as drug delivery systems (DDS) and to this end, their simultaneous incorporation with lipids in the same nano-assembly and the formulation of a biodegradable DDS from renewable sources with innovative properties were the endeavor of this study.[303]

In the present study, the block copolymer methoxy poly-ethylene glycol-co-poly(delta-decalactone) ($mPEG_x$-PDL_y) was incorporated into 1,2-dipalmitoyl-sn-glycero-3-phosphocho-line (DPPC) and 1,2-distearoyl-sn-glycero-3-phosphocholine (DSPC) lipid bilayers. The interactions between the polymer and the lipids were investigated using DSC and the effect of the composition and molecular weight of the block copolymers on these interactions was evaluated. After gaining an insight on the thermotropic behavior of the biomaterials, chimeric liposomes were prepared by the most promising systems. The resulted liposomes were studied in regards with their physicochemical properties, their colloidal stability and their *in vitro* toxicity. The described functionality of the new proposed nanosystems may have a high impact to the emerging need of innovative platforms based on nanotechnology. To the best of our knowledge this is the first time that a chimeric liposome composed of a PEG-PDL block copolymer is prepared and characterized.

2. Material and methods

2.1. Materials

Methoxy poly(ethylene glycol) (mPEG) 1.9 kDa were purchased from Polysciences (Eppelheim, Germany), while mPEG 0.55 kDa, 1,5,7-Triazabicyclo[4.4.0]dec-5-ene (TBD) and d-decalactone were purchased from Sigma-Aldrich (Milan, Italy). The phospholipids used for the chimeric formulations were 1,2-dipalmitoyl-sn-glycero-3-phosphocholine (DPPC) and 1,2-distearoyl-sn-glycero-3-phosphocholine (DSPC). They were purchased from Avanti Polar Lipids Inc. (Alabaster, AL, USA) and used without further purification. All other reagents were standard reagent grade or higher and used without further purification.

303 K. K. Bansal, et al., *New biomaterials from renewable resources – amphiphilic block copolymers from δ-decalactone, Polymer chemistry*, **2015**, *6*(40), 7196–7210.

2.2. Synthesis of methoxy polyethylene glycol-co-poly(δ-decalactone) block copolymers

The $mPEG_x$-PDL_y block copolymers were synthesized by ring opening polymerization (ROP) of δ-decalactone monomer using mono-hydroxy terminated PEG of different MW (namely 0.55 and 1.9 kDa). The mPEG was added to a Schlenk tube and melted at 60 °C, under magnetic stirring and nitrogen gas. δ-Decalactone was then added into the flask and stirred for 10 min until a homogeneous mixture was obtained. Finally, TBD was added, and the mixture was allowed to react for 24 h at 60 °C. The reaction mixture was quenched by adding a benzoic acid solution in acetone and was then cooled to room temperature. Dichloromethane was added, and the viscous solution was poured into cold diethyl ether, under stirring, to precipitate the copolymers. The precipitated material was then dialyzed against water for 24 h and freeze-dried. The obtained wax-like solid was stored at 4 °C for further investigations. The copolymers were characterized by ^{1}H-NMR and SEC and they were found to have the molecular characteristics reported on **Scheme 1**.

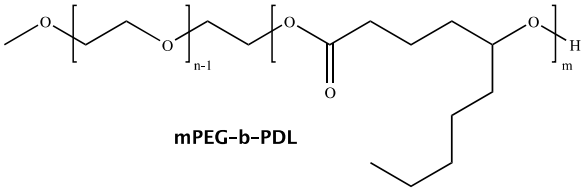

Code	Mw (^{1}H-NM)	FORM
$mPEG_{1.9}$-PDL_{10}	12 kDa	White waxy
$mPEG_{1.9}$-PDL_{24}	26 kDa	White waxy
$mPEG_{1.9}$-PDL_{96}	98 kDa	White waxy
$mPEG_{0.55}$-$PDL_{9.5}$	10 kDa	White waxy
$mPEG_{0.55}$-$PDL_{29.5}$	30 kDa	White waxy

Scheme 1. Chemical structure of $mPEG_x$-PDL_y and its molecular characteristics

2.3. Preparation of bilayer

Pure lipid and chimeric bilayers were prepared by mixing the appropriate amounts of DSPC/ DPPC and $mPEG_x$-PDL_y in chloroform solutions and the subsequent evaporation of the solvents under vacuum and heat. Briefly, stock solutions were prepared by dissolving the copolymer $mPEG_x$-PDL_y in chloroform. Appropriate amounts of DSPC or DPPC were mixed with the copolymer solutions, in order to obtain the desired molar ratios (9:0.1 and 9:0.5), and

the solutions were transferred into vials. Chimeric phospholipid/block copolymer films were formed by removing the solvent at 45 °C. The films were maintained under vacuum for 2 h and then in a desiccator for at least 24 h, in order to remove traces of solvent. The obtained laminated bilayers were hydrated in PBS (pH=7.4) and then studied by DSC.

2.4. Differential scanning calorimetry analysis

DSC experiments were performed on an 822^{e}Mettler-Toledo (Schwerzenbach, Switzerland) calorimeter calibrated with pure indium (T_m= 156.6 °C) and water. Sealed aluminium 40 μL crucibles were used as sample holders. The samples investigated were DSPC and DPPC pure and in the presence of the block copolymers in different weight ratios (i.e. 9:0.1 and 9:0.5), while samples without the block copolymers were used as controls. An empty aluminium crucible was used as reference. Prior to measurements, the crucibles were subjected to a temperature over the transition of DPPC (41.7 °C), to ensure equilibration. All samples were scanned repeatedly until identical curves were obtained. Three cooling-heating cycles were performed; 10–60 °C at 20 and 2 °C min^{-1} scanning rate, respectively. The second heating and cooling runs were taken into account. All experiments were performed in triplicate. Enthalpy changes and characteristic transition temperature were calculated with Mettler-Toledo STAR^e software.

2.5. Preparation of chimeric liposomes

Liposomes composed of DSPC with incorporated $mPEG_x$-PDL_y polymer were prepared in 9:0.5 weight ratio, by utilizing the thin-film hydration method. To this end, appropriate amounts of lipid and polymer were dissolved in chloroform and transferred into a round flask, connected to a rotary evaporator (Rotavapor R-114, Buchi, Switzerland). Vacuum was applied and the thin film was formed by slow removal of the solvent at 45 °C. The mixed film was maintained under vacuum for at least 24 h in a desiccator to remove traces of solvent. Subsequently, it was hydrated with PBS (pH= 7.4), by slowly stirring for 1 h in a water bath, above the phase transition temperature of the lipid, for a total concentration of 5 mg/mL. The resultant structures (apparently multilamellar vesicles, MLVs) were subjected to two 5-min sonication cycles (amplitude 70%, cycle 0.5 s) interrupted by a 5-min resting period, using a probe sonicator (UP 200S, Dr. Hielsher GmbH, Berlin, Germany). The resultant chimeric nanostructures (tentatively assigned as small unilamellar vesicles, SUVs) were allowed to anneal for 30 min.

2.6. Light scattering measurements

The size, polydispersity, and f-potential of the prepared chimeric liposomes were investigated by dynamic and electrophoretic light scattering (DLS and ELS). The physicochemical characteristics were measured immediately after preparation (T= 0 days), as well as over a period of 30 days, in order to monitor their physical stability. In addition, the intensity of the samples is presented, as well as their particle distribution per intensity (D_I). For DLS and ELS, 200 μL aliquots were 30-fold diluted in HPLC-grade water. Measurements were performed at a detection angle of 90 and at 25 °C, in a photon correlation spectrometer (Zetasizer 3000 HSA, Malvern, UK) and analyzed by the CONTIN method (MALVERN software). Details on the methods have been previously published.[304]

2.7. Cell culture experiments

HEK-293 cells (a human embryonic kidney cell line) were grown in DMEM High Glucose culture medium (Biosera) containing 10% FBS, 2 mmol/L glutamine, 100 U/mL penicillin and 100 g/mL streptomycin at 37 °C. Every 48 h the medium was changed, and cells were passaged using standard trypsin-EDTA concentration weekly.

2.8. Chimeric liposomes exposure and viability (MTT) assay

MTT assay was used to quantify the viability of cells exposed to four different chimeric liposome types (DSPC:mPEG$_{1.9}$-PDL$_{24}$, DSPC:mPEG$_{1.9}$-PDL$_{96}$, DSPC:mPEG$_{0.55}$-PDL$_{9.5}$ and DSPC:mPEG$_{0.55}$-PDL$_{29.5}$) at various concentrations (25, 50, 100, 200, 300, 400 and 500 μg/mL). During this assay the yellow tetrazolium (3–(4,5-dimethyltihazolyl-2)–2,5-diphenyltetrazolium bromide (Thermo Fisher Scientific, Cat. No. M6494) is reduced to the insoluble formazan. This reaction is catalyzed by the mitochondrial dehydrogenase enzymes that consume NAD(P)H; formazan crystals are only formed inside living cells. Formazan is then solubilized, and its levels are quantified using spectrophotometry. In this assay, approximately 5000 cells per well were loaded in a 96-well plate (Corning-Costar, Corning NY). These cells were then incubated for 16–24 h with the liposome types and concentrations described above. After the incubation period, the cells were rinsed and 100 μL of serum-free medium containing 0.5 mg/mL MTT were added. After an incubation of approximately 2 h at 37 °C, the formazan crystals were solubilized by adding 100 μL/well of SDS-HCl and mixed thoroughly. A final incubation of 1.5 h at 37 °C followed. The optical densities were read by using a microplate spectrophotometer (SPECTROstar^{Nano}, BMG LABTECH) at 570 nm. The

304 N. Pippa, et al., *PEO-b-PCL grafted DPPC liposomes: physicochemical characterization and stability studies of novel bio-inspired advanced drug delivery nanosystems (aDDnSs), Journal of nanoscience and nanotechnology*, **2014**, *14*(8), 5676–5681.

reference filter was set at 690 nm. Absorbances were normalized with respect to the untreated cultures to calculate changes in cell viability.

3. Result and discussion

3.1. Thermal characterization of the interactions between lipids and co-polymers

DSC has been used to investigate the interactions between lipid bilayers and $mPEG_x$-PDL_y. We used two different lipid membrane models; the first one composed of DSPC with T_m= 55 °C and the second one composed of DPPC with T_m= 41 °C. Both these two phospholipids belong to the category of phosphatidylcholines, containing two identical, saturated, linear fatty acyl chains. The difference between them is their chain length, which results in their different phase transition temperature.[305][306] [307]During heating of these lipids, there are variations in the packing arrangement of the hydrocarbon chains that alter the bilayer geometry and lead to extensive polymorphism. We also utilized block copolymers with different compositions (i.e. the different ratio between the lipophilic and hydrophilic component) and different molecular weights. **Table 5** and **Table 6** present the calorimetric profiles of DSPC and DPPC lipid bilayers after heating, where different weight ratios of the polymeric guest have been incorporated, while **Figure 13** and **Figure 14** include the DSC heating and cooling scans of DSPC and DPPC, respectively.

305 R. Koynova, M. Caffrey, *Phases and phase transitions of the phosphatidylcholines, Biochimica et biophysica acta,* **1998**, *1376*(1), 91–145.

306 C. Demetzos, *Differential scanning calorimetry (DSC): a tool to study the thermal behavior of lipid bilayers and liposomal stability, Journal of liposome research*, **2008**, *18*(3), 159–173.

307 A. G. Lee, *Lipid phase transitions and phase diagrams I. Lipid phase transitions, Biochimica et biophysica acta*, **1997**, *472*(2), 237–281

Sample	Weight ratio	$T_{onset.m}$ (°C)	T_m (°C)	$\Delta T_{1/2.m}$ (°C)	ΔH_m (J/mol)	$T_{onset.s}$ (°C)	T_s (°C)	$\Delta T_{1/2.s}$ (°C)	ΔH_s (J/mol)
DSPC	-	54.2	55.3	1.18	357.0	50.5	52.3	2.08	30.1
DSPC:$mPEG_{1.9}$-PDL_{10}	9:0.1	54.1	55.0	1.07	362.0	43.6	47.2	3.48	118.0
DSPC:$mPEG_{1.9}$-PDL_{24}	9:0.1	54.0	55.0	1.20	475.0	48.8	50.7	2.21	31.8
DSPC:$mPEG_{1.9}$-PDL_{96}	9:0.1	54.1	54.9	0.95	221.0	49.7	51.6	2.02	20.6
DSPC:$mPEG_{0.55}$-$PDL_{9.5}$	9:0.1	54.0	54.9	1.09	460.3	48.9	50.9	2.35	26.9
DSPC:$mPEG_{0.55}$-$PDL_{29.5}$	9:0.1	54.1	55.0	1.33	517.6	50.4	52.0	1.80	56.9
DSPC:$mPEG_{1.9}$-PDL_{10}	9:0.5	51.0	53.5	2.16	343.0	-	-	-	-
DSPC:$mPEG_{1.9}$-PDL_{24}	9:0.5	52.7	54.3	1.53	408.0	-	-	-	-
DSPC:$mPEG_{1.9}$-PDL_{96}	9:0.5	53.5	54.8	1.38	382.2	-	-	-	-
DSPC:$mPEG_{0.55}$-$PDL_{9.5}$	9:0.5	53.8	54.8	1.26	300.8	-	-	-	-
DSPC:$mPEG_{0.55}$-$PDL_{29.5}$	9:0.5	53.6	54.6	1.07	95.6	-	-	-	-

Table 5. Calorimetric profiles of DSPC lipid bilayers after heating. **T_{onset}:** temperature at which the thermal event starts; **$T_.$:** temperature at which heat capacity (ΔC_p) at constant pressure. is maximum; **$\Delta T_{1/2}$:** width at half peak height of the transition; **ΔH:** transition enthalpy normalized per mol of lipid system. **m:** main transition; **s:** secondary transition.

Sample	Weight ratio	$T_{onset.m}$ (°C)	T_m (°C)	$\Delta T_{1/2.m}$ (°C)	ΔH_m (J/mol)	$T_{onset.s}$ (°C)	T_s (°C)	$\Delta T_{1/2.s}$ (°C)	ΔH_s (J/mol)
DPPC	-	40.9	41.9	1.02	402.4	34.2	36.5	1.00	63
DPPC:$mPEG_{1.9}$-PDL_{10}	9:0.1	38.1	40.2	1.36	271.0	-	-	-	-
DPPC:$mPEG_{1.9}$-PDL_{24}	9:0.1	38.8	40.5	1.25	369.4	-	-	-	-
DPPC:$mPEG_{1.9}$-PDL_{96}	9:0.1	40.4	41.3	2.21	359.8	-	-	-	-
DPPC:$mPEG_{0.55}$-$PDL_{9.5}$	9:0.1	39.3	40.8	3.14	512.1	-	-	-	-
DPPC:$mPEG_{0.55}$-$PDL_{29.5}$	9:0.1	40.7	41.9	1.98	382.6	-	-	-	-
DPPC:$mPEG_{1.9}$-PDL_{10}	9:0.5	38.1	40.2	1.98	1318.2	-	-	-	-
DPPC:$mPEG_{1.9}$-PDL_{24}	9:0.5	34.9	37.6	3.61	270.5	-	-	-	-
DPPC:$mPEG_{1.9}$-PDL_{96}	9:0.5	40.3	41.3	1.69	221.5	-	-	-	-
DPPC:$mPEG_{0.55}$-$PDL_{9.5}$	9:0.5	39.3	40.8	2.61	227.1	-	-	-	-
DPPC:$mPEG_{0.55}$-$PDL_{29.5}$	9:0.5	40.2	41.3	1.67	307.4	-	-	-	-

Table 6. Calorimetric profiles of DPPC lipid bilayers after heating. **T_{onset}:** temperature at which the thermal event starts; **$T_.$:** temperature at which heat capacity (ΔC_p) at constant pressure. is maximum; **$\Delta T_{1/2}$:** width at half peak height of the transition; **ΔH:** transition enthalpy normalized per mol of lipid system. **m:** main transition; **s:** secondary transition.

The presence of $mPEG_x$-PDL_y did not cause any decrease in the T_m of DSPC (**Table 5**). The presence of $mPEG_{1.9}$-PDL_{24}, $mPEG_{0.55}$-$PDL_{9.5}$ and $mPEG_{0.55}$-$PDL_{29.5}$ into the DSPC lipid bilayers at 9:0.1 weight ratio, however, causes a significant increase of the transition enthalpy, meaning that the whole system needs more energy to melt. This phenomenon is evidence that

the hydrophobic part of the polymer incorporates into the chain of the phospholipids. The pre-transition remains unaffected in the presence of the $mPEG_x$-PDL_y, as indicated by the T_s values (**Table 5**). On the other hand, the molecular weight of the block copolymer at 9:0.1 weight ratio influences the pre-transition enthalpy in a composition dependent manner. More specifically, when the molecular weight of PEG is 1.9 kDa, as the molecular weight (or equally, the hydrophobic part) increases, the ΔH_s decreases significantly (**Table 5**). The long hydrophobic part probably influences the mobility of the head groups, apart from the alkyl chains.[308;309,310,311] On the contrary, for $mPEG_{0.55}$-PDL_y block copolymer, we observed the opposite phenomenon. The increase of the PDL block caused an increase of the ΔH_s for 9:0.1 weight ratio. For the higher weight ratio 9:0.5, the pretransition disappears for all the block copolymers (**Table 5** and **Figure 13**(**B**)).

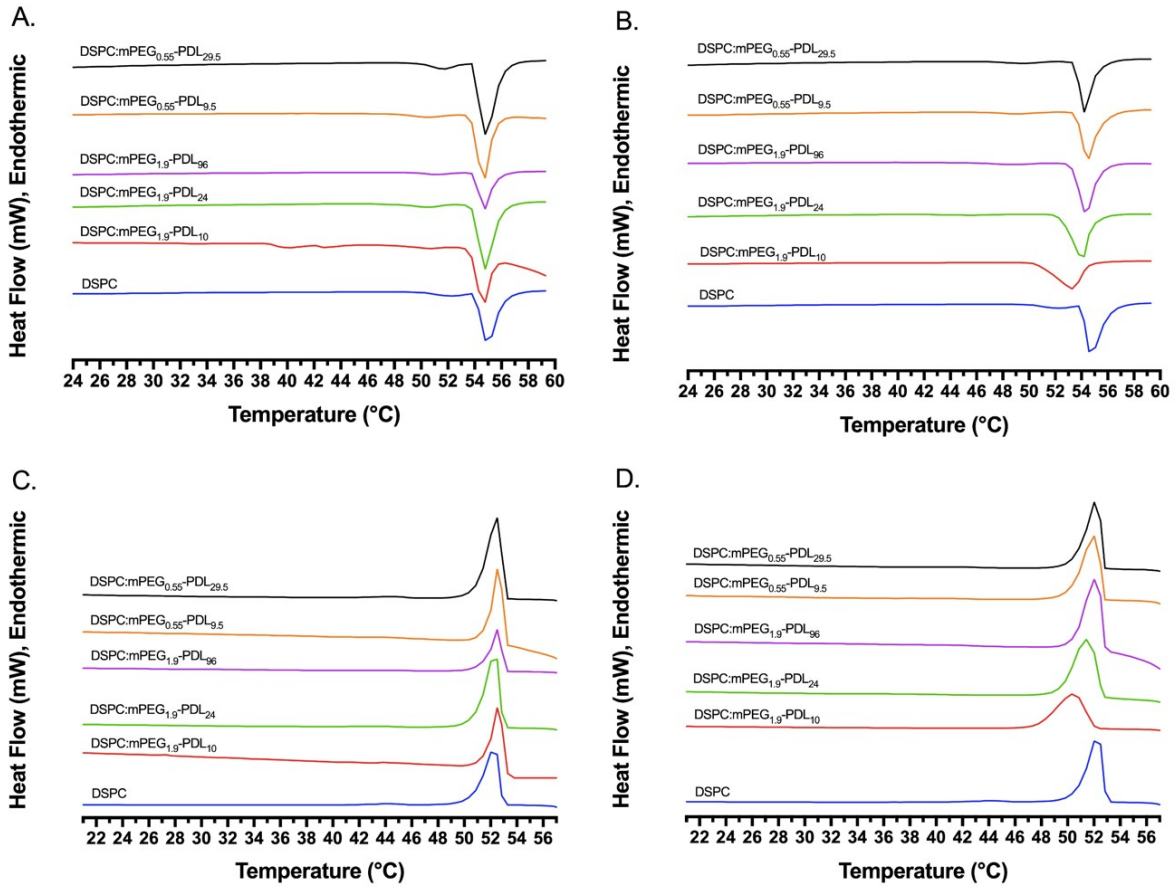

Figure 13. DSPC:Polymer Thermal analysis: A-B DSC heating scans and **C-D** DSC cooling scans; **A, C** 9:0.1 and **B, D** 9:0.5 weight ratio. The limits for the calculation of thermotropic parameters are from 20°C to 60°C.

308 T. Hashizaki, et al., *Calorimetry and cryo-transmission electron microscopic studies of PEG2000-grafted liposomes. Chemical & pharmaceutical bulletin*, **2006**, *54*(4), 561–563.

309 A. A. Yaroslavov, et al., *Multi-liposomal containers, Advances in col-loid and interface science*, **2015**, *226*, 54–64.

310 A. A. Efimova, et al., *Effect of cholesterol on the phase state and permeability of mixed liposomes composed of anionic diphosphati-dylglycerol and switteroonicdipalmitoylphosphadilcholine, Mendeleev communications*, **2016**, *26*(2), 99–100.

311 D. Paolino, et al., *Interactions between PEG lipid and DSPE/DSPC phospholipids: an insight of PEGylation degree and kinetics of de-PEGylation, Colloids surf B biointerfaces*, **2017**, *155*, 266–275.

This means that the weight ratio of the polymeric guest influences the mobility of the polar head groups and when the entry points of the block copolymers increase, the head groups become more mobile due to various interactions (i.e. van der Waals interactions and hydrogen bonds).[312] Regarding the main transition of the DSPC, we did not observe significant differences in the calorimetric values (**Table 5** and **Figure 13**), except for the $mPEG_{0.55}$-$PDL_{29.5}$, which was responsible for system enthalpy decrease (**Table 5**). The presence of the block copolymers influences in a different way the thermodynamic behavior of the DPPC bilayers. Firstly, the pretransition of the DPPC disappeared in the presence of lower weight ratios of the block copolymers (**Table 6**). Generally, at lower weight ratios of the polymeric guests, the ΔH_m decreased slightly, except for the $mPEG_{0.55}$-$PDL_{9.5}$ (**Table 6**). All the other calorimetric values remained more or less the same with those of the pure lipid bilayers (**Table 6** and **Figure 14**).

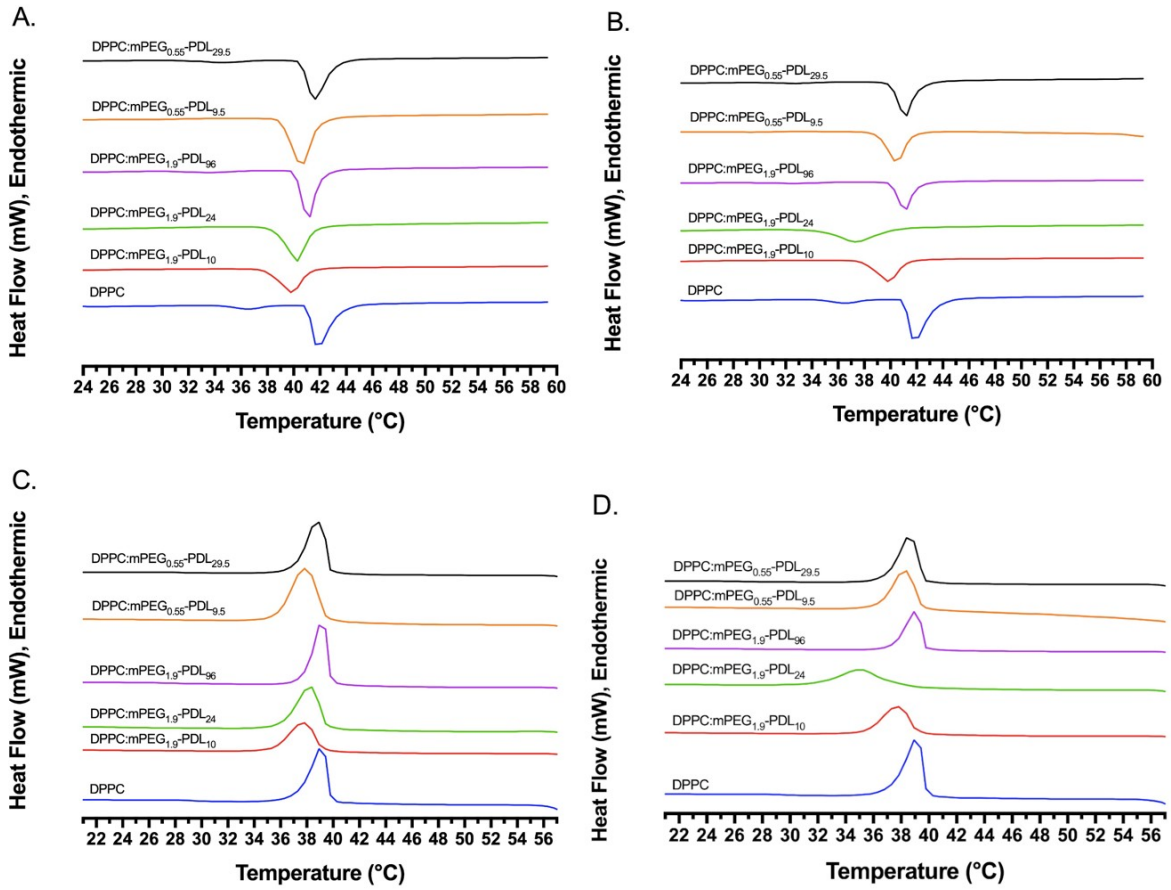

Figure 14. DPPC:Polymer Thermal analysis: A-B DSC heating scans and **C-D** DSC cooling scans; **A, C** 9:0.1 and **B, D** 9:0.5 weight ratio. The limits for the calculation of thermotropic parameters are from 20°C to 60°C.

312 N. Pippa, S. Pispas, C. Demetzos, *The metastable phases as modulators of biophysical behavior of liposomal membranes, Journal of thermal analysis and calorimetry*, **2015**, *120*(1), 937–945.

The increase of the weight ratio of the $mPEG_x$-PDL_y caused a significant decrease of the melting enthalpy, except for the case of $mPEG_{1.9}$-PDL_{10}. Regarding the main transition, the $mPEG_{1.9}$-PDL_{10} acts as 'impurity', because the melting enthalpy increased 3 times, in comparison to pure DPPC lipid bilayers. The incorporation and probably the conformation of the PDL part inside the DPPC lipid bilayer caused rafts, which require a higher amount of energy to melt. The DSC cooling scans are illustrated in **Figure 13** (**C–D**) and **Figure 14** (**C–D**). A small hysteresis of the main transition temperature in the cooling curves is observed (**Table 7** and **Table 8**), a common phenomenon, well-established in the literature.[13]

Sample	Weight ratio	$T_{onset.m}$ (°C)	T_m (°C)	$\Delta T_{1/2.m}$ (°C)	ΔH_m (J/mol)	$T_{onset.s}$ (°C)	T_s (°C)	$\Delta T_{1/2.s}$ (°C)	ΔH_s (J/mol)
DSPC	-	52.7	51.8	1.35	420.2	-	-	-	-
DSPC:$mPEG_{1.9}$-PDL_{10}	9:0.1	53.2	52.2	1.28	794.3	-	-	-	-
DSPC:$mPEG_{1.9}$-PDL_{24}	9:0.1	52.8	51.8	1.28	516.6	-	-	-	-
DSPC:$mPEG_{1.9}$-PDL_{96}	9:0.1	52.8	52.0	1.04	244.3	-	-	-	-
DSPC:$mPEG_{0.55}$-$PDL_{9.5}$	9:0.1	53.1	52.2	1.15	555.2	-	-	-	-
DSPC:$mPEG_{0.55}$-$PDL_{29.5}$	9:0.1	52.9	52.1	1.35	1555.2	-	-	-	-
DSPC:$mPEG_{1.9}$-PDL_{10}	9:0.5	51.6	50.1	2.36	355.2	-	-	-	-
DSPC:$mPEG_{1.9}$-PDL_{24}	9:0.5	52.3	51.1	1.78	480.7	-	-	-	-
DSPC:$mPEG_{1.9}$-PDL_{96}	9:0.5	52.7	51.6	1.51	564.2	-	-	-	-
DSPC:$mPEG_{0.55}$-$PDL_{9.5}$	9:0.5	52.4	51.5	1.38	428.4	-	-	-	-
DSPC:$mPEG_{0.55}$-$PDL_{29.5}$	9:0.5	52.6	51.7	1.25	403.2	-	-	-	-

Table 7. Calorimetric profiles of DSPC lipid bilayers after cooling; **T_{onset}:** temperature at which the thermal event starts; **$T_.$:** temperature at which heat capacity (ΔC_p) at constant pressure. is maximum; **$\Delta T_{1/2}$:** width at half peak height of the transition; **ΔH:** transition enthalpy normalized per mol of lipid system. **m:** main transition; **s:** secondary transition.

Sample	Weight ratio	$T_{onset.m}$ (°C)	T_m (°C)	$\Delta T_{1/2.m}$ (°C)	ΔH_m (J/mol)	$T_{onset.s}$ (°C)	T_s (°C)	$\Delta T_{1/2.s}$ (°C)	ΔH_s (J/mol)
DPPC	-	40.0	38.8	0.97	304.9	-	-	-	-
DPPC:$mPEG_{1.9}$-PDL_{10}	9:0.1	38.8	37.4	1.02	285.3	-	-	-	-
DPPC:$mPEG_{1.9}$-PDL_{24}	9:0.1	39.1	37.9	1.52	379.1	-	-	-	-
DPPC:$mPEG_{1.9}$-PDL_{96}	9:0.1	39.7	38.8	1.43	392.4	-	-	-	-
DPPC:$mPEG_{0.55}$-$PDL_{9.5}$	9:0.1	39.1	37.6	1.85	522.1	-	-	-	-
DPPC:$mPEG_{0.55}$-$PDL_{29.5}$	9:0.1	39.6	38.4	2.05	403.7	-	-	-	-
DPPC:$mPEG_{1.9}$-PDL_{10}	9:0.5	38.8	37.4	1.52	288.4	-	-	-	-
DPPC:$mPEG_{1.9}$-PDL_{24}	9:0.5	37.4	34.8	1.87	221.2	-	-	-	-
DPPC:$mPEG_{1.9}$-PDL_{96}	9:0.5	39.6	38.6	1.85	237.4	-	-	-	-
DPPC:$mPEG_{0.55}$-$PDL_{9.5}$	9:0.5	39.2	37.9	2.01	364.6	-	-	-	-
DPPC:$mPEG_{0.55}$-$PDL_{29.5}$	9:0.5	39.4	37.9	2.12	323.8	-	-	-	-

Table 8. Calorimetric profiles of DPPC lipid bilayers after cooling; **T_{onset}:** temperature at which the thermal event starts; **$T_.$:** temperature at which heat capacity (ΔC_p) at constant pressure. is maximum; **$\Delta T_{1/2}$:** width at half peak height of the transition; **ΔH:** transition enthalpy normalized per mol of lipid system. **m:** main transition; **s:** secondary transition.

3.2. Physicochemical characteristics of chimeric liposomes and stability studies

The most promising chimeric systems, in terms of thermotropic behavior, were chosen to be developed as liposomes. Based on the enthalpy of the main transition, those were

DSPC:polymer 9:0.5. The physicochemical properties of the developed chimeric lipid/polymer nanosystems are presented in **Table 9**.

System	Weight ratio	Dispersion Medium	D_h[a] (nm)	PDI[b]	ζ-pot[c] (mV)	I[d] (KCps[e])
DSPC:$mPEG_{1.9}$-PDL_{24}	9:0.5	PBS	89.9±0.7	0.271±0.002	-2.9±0.9	266.6±3.9
DSPC:$mPEG_{1.9}$-PDL_{96}	9:0.5	PBS	89.6±0.8	0.270±0.020	4.6±0.7	325.8±2.5
DSPC:$mPEG_{0.55}$-$PDL_{9.5}$	9:0.5	PBS	172.9±2.4	0.625±0.019	-0.4±0.3	479.8±10.6
DSPC:$mPEG_{0.55}$-$PDL_{29.5}$	9:0.5	PBS	573.3±59.2	1.000±0.000	-2.7±0.2	281.9±9.5

Table 9. Physicochemical characteristics of the chimeric systems; [a]**D_h:** hydrodynamic diameter [b]**PDI:** polydispersity index [c]**ζ-pot:** zeta potential [d]**I:** intensity [e]**KCps:** kilo counts per second

These include the particle size (D_h), polydispersion index (PDI), zeta potential (ζ-pot) and scattered light intensity (I). In addition, **Figure 15** provide the physical stability studies of the systems. All the formulations were developed in PBS solution since this medium simulates well the physiological environment in terms of pH (7.4) and ionic strength.

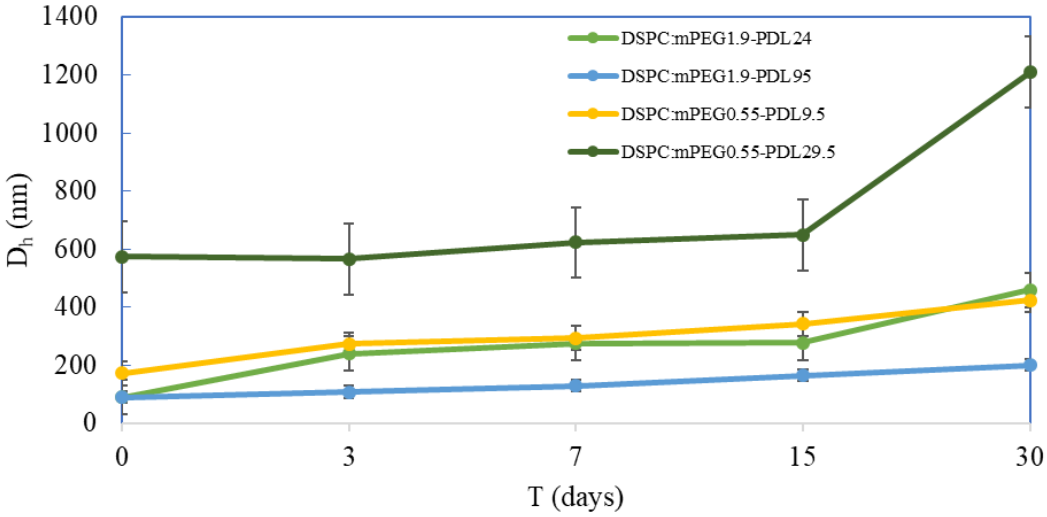

Figure 15. Stability assessment of the chimeric systems.

Regarding the size and polydispersity of the chimeric liposomes, we observed a high dependence on the nature of the utilized copolymer. In particular, the hydrophilic-to-hydrophobic balance of the copolymer affected those parameters greatly (**Table 5**). In the case of $mPEG_{1.9}$, the length variation of PDL did not alter the liposomal diameter, leading to a size of 90 nm, while the polydispersity was also stable at 0.270, indicating homogeneity of the systems. These properties are promising for further *in vivo* investigation of these chimeric nanoparticles.[313] However, when a copolymer with different hydrophilic and hydrophobic

313 N. Hoshyar, et al., *The effect of nanoparticle size on in vivo pharmacokinetics and cellular interaction. Nanomed. Nanomedicine*, London, England, **2016**, *11*(6), 673–692.

segments is incorporated inside the phospholipid membrane, these properties change dramatically. Namely, for $mPEG_{0.55}$- $PDL_{9.5}$, liposomal size is almost doubled (170 nm) and particle distribution becomes heterogeneous (PDI : 0.625). This phenomenon comes hand-in-hand with the alteration of the thermodynamic content of the specific system. The same also applies for DSPC:$mPEG_{0.55}$-$PDL_{29.5}$, where the transition enthalpy was measured to be significantly lower than the rest of the 9:0.5 systems and at the same time, the prepared particles were around 570 nm and fully heterogeneous. These results are indications of the formation of other types of nanostructures, besides liposomes, which exhibit larger hydrodynamic diameter in a broad range of size and probably even different morphology.[314] The relatively higher hydrophobic balance of these copolymers could be the reason for self-assembly in larger aggregates since the hydrophilic segment is low in amount and possibly cannot drive the process in favor of the membrane incorporation. Therein, we observed the formation of two types of populations and as expected, the one of larger hydrodynamic diameter dominates in the case of DSPC:$mPEG_{0.55}$-$PDL_{29.5}$, where the high hydrophobicity of the copolymer prevails during the self-assembly process, due to hydrophobic interactions and leads to the formation of larger aggregates.[315]

The zeta potential of the developed liposomes was close to zero, which means an absence of net charge around the particle surface (**Table 9**). According to the literature, the pure DSPC/DPPC liposomes have zero surface charge, due to the zwitterionic nature of these phospholipids. The zeta-potential values of the chimeric liposomes are also found near zero (absence of surface charge). This phenomenology means that the addition of the polymer into the lipid bilayer did not alter the surface charge and the net charge of the prepared structures. Furthermore, the different molecular composition of the polymers did not affect the liposomal surface charge (**Table 9**). This property was expected since no charged phospholipid was utilized and on top of that, the copolymers consist of backbone and alkyl groups that are not charged.[316] As a result, the observed physical stability of certain systems is not attributed to electrostatic interactions between nanoparticles (**Figure 15**). Instead, it is a property provided by the hydrophilic corona of mPEG chains that surround each liposome. This results in enthalpic stabilization each time one particle approaches another, forcing of water molecules

314 N. Naziris, *et al., Morphological diversity of block copolymer/ lipid chimeric nanostructures, Journal of nanoparticle research*, **2017**, *19*, 347.

315 G. Mountrichas, P. Petrov, et al., *Nano-sized polymer structures via self-assembly and co-assembly approaches. In: S. Fakirov, ed. Nano-size polymers: preparation, properties, applications,* New York, USA: Springer International Publishing, **2016**, 19–48.

316 Y. Takechi-Haraya, K. Sakai-Kato, Y. Goda, *Membrane rigidity determined by atomic force microscopy is a parameter of the perme-ability of liposomal membranes to the hydrophilic compound calcein, AAPS Pharm. Sci. Tech*., 2017, 18 (5), 1887–1893

out of the hydrated chains and ultimately, steric repulsion between particles and colloidal stability.[317,318] Most nanosystems were characterized by such behaviour, especially DSPC:mPEG$_{0.55}$-PDL$_{29.5}$ 9:0.5. Only the system with larger aggregates exhibited a steep size increase from day 15 to day 30.

3.3. Toxicity of chimeric liposomes

Of all the liposomes tested, the DSPC:mPEG$_{1.9}$-PDL$_{24}$ appeared to be the most toxic for HEK-293 cells; after the incubation period, cell viability was decreased to less than 60% even at the lowest concentration. DSPC:mPEG$_{1.9}$-PDL$_{96}$ liposomes showed greater variance on toxicity since the observed viability ranged from unaffected to a reduced at 60%. The DSPC:mPEG$_{0.55}$-PDL$_{9.5}$ and DSPC:mPEG$_{0.55}$-PDL$_{29.5}$ liposomes showed similar toxicity rates since most of the concentrations tested led to a decreased viability of 80% (**Figure 16**).

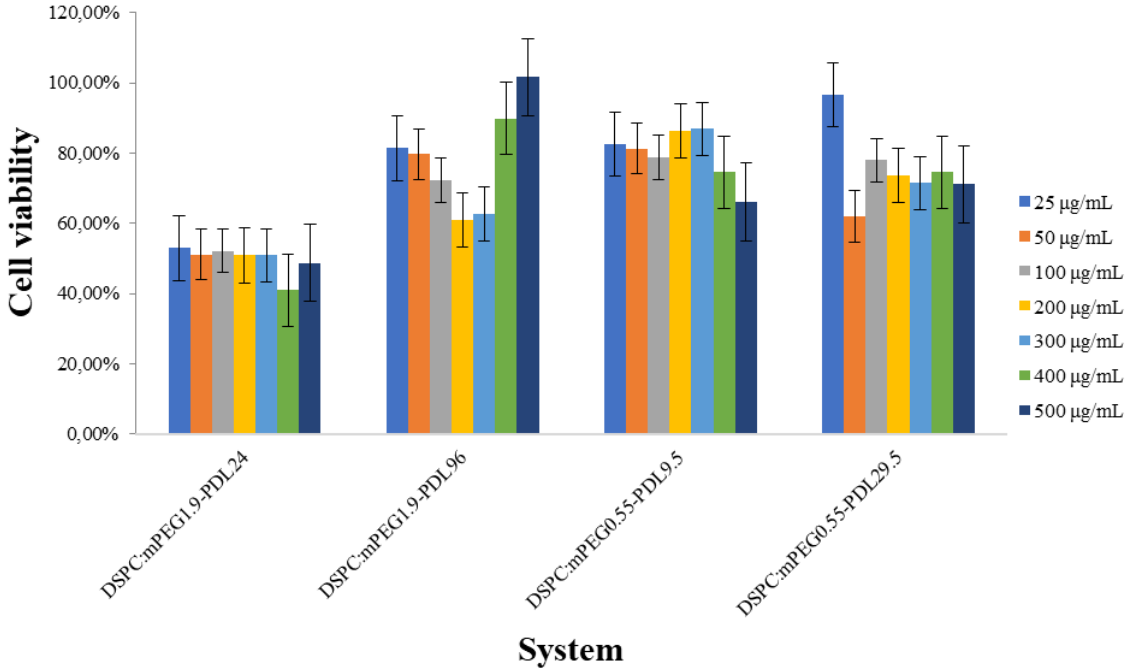

Figure 16. MTT cell viability assay after 24h treatment of HEK-293 with various concentrations of chimeric liposomes. Cell viability is expressed as % cell viability ± SD between two experiments.

These results agree with Bansal et al., who also used chimeric liposomes (mPEG-PCL and mPEG-b-PDL) and found comparable cell viability on HCT116 cells. However, data regarding cell viability upon exposure to bare chimeric liposomes are scarce and further research is required to understand the mechanisms that induce toxicity.

317 D. Attwood, *A. T. Florence, Physical pharmacy, 2nd ed.; Pharmaceutical Press:* London, UK, **2008**, 67-69.
318 C. Tribet, F. Vial, *Flexible macromolecules attached to lipid bilayers: impact on fluidity, curvature, permeability and stability of the membranes, Soft matter,* **2008**, *4*(1), 68–81

4. Conclusion

The utilization of different in nature biomaterials for the purpose of building innovative and sophisticated nano-entities for biomedical applications has drawn great interest in recent years. In the present study, a series of nanosystems were built by combining phospholipid DSPC or DPPC with one of the $mPEG_x$-PDL_y block copolymers. DSC analysis revealed the thermotropic effect of the copolymers on the two types of membranes in two different weight ratios, 9:0.1 and 9:0.5. The most profound alterations regard the transition enthalpy, reflecting the organization of the membranes, which was assessed and based on that, liposomes were rationally developed. Specifically, the combination of higher copolymer ratio on DSPC membranes was promising in terms of thermodynamics. The resulting vesicles presented physicochemical properties that depend on the ratio between copolymer blocks, with the smallest particle size and homogeneity observed in the case of larger mPEG segment. Physical stability of the liposomes was obtained in most cases, due to the presence of mPEG chains around the liposomal membranes and the preventing of aggregation phenomena. Finally, one of the four systems, namely DSPC:$mPEG_{1.9}$-PDL_{24}, was the most toxic *in vitro*, with the others being more tolerable, especially at certain concentrations. As a result, depending on their thermodynamic, physicochemical and toxicity profiles, chimeric polymer-grafted liposomes could be promising candidates for further *in vitro* and *in vivo* investigations for future drug delivery applications.

SECTION III

GLYCOLIPID-MEDIATED LIPOSOME TARGETING IN ZEBRAFISH EMBRYOS

F. Biondo, S. Romeijn, L. Marino, W. Jiskoot, L. Casettari, J. Bussmann, manuscript in preparation

Abstract

Purpose: Liver sinusoidal endothelial cells (LSECs) form the vascular lining of the liver and have key roles in lipid metabolism, blood clearance, antigen presentation and liver repair. Drug delivery systems for intracellular delivery in LSECs are an attractive strategy for the induction of immune tolerance and to prevent the progression of liver fibrosis. The most abundant endocytic receptor on LSECs is the Mannose Receptor (mrc1). In this project we have developed a liposomal drug delivery system based on mannosylated liposomes to target this receptor, tested its receptor- specificity and potential for delivery to LSECS in our recently established zebrafish embryo model.

Synthesis and characterization of glycolipids: Three different glycolipids were synthesized by one reaction step. 6-O-oleoyl-glucose and 6-O-oleoyl-mannose were obtained through enzymatic esterification, while 2-Oleoyl-fucose was chemically synthesized. Nuclear magnetic resonance spectroscopy analysis was performed to characterize these glycolipids. The complete ^{1}H-NMR and ^{13}C NMR assignments of the compounds were carried out by using DEPT, HMBC, HSQC, NOESY and ^{1}H–^{1}H COSY spectra.

Formulation and characterization of glyco-liposomes: DOPC-Glyclopid-Rhodamine/DPPE liposomes, in the molar ratio 79:20:1 respectively, were prepared by thin film method followed by extrusion. The delivery systems were characterized by DLS and zeta-potential measurement. UPLC-ELSD analysis were carried out for the quantification of the different glycolipids incorporated. Intravenous injection into zebrafish embryos was used to model LSEC targeting *in vivo* and to visualize liposome biodistribution. To test the specificity of the LSECs targeting we compared it to the alternative glycolipid-based liposomes (glucosylated & fucosylated), competitively inhibited Mrc1 using mannan, and injected embryos with a targeted mutation in mrc1a.

Results: The glyco-liposomes of 100nm, <0.1 PDI and Z-potential ~-18 mV were obtained. After intravenous injection into zebrafish embryos, mannosylated liposomes – but not glucosylated, fucosylated or control liposomes - were removed from circulation within 4 hours and accumulated specifically in LSECs and macrophages. LSECs targeting was prevented in embryos preinjected with Mannan and in *mrc1a* mutants – but not *stab1/2* mutants showing precise specificity towards the Mannose Receptor.

Conclusion: We have successfully generated a LSEC-targeted liposomal drug delivery system with precise and *in vivo* confirmed specificity towards LSECs through interaction with the mrc1 receptor.

1. Introduction

Liver sinusoidal endothelial cells, called LSECs, form the vascular lining cells and the wall of the liver sinusoids.[319] LSECs are highly specialized endothelial cells (ECs), that have pores, so-called fenestrae, approximately 100 to 150 nm in size. Wisse, in 1970, described in his early report that LESC contained mant fenestrae.[320] He also noticed that, those fenestrae, creating open channels for the exchange of substances between the blood and liver parenchyma.[321] Liver sinusoidal endothelial cells have unique and indispensable functions in physiology of the liver and thus participate in some pathological processes of this organ. LSECs contribute to regulating the sinusoidal blood flow; to have a role in triggering of liver regeneration; taking part to hepatic complications as well as liver fibrosis, atherosclerosis and liver metastasis.[322,323,324,325] In combination with Kupffer cells, LSECs constitute the most powerful scavenger system in the mammalian body. These two cell types play complementary roles in the hepatic blood clearance of macromolecules and nanoparticles. The LSECs are specialized in endocytosis uptake of material roughly <200 nm, while the Kupffer cells taking care of the clearance of larger material by phagocytosis.[326,327,328]

319 E. Maslak, A. Gregorius, S. Chlopicki, *Liver sinusoidal endothelial cells (LECs) function and NAFLD; NO-based therapy targeted to the liver, Pharmacol. Rep.*, **2015**, *67*, 689-694.
320 E. Wisse, *An electron microscopic study of the fenestrated endothelial lining of rat liver sinusoids, J. Ultrastruct. Res*., **1970**, *31*, 125-150.
321 B. Le Bail, P. Bioulac-Sage, R. Senuita, A. Quinton, J. Saric, C. Balabaud, *Fine structure of hepatic sinusoids and sinusoidal cells in disease, J. Electron Microsc. Tech*., **1990**, *14*, 257-282.
322 R. S. McCuskey, *Morphological mechanisms for regulating blood flow through hepatic sinusoids, Liver*, **2000**, *20*, 3-7.
323 N. Moniaux, J. Faivre, *Key role of sinusoidal endothelial cells in the triggering of liver regeneration, J. Hepatol*., **2011**, *55*, 488-490.
324 L. D. De Leve, *Liver sinusoidal endothelial cells in hepatic fibrosis, Hepatol*., **2015**, *61*(5), 1740, 1746.
325 R. Fraser, V. C. Cogger, B. Dobbs, H. Jamieson, A. Warren, S. N. Hilmer, *The liver sieve and atherosclerosis, Phatol*., **2012**, *44*(3), 181-186.
326 T. Seternes, K. Sorensen, B. Smedsrod, *Scavenger endothelial cells of vertebrates: A nonperipheral leukocyte system for high-capacity elimination of waste macromolecules, Proc. Natl. Acad. Sci*., **2002**, *99*, 7594-7597.
327 B. Smedsrod, *Clearance function of scavenger enfothelial cells, Comp. Hepatol*., **2004**, *3*, 22.
328 K. K. Sorensen, P. McCourt, T. Berg, C. Crossley, D. L. Couteur, K. Wake, B. Smedsrod, *The scavenger endothelial cell: a new player in homeostasis and immunity, Am. J. Physiol. Regul. Integr. Comp. Physiol*., **2012**, *303*, 1217-1230.

LSECs are equipped with surface receptors that enable them to scavenge macromolecules and pathogenic agents from sinusoidal blood.[329] The receptors, associated with scavenger function, are CD14, CD36, TLR4, TLR9, L-SIGN, Fcγ receptors, LSECtin, Stabilin 1 and 2, and the mannose receptors.[330] Most of them are pattern recognition receptors that recognize pathogen-associated patterns (PAMPS).[331]

The multifunctional scavenger receptor Stabilin-1 is expressed on tissue macrophages and sinusoidal endothelial cells, and its expression is induced during chronic inflammation and tumor progression. Stabilin-1 in the mammalian body is a transmembrane receptor that mediates endocytic and phagocytic clearance of unwanted-self components.[332] Stabilin-2 has a very similar extracellular domain organization with stabilin-1, but differs from this one, by its absence on macrophages, and by performing a solely classical endocytic function.[333,334] Stabilin-2 ligands include hyaluronic acid, AGE-modified BSA (advanced glycation end product-conjugated bovine serum albumin, formaldehyde-treated BSA, Collagen N-terminal propeptides etc.[335] Stabilin-1 and -2 together seem to guarantee proper clearance of the peripheral blood from potentially noxious agents and thus contribute to tissue homeostasis though out the whole body.[336] *In vivo*, these two receptors were shown to bind anionic macromolecules. The mannose receptor (Mrc1), is a C-type lectin with roles in immunity and glycoprotein homeostasis.[337,338]

In mammals, the receptor is expressed in several cell types, including most tissue macrophages, subsets of immature dendritic cells, LSECs, and lymph node sinusoidal

329 S. A. Mousavi, C. Fladeby, R. Kjeken, N. Boris, T. Berg, *Receptor-mediated endocytosis of immune complexes in rat liver sinusoidal endothelial cells is mediated by FcγRIIb2, Hepatology*, **2007**, *46*(3), 871-884.

330 D. M. E. Bowdish, K. Sakamoto, M. J. Kim, M. Kroos, S. Mukhopadhyay, C. A. Leifer, K. Tryggvason, S. Gordon, D. G. Russell, *MARCO, TLR2, and CD14 are required for macrophage cytokine responses to Mycobacterial trehalose dimycolate and Mycobacterium tuberculosis, PLoS Pathogens*, **2009**, *5*(6), 1-14.

331 T. H. Mogensen, *Pathogen recognition and inflammatory signaling in innate immune defenses, Clin. Microbiol. Rev*., **2009**, *22*(2), 240-273.

332 J. Kzhyshkwska, A. Gratchev, J. H. Martens, O. Pervushina, S. mamidi, S. Johansson, K. Schledzewski, B. Hansen, X. He, J. Tang, K. Nakayama, S. *Goerdt, Stabilin-1 localized to endosomes and the trans-Golgi network in human macrophages and interacts with GGA adaptors, J. Leukoc. Bio*l., **2004**, *76*, 1151-1161.

333 O. Politz, A. Gratchev,P. A. McCourt, K. Schledzewski, P. Guillot, S. Johansson, G. Svineng, P. Franke, C. Kannicht, J. Kzhyshkowska, P. Longati, F. W. Veltem, S. Johansson, S. Goerdt, *Stabilin-1 and -2 constitute a novel family of fasciclin-like hyaluronan receptor homologues, Biochem. J*., **2002**, *362*, 155-164.

334 M. Falkowski, K. Schledzewski, B. Hansen, S. Goerdt, *Expression of stabilin-2, a novel fasciclin-like hyaluronan receptor protein in murine sinusoidal endothelia, avascular tissues and at solid/liquid interfaces, Histochem. Cell. Biol*., **2003**, *120*, 321-369.

335 Y. Tamura, H. Adachi, J. Osuga, K. Ohashi, N. Yahagi, M. Sekiya, H. Okazaki, S. Tomita, Y. Iizuka, H. Shimano, R. Nagai, S. Kimura, M. Tsujimoto, S. Ishibashi, *FEEL-1 and FEEL-2 are endocytic receptors for advanced glycation end products. J. Biol. Chem.*, **2003**, *278*, 12613–12617.

336 B. Hansen et al., *Stabilin-1 and Stabilin-2 are both directed into early endocytic pathway in hepatic sinusoidal endothelium via interaction with clathrin/AP-2, independent of ligand binding, Exp. Cell. Res.,* **2005**, *303*(1), 160-173.

337 E. P. McGreal, L. Martinez-Pomares, S. Gordon, *Divergent roles for C-type lectins expressed by cells of the innate immune system, Mol. Immunol.*, **2004**, *41*, 1109-1121.

338 S. J. Lee, S. Evers, D. Roeder, A. F. Parlow, J. Risteli, L. Risteli, et al., *Mannose receptor-mediated regulation of serum glycoprotein homeostasis, Science*, **2002**, *295*, 1898-1901.

endothelial cells.[339,340] The Mrc1 has several domains responsible for its broad ligand-binding specificity.[341] These include eight C-type lectin-like domains, which are capable to bind carbohydrates with terminal D-mannose, L-fucose, or N-acetyl-D-glucosamine, an outer cysteine-rich domain, which binds some sulfated sugars, and fibronectin type II repeat, which binds collagens.[342,343,344,345] From this information, we can say that, scavenger receptors (SRs) comprise a large family of transmembrane cell surface glycoproteins and are mainly expressed in macrophages, dendritic cells and liver sinusoidal endothelial cells.[346] Their ability is to recognize and internalize modified low-density lipoproteins (LDLs), such as oxidized LDL and acetylated LDL. SRs have also many other important functions, for example, they are involved in the clearance of pathogens, nanoparticles and macromolecules, they participate in transport of cargo within cells, and in lipid transport.[347,348,349]

Many homologs of the mammalian scavenger receptor family were identified, not in the liver, but in in various other organs in the zebrafish genome.[8,350] In Danio rerio embryonic zebrafish, scavenger endothelial cells (SECs), were shown to be present in several large veins, including the posterior, common cardinal vein (PCV, CCV), and the caudal vein (CV), where they clear substances, colloidal nanoparticle waste and viral particles from the blood circulation as early as 28 h post fertilization (hpf). In **Figure 17**, the vascular anatomy of the developing zebrafish embryo has been shown in detail and has a high structural homology to other vertebrates.[351]

339 S. E. Pontow, V. Kery, P. D. Stahl, *Mannose receptor, Int. Rev. Cytol.*, **1992**, *137B*, 221-244.
340 K. H. Elvevold, G. I. Nedredal, A. Revhaug, B. Smedsrod, *Scavenger properties of cultivated pig liver endothelial cells, Comp. Hepatol.,* **2004**, *3*(4), 1-11.
341 S. Magnusson, T. Berg, *Extremely rapid endocytosis mediated by the mannose receptor of sinusoidal endothelial rat liver cells, Biochem. J*., **1989**, *257*, 651-656.
342 M. E. Taylor, K. Bezouska, K. Drickamer, *Contribution to ligand binding by multiple carbohydrate-recognition domains in the macrophage mannose receptor, J. Biol. Chem*., **1992**, *267*, 1719-1726.
343 D. J. Fiete, M. C. Beranek, J. U. Baenziger, *A cysteine-rich domain of the "mannose" receptor mediates GalNAc-4-SO4 binding, Proc. Natl. Acad. Sci.*, **1998**, *95*, 2089-2093
344 C. E. Napper, K. Drickamer, M. E. Taylor, *Collagen binding by the mannose receptor mediated through the fibronectin type II domain, Biochem. J*., **2006**, *395*, 579-586.
345 L. Martinez-Pomares, D. Wienke, R. Stillion, E. J. McKenzie, J. N. Arnold, J. Harris, et al., *Carbohydrate-independent recognition of collagens by the macrophage mannose receptor, Eur. J. Immunol.*, **2006**, *36*, 1074-1082.
346 J. E. Murphy, P. R. Tedbury, S. Homer-Vanniasinkam, J. H. Walker, S. Ponnambalam, et al., *Biochemistry and cell biology of mammalian scavenger receptors, Atherosclerosis,* **2005**, *182*, 1-15.
347 J. L. Goldstein, Y. K. Ho, S. K. Basu, M. S. Brown, *Binding site on macrophages that mediates uptake and degradation of acetylated low density lipoprotein, producing massive cholesterol deposition, Proc. Natl. Acad. Sci.*, **1979**, *76*, 333-337.
348 S. Xu, M, Laccotripe, X. Huang, A. Rigotti, V. I. Zannis, M. Krieger, *Apolipoproteins of HDL can directly mediate binding to the scavenger receptor SR-BI, an HDL receptor that mediates selective lipid uptake, J. Lipid Res*., **1997**, *38*, 1289-1298.
349 S. Pollock, R. Antrobus, L. Newton, B. Kampa, J. Rossa, S. Latham, et al., *Uptake and trafficking of liposomes to the endoplasmic reticulum, FASEB. J.*, **2010**, *24*, 1866-1878.
350 M. van der Vaart, H. P. Spaink, A. H. Meijer, *Pathogen Recognition and Activation of the Innate Immune Response in Zebrafish, Adv. Hematol*., **2012**, *2012*, 1-19.
351 S. Isogai, M. Horiguchi, B. M. Weinstein, *The vascular anatomy of the developing zebrafish: an atlas of embryonic and early larval development, Dev. Biol*., **2001**, *230*, 278-301.

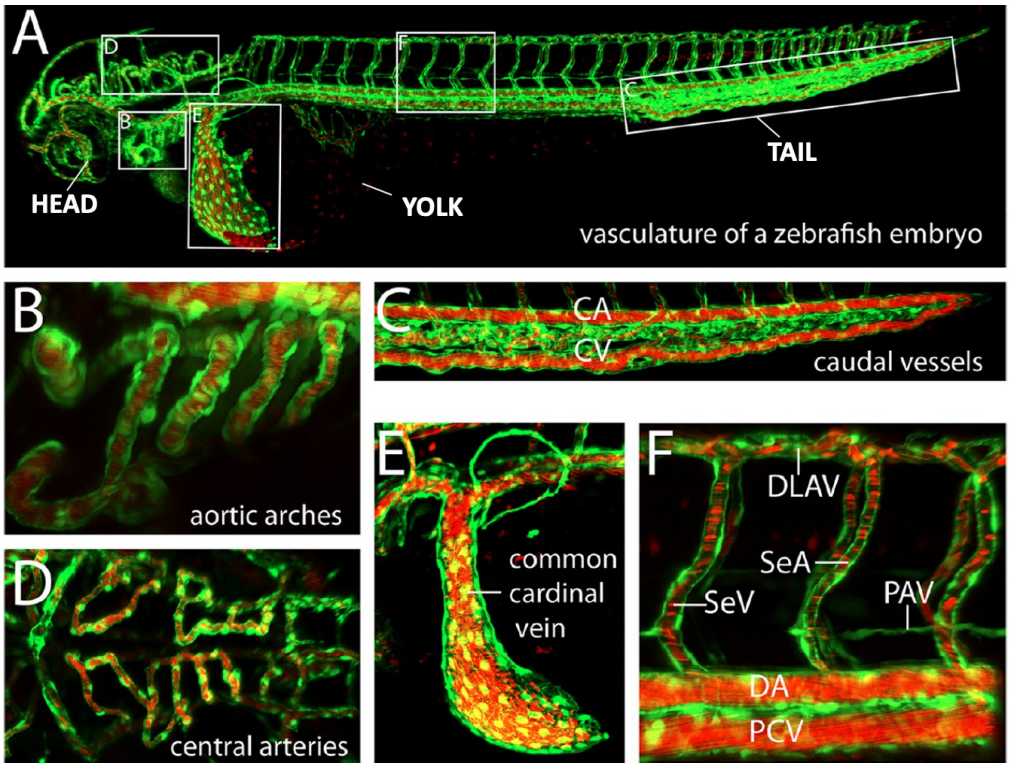

Figure 17. The vasculature of a double transgenic zebrafish embryo at 60 hpf. The vasculature is shown in green and was visualized by transgenic GFP expression. Blood cells, erythrocytes, are shown in red. (A–C), (E–F): later views; (D) dorsal view; (B–F) higher magnifications, showing in (B) the aortic arches; in (C) the caudal tail region including the caudal aorta (CA), The caudal vein (CV), and the caudal vein plexus; in (D) the central arteries (dorsal view); in (E) the common cardinal vein (CCV) and in (F) the intersegmental vessels (Se/ISV), consisting of intersegmental arteries (SeA) and intersegmental veins (SeV), the dorsal longitudinal anastomic vessel (DLAV), the parachordal vessel (PAV), and the dorsal aorta (DA) and posterior cardinal vein (PCV).[352]

The uptake of negative molecule by SECs in the CV is mainly dependent on the transmembrane receptor Stabilin-1 and -2.[353] Furthermore, zebrafish homologous of mammalian mannose receptor, called *mrc1a*, has been found in the cardinal vein, the tail plexus region and venous head vessels.[354] *Mrc1a* in zebrafish, as well as mrc1 in the mammalian cells, plays a role in the innate immune system by participating in the phagocytosis of microorganisms and in the antigen recognition and processing and in regulating serum glycoprotein homeostasis.[355,356]

352 A. Schuermann, C. S. M. Helker, W. Herzog, *Angiogenesis in zebrafish, Semin. Cell. Dev. Biol.*, **2014**, *31*, 106-114.
353 F. Campbell, F. L. Bos, S. Sieber, G. Arias-Alpizar, B. E. Koch, J. Huwyler, A. Kros, J. Bussmann, *Directing nanoparticle biodistribution through evasion and exploitation of stab2-dependent nanoparticle uptake, ACS nano,* **2018**, *12*, 2138-2150.
354 K. S. Wong, K. Proulx, M. S. Rost, S. Sumanas, *Identification of vasculature-specific genes by microarray analysis of Etsro/Etv2 overexpressing zebrafish embryos, Dev. Dyn*., **2009**, *238*, 1836-1850.
355 L. East, C. M. Isacke, *The mannose receptor family, Biochim. Biophys. Acta*., **2002**, *1572*, 364-386.
356 D. Lee, C. Park, H. Lee, J. J. Lugus, S. H. Kim, E. Arentson, Y. S. Chung, G. Gomez, M. Kyba, S. Lin, R. Janknecht, D. S. Lim, K. Choi, *ER71 acts downstream of BMP, Notch, and Wnt signaling in blood vessel progenitor specification, Cell. Stem. Cell.,* **2002**, *2*, 487-507.

On the basis of these considerations, the zebrafish shares a high degree of conservation with mammalian systems. Indeed, the genomes of the zebrafish and humans are highly related and contain orthologous genes encoding enzymes and regulatory molecules that control similar aspects of development and body homeostasis.[357] Moreover, many therapeutic agents used to treat human diseases have comparable effects in zebrafish embryos and humans.[358,359] The zebrafish are transparent during early larval stages, allowing investigators to directly observe internal structure development. Their small size, rapid development and short life cycle make zebrafish embryos logistically attractive for rapidly evaluating nanoparticle biodistribution effects.[360,361] The aim of the present work was to design and characterize a novel drug delivery nanosystem, based on glycolipid liposomes, for intracellular delivery in LSECs.

A novel drug delivery system was obtained by combining the advantages of synthetic sugar fatty acid esters and liposomes. In the Section II, liposomes were well established as carrier systems that accommodate therapeutic agents and deliver them to various sites in the body. Furthermore, liposomes can sustain the release of the entrapped active materials, hence enhancing the therapeutic outcome.[362] Fatty acid sugar esters, belonging to glycolipids, are amphiphilic, non-ionic molecules that consist of a hydrophilic carbohydrate moiety and one or more fatty acids as lipophilic tail.[363] The carbohydrate moieties, were amongst others monosaccharides like glucose, mannose, galattose or fucose, di- and trisaccharides like saccharose, fructose, lactose or maltose and oligo- and polysaccharides like starch, cellulose and pectin.[364,365,366,367] The substrate could be acylated using different fatty acids or other fatty

357 S. Saleem, R. R. Kannan, *Zebrafish: an emerging real-time model system to study Alzheimer's disease and neurospecific drug discovery, Cell Death Discovery*, **2018**, *4*(45), 1-13.

358 R. T. Peterson, S. Y. Shaw, T. A. Peterson, D. J. Milan, T. P. Zhong, S. L. Shreiber, C. A. MacRae, M. C. Fishman, *Chemical suppression of a genetic mutation in a zebrafish model of aortic coarcation, Nat. Biotechnol*., **2004**, *22*, 595-599.

359 L. I. Zon, R. T. Peterson, *In vivo drug discovery in the zebrafish, Nat. Rev. Drug. Discov*., **2005**, *4*, 35-44.

360 A. L. Rubinstein, *Zebrafish: from disease modelling to drug discovery, Curr. Opin. Drug Discov. Devel*., **2003**, *6*(2), 218-223.

361 A. Dodd, P. M. Curtis, L. C. Williams, D. R. Love, *Zebrafish: bridging the gap between development and disease, Hum. Mol. Genet.*, **2000**, *9*(16), 2443, 2449.

362 F. Szoka, D. Papahadjopoulos, *Comparative properties and methods of preparation of lipid vesicles (liposome), Annu. Rev. Biophys. Bioeng.*, **1980**, *9*, 467-508.

363 F. J. Plou, M. Cruces, M. Ferrer, G. Fuentes, E. Pastor, M. Bernabé, M. Christensen, F. Comelles, J. L. Parra, A. Ballesteros, Enzymatic acylation of di-and trisaccharides with fatty acids: choosing the appropriate enzyme, support and solvent, Journal of Biotechnology, **2002**, *96*, 55-66.

364 P. Degn, L. H. Pedersen, J. O. Duus, W. Zimmermann, *Lipase-catalysed synthesis of glucose fatty acid esters in tert-butanol, Biotechnology Letters*, **1999**, *21*, 275-280.

365 P. Pouillart, O. Douillet, B. Scappini, G. Antonella, V. Santini, A. Grossi, G. Pagliai, P. Strippoli, L. Rigacci, G. Ronco, P. Villa, *Regioselective synthesis and biological profiling of butyric and phenylalkylcarboxylic esters derivated from D-mannose and xylitol: influence of alkyl chain length on acute toxicity, European Journal of Pharmaceutical Sciences,* **1999**, *7*, 93-106.

366 G. Fregapane, D. B. Sarney, E. N. Vulfson, *Enzymic solvent-free synthesis of sugar acetal fatty acid esters, Enzyme and Microbial Technology,* **1991**, *13*, 796-800.

367 L. Lay, L. Panza, S. Riva, M. Khitri, S. Tirendi, *Regioselective acylation of disaccharides by enzymatic transesterification, Carbohydrate Research,* **1996**, *291*, 197-204.

acid derivates with varying chain length.[368,369] These sugar ester showing high emulsifying, stabilizing and detergent properties. They find application in different food, cosmetic, pharmaceutical cleaning products. They are also non-toxic, odor- and tasteless, completely biodegradable.[370,371]

The first objective of this work was to selectively produce novel glycolipids, using substrates originating from renewable resources. Three different glycolipids (MX_C18) were synthetized by one reaction step. Oleic monoesters of Glucose (MG_C18) and Mannose (MM_C18), were obtained by enzymatic reaction using Novozym 435.[372] Fucose oleic monoester was synthesized by chemical reaction under basic condition, using Pyridine and 2-(1H-Benzotriazole-1-yl)-1,1,3,3-tetramethylaminium tetrafluoroborate (TBTU) as catalyst.[373] The complete ^{1}H-NMR and ^{13}C NMR assignments of the compounds were carried out by using DEPT, HMBC, HSQC, NOESY and ^{1}H–^{1}H COSY spectra.

After that we worked on the preparation and characterization of all glyco-liposomes, that were prepared by thin film method. The synthetic glycolipid was incorporated into the lipid bilayer of DOPC fluorescent liposomes. These glyco-liposome nanosystems were used to identify the influence of glycolipid composition on liposome biodistribution and the mechanisms of liposome uptake by cells. Furthermore, liposome clearance by macrophages was studied using transgenic zebrafish embryos, lacking Stab-1, Stab-2 and mrc1a receptors, with fluorescently labeled glycol-liposomal formulations. The ultimate goal was tested the glico-liposomes mannose (mrc1) receptor-specificity and study their potential for delivery to LSECs in our recently zebrafish embryo model after intravenous injection.

2. Material and methods

1,2-dioleoyl-sn-glycero-3-phosphocholine (DOPC) was from Avanti Polar Lipids (Alabaster, AL), Lipase acrylic resin from Candida antartica (Novozym 435), D-Glucose, D-Mannose and L-Fucose were obtained from Sigma Aldrich Chemical (Steinheim, Germany) and 1,2-

368 N. R. Pedersen, R. Wimmer, R. Matthiesen, L. H. Pedersen, A. Gessesse, *Synthesis of sucrose laurate using a new alkaline protease, Tetrahedron-Asymmetry,* **2003**, *14*, 667-673.

369 J. F. Cramer, M. S. Dueholm, S. r. B. Nielsen, D. S. Pedersen, R. Wimmer, L. H. Pedersen*, Controlling the degree of esterification in lipase catalysed synthesis of xylitol fatty acid esters, Enzyme and microbial technology*, **2007**, *41*, 346-352.

370 Y. Yan, U. T. Bornscheuer, L. Cao, R. D. Schmid, *Lipase-catalyzed solid-phase synthesis of sugar fatty acid esters: removal of byproducts by azeotropic distillation, Enzyme and microbial technology,* **1999**, *25*, 725-728.

371 S. Sabeder, M. Habulin, Z. Knez, *Lipase-catalyzed synthesis of fatty acid fructose esters, Journal of Food Engineering*, **2006**, *77*, 880-886.

372 D. Coulon, A. Ismail, M. Girardin, B. Rovel, M. Ghoul, *Effect of different biochemical parameters on the enzymatic synthesis of fructose oleate, Journal of biotechnology*, **1996**, *51*, 115-121.

373 B. Tang, K. H. Row, *Recent developments in deep eutectic solvents in chemical sciences, Monatshefte für Chemie-Chemical Monthly*, **2013**, *144*, 1427-1454.

dipalmitoyl-sn-glycero-3-phosphoethanolamine-N-(lissamine rhodamine B sulfonyl) ammonium salt (DPPE-Rho) was purchased from Avanti Polar Lipids (Birmingham, AL, USA). Oleic acid and O-(Benzotriazol-1-yl)-N,N,N',N'-tetramethyluronium tetrafluoroborate (TBTU) were from Fluorchem. All organic solvents used in the study were purchased from Sigma and prior to use, acetone was dried with molecular sieves with an effective pore diameter of 4 Å. Column chromatography purifications were performed under "flash" conditions using Merck 230–400 mesh silica gel. TLC was carried out on Merck silica gel 60 F254 plates, which were visualized by exposure to ultraviolet light and by exposure to an aqueous solution of ceric ammonium molybdate (CAM). The structures of compounds were characterized by ^{1}H NMR,^{13}C NMR, and High-resolution mass spectrometry (HRMS). ^{1}H-NMR, ^{13}C-NMR, DEPT, HMBC, HSQC, NOESY and ^{1}H–^{1}H COSY spectra were recorded on a Bruker AV-500 (500 and 125 MHz respectively) or a Bruker DMX-600 (600 and 151 MHz) spectrometer in DMSO. Chemical shifts are given in ppm relative to the residual solvent peak as internal standard. Coupling constants are given in Hz. High-resolution mass spectrometry (HRMS) analysis was performed with a LTQ Orbitrap mass spectrometer (Thermo Finnigan), equipped with an electronspray ion source in positive mode (source voltage 3.5 kV, sheath gas flow 10 mL/min, capillary temperature 250°C) with resolution R = 60000 at m/z 400 (mass range m/z = 150 - 2000) and dioctyl phthalate (m/z = 391.28428) as a "lock mass". The high resolution mass spectrometer was calibrated prior to measurements with a calibration mixture (Thermo Finnigan). All organic solvents used in the study were purchased from Sigma and prior to use, acetone was dried with molecular sieves with an effective pore diameter of 4 Å. Phosphate-buffered saline, (PBS: 140 mM NaCl, 8.7 mM Na_2HPO_4. 12 H_2O, 1.8 mM NaH_2PO_4 2 H_2O, pH 7.4), was purchased from B. Braun (Meslungen, Germany) PBS-buffer was diluted with deionized water to obtain 10 mM PBS, which was used for liposome formulations.

2.1. Synthesis of MX_C18 glycolipids

MX_C18 was synthesized and purified as described below. The final identity and purity of the resulting compounds were confirmed by NMR techniques.

2.1.1. Synthesis and characterization of 6-O-Oleoyl-Glucose (1a)

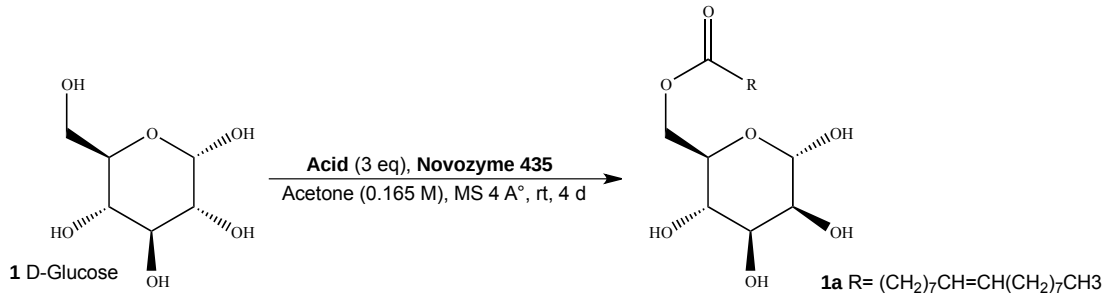

Scheme 2. Synthesis of MG_C18.

Novozym 435 (0.168 g) was added to a solution of oleic acid (0.475 g, 1.68 mmol, 0.531 mL), molecular sieves (0.336 g) and D-(+)-glucose (**1**) (0.100 g, 0.56 mmol) in 3.39 mL of acetone (0.165 M). The mixture was stirred at 25°C for 4 days, diluted with acetone, then filtered, and the filtrate was concentrated. The purification of the residue by column chromatography (cyclohexane/ethyl acetate 6:4) gave **1a** (GM_C18) pale white oil. Yield: 20% (0.050 g).[374]

^{1}H NMR (500 MHz, DMSO-d_6) δ 6.33 (d, J = 4.5 Hz, 1H, OH^{1}), 5.32 (ddd, J = 4. 9, 4.2, 1.0 Hz, 2H, H^{15}, H^{16}), 5.02 (d, J = 5.1 Hz, 1H, H^{4}), 4.89 (dd, J = 3.8 Hz, 1H, H^{1}), 4.74 (bs, 1H, OH^{3}), 4.51 (d, J = 5.0 Hz, 1H, OH^{2}), 4.26 (dd, J = 1.9, 11.6 Hz, 1H, H^{6}), 3.99 (dd, J = 5.5, 17.9 Hz, 1H, $H^{6'}$), 3.77 (ddd, J = 2.0, 6.2, 10.1, Hz, 1H, H^{5}), 3.42 (dd, J = 9.2 Hz, 1H, H^{3}), 3.12 (m, 1H, H^{2}), 3.04 (ddd, J = 4.2, 9.2 Hz, 1H, H^{4}), 2.26 (t, J = 7.5, Hz, 2H, H^{8}), 1.98 (m, 4H, H^{14}, H^{17}), 1.49 (m, 2H, H^{9}), 1.33 – 1.19 (m, 20H, -CH2- chain length oleic acid), 0.87 – 0.83 (t, J = 14.07, 3H, H^{24}) ppm. **^{13}C NMR** (500 MHz, DMSO-d_6) δ 172.88 (C^{7}), 129.63 (C^{15}, C^{16}), 92.27 (C^{1}), 72.85 (C^{3}), 72.18 (C^{2}), 70.55 (C^{4}), 69.12 (C^{5}), 63.87 (C^{6}), 40.01, 39.84, 39.68, 39.51, 39.34, 39.18, 39.01, 33.42 (C^{8}), 31.26, 29.08, 28.82, 28.67, 28.59, 28.57, 28.48, 28.42, 26.58 (C^{14}), 26.55 (C^{17}), 24.45 (C^{9}), 22.07, 13.93 (C^{24}) ppm. NOESY (500 MHz, DMSO-d_6) showed α anomer formation. HRMS measured value: [M+Na^{+}] 467.29779; calculated: 467.29848.

2.1.2. Synthesis and characterization of 6-O-Oleoyl-Mannose (2a)

374 S. Lucarini, et al., *Unsaturated fatty acids lactose esters: Cytotoxicity, permeability enhancement and antimicrobial activity, Eur. J. Pharm. Biopharm*., **2016**, *107*, 88-96.

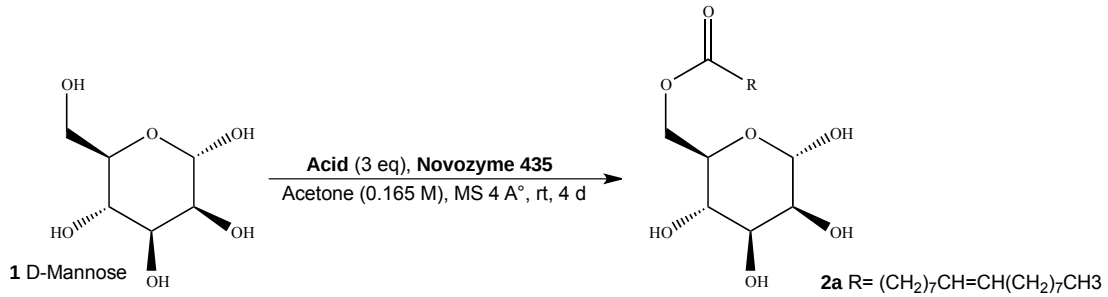

Scheme 3. Synthesis of MM_C18.

Novozym 435 (0.168 g) was added to a solution of oleic acid (0.475 g, 1.68 mmol, 0.531 mL), molecular sieves (0.336 g) and D-(+)-mannose (**1**) (0.100 g, 0.56 mmol) in 3.39 mL of acetone (0.165 M). The mixture was stirred at 25°C for 4 days, diluted with acetone, then filtered, and the filtrate was concentrated. The purification of the residue by column chromatography (cyclohexane/ethyl acetate 6:4) gave **2a** (**MM_C18**) pale white oil. Yield: 48% (0.120 g).

^{1}H NMR (500 MHz, DMSO-d_6) δ 6.34 (d, J = 4.2 Hz, 1H, OH^{1}), 6.22 (d, J = 8.4 Hz, 1H, $OH^{1'}$), 5.32 (m, 2H, H^{15},H^{16}), 4.85 (bs, 2H, H^{1}, OH^{4}), 4.59 (d, J =3.7 Hz, 1H, OH^{2}), 4.57 (bs, 1H, OH^{3}), 4.28 (dd, J = 11.5, 1.9 Hz, 1H, H^{6}), 4.00 (dd, J = 11.8, 6.9 Hz, ^{1}H, $H^{6'}$), 3.70 (dd, J = 15.5 Hz, 1H, H^{5}), 3.60 – 3.46 (m, 2H, H^{3}, H^{2}), 3.39 (m, 1H, H^{4}), 2.27 (d, J = 7.3 Hz, 2H, H^{8}), 1.98 (m, 4H, H^{14}, H^{17}), 1.51 (m, 2H, H^{9}), 1.26 (m, 20H, -CH2- oleate), 0.85 (t, J = 6.8 Hz, 3H, H^{24}). **^{13}C NMR** (500 MHz, DMSO-d_6) δ 172.95 (C^{7}), 129.62 (C^{15}, C^{16}), 94.05 (C^{1}), 71.29 (C^{2}), 70.37 (C^{5}), 70.36 (C^{3}), 67.15 (C^{6}), 64.25 ($C^{6'}$), 40.01, 39.84, 39.68, 39.51, 39.34, 39.18, 39.01, 33.45 (C^{8}), 33.40, 31.28, 29.11, 28.84, 28.69, 28.63, 28.60, 28.52, 28.49 (C^{14}), 26.61 (C^{17}), 26.57, 24.45 (C^{9}), 22.09, 13.93 (C^{24}). NOESY (500 MHz, DMSO-d_6) showed α and β anomers formation 3:7 respectively. NOESY (500 MHz, DMSO-d_6) showed α/β anomer formation with a ratio of approximately 7:3. HRMS measured value: [M+Na^{+}] 467.29771; calculated: 467.29848.

2.1.3. Synthesis and characterization of 2-O-Oleoyl-Fucose (3a)

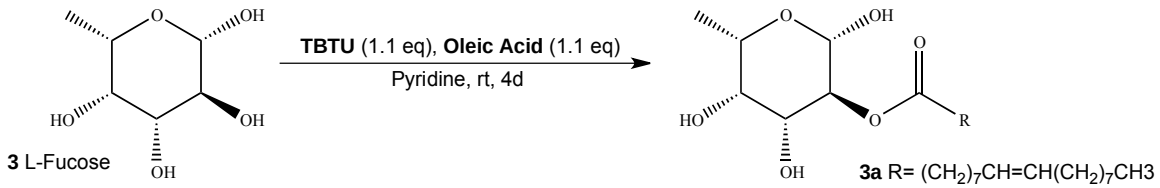

Scheme 4. Synthesis of MF_C18.

Oleic acid (0.282 g, 1.0 mmol) and TBTU (0.321 g, 1.0 mmol) were dissolved in anhydrous pyridine (5 mL) in a oven-dried round-bottomed flask. The resulting mixture was stirred at rt for 30 min under nitrogen atmosphere. A solution of L-Fucose (**3**) (0.150 g, 0.91 mmol) in pyridine (3 mL) was then injected into the reaction mixture and stirring was continued at room temperature for 4 days. The reaction was then diluted with dichloromethane, washed with 10 mL of saturated sodium bicarbonate solution for three times. The combined organic phases were dried over Na_2SO_4 and the solvent was removed under reduced pressure.[375] The residue was crystallized from diethyl ether and pentane giving **3a** (**FM_C18**). Yield: 10% (0.040 g)

^{1}H NMR (500 MHz, DMSO-d_6) δ 6.56 (d, J = 6.4 Hz, 1H, OH^1), 5.35 – 5.29 (m, 2H, H^{15}, H^{16}), 4.74 (dd, J = 9.6, 7.9 Hz, 1H, H^2), 4.67 (m, 2H, OH^3, OH^4), 4.41 (dd, J = 7.9, 6.4 Hz, 1H, H^1), 3.55 (m, 1H, H^5), 3.49 – 3.42 (m, 2H, H^3, H^4), 2.25 (td, J = 7.4, 2.6 Hz, 2H, H^8), 2.00 – 1.95 (m, 4H, H^{14}, H^{17}), 1.50 (t, J = 7.2 Hz, 2H, H^9), 1.28 – 1.17 (m, 20H, -CH2- oleate), 1.12 (d, J = 6.4 Hz, 3H, $-CH_3{}^6$), 0.85 (t, J = 7.1, 7.0, 0.6 Hz, 3H, H^{24}). **^{13}C NMR** (500 MHz, DMSO-d_6) δ 172.08 (C^7), 129.63 (C^{15}, C^{16}), 94.67 (C^1), 73.50 (C^2), 71.40 (C^3), 71.28 (C^4), 69.77 (C^5), 40.01, 39.84, 39.68, 39.51, 39.34, 39.18, 39.01, 33.80 (C^8), 31.27, 29.11, 29.09, 28.83, 28.68, 28.65, 28.59, 28.52, 28.39 (C^{14}), 26.61(C^{17}), 26.57, 24.56 (C^9), 22.09, 16.55 ($-CH_3{}^6$), 13.95 (C^{24}). NOESY (500 MHz, DMSO-d_6) showed β anomer formation. HRMS measured value: [M+Na^+] 451.30269; calculated: 451.30356.

2.2. Glyco-liposome preparation

All glyco-liposomes were prepared by thin film method as describes previously.[376,35] Appropriate amounts of DOPC, glycolipid (**XM_C18**) and DPPE-Rho were dissolved in $CHCl_3$–MeOH (2:1, v/v) and mixed in a clean vial, at a molar ratio 79: 20: 1 respectively, to obtain a final lipid concentration of 1.5 mg/mL. The solvents were evaporated under a stream of N_2 at 40°C and then 1h under vacuum until complete dryness. The lipid film was formed and rehydrated with 1 mL of PBS (10 mM, pH 7.4) at 65°C. The mixture was vortexed for 3 minutes and then the multilamellar vesicles were sized by extrusion at 65°C (Mini-extruder with heating block, Avanti Polar Lipids, Alabaster, US). The hydrated lipids were passed 11 times through 2 × 400 nm polycarbonate (PC) membranes (Nucleopore Track-Etch

375 K. P. Nawal, K. T. Jeand-d'Amour,T. B. Grindley, Direct Synthesis of Marolipids and other Trehalose 6-Monoesters and 6,6'-Diesters, J. Org. Chem., 2013, 78(2), 363-369.

376 A. D. Bangham, M. M. Standish, J. C. Watkins, *J. Mol. Biol*., *Diffusion of univalent ions across the lamellae of swollen phospholipids*, **1965**, *13*, 238-252.

membranes, Whatman), followed by 11 times through 2 × 100 nm PC pores, to obtain monodisperse liposomes. Liposomes were stored at 4 °C and used for further experiments.

2.2.1. Glyco-liposome characterization

Size, polydisperity, zeta-potential, NTA and UPLC analysis – The *Z*-average diameter (Z_{ave}) and polydispersity index (PDI) of the liposomes were measured by dynamic light scattering (DLS) using a NanoZS Zetasizer (Malvern Ltd., Malvern, UK). Zeta-potential was determined by using laser Doppler electrophoresis using the same instrument. For measurements, the liposomes were diluted 10-fold in 10 mM saline phosphate buffer at pH 7.4 to a total volume of 1 mL. NanoSight NS500 instrument (Malvern Panalytical, UK) was used for particle size determination, in this case the liposomes were diluted 100-fold in 10 mM PBS buffer to a volume of 100 µl. A reversed-phase UPLC (Waters ACQUITY UPLC, Waters, MA, USA) analysis, with evaporative light-scattering (ELSD) and fluorescence detectors, were adapted to determine the concentrations of DOPC, glycolipid (XM_C18) and DPPE-Rho.[377] For this, 10 µl of the sample was injected into a C18 column (ACQUITYUPLC®BEHC18 1.7 µm, 2.1 × 50 mm). The column temperature and the temperature of the sample were set at 40 °C. The mobile phases were Milli-Q water (solvent A) and acetonitrile with 0.1% TFA (solvent B). For detection, the mobile phases were applied in a linear gradient from 55% to 100% solvent B over 6 min at a flow rate of 0.500 mL/min (**Table 10.**)

Time	Flow (mL/min)	% Solvent A	% Solvent B
Initial	0.500	45.0	55.0
2.00	0.500	0.0	100.0
8.00	0.500	0.0	100.0
8.10	0.500	45.0	55.0

Table 10. Gradient elution method for quantitative analysis of DOPC, glycolipid (XM_C18) and Rho-DPPE.

Cryo-TEM – Morphological analysis was carried out by cryo-Transmission Electron Microscopy (cryo-TEM) using a Talos L120C transmission electron microscope (Philips, Leiden, The Netherlands).[378] Samples for cryo-TEM were prepared under controlled temperature and humidity conditions within an environmental vitrification system. A small droplet (4 µL) of undiluted samples, was deposited onto a Pelco easiGlow Formvar carbon-

377 G. A. Hayner, S. Khetan, M. G. Paulick, Quantification of the Disaccharide Trehalose from Biological Samples: A comparison of Analytical Methods.

378 M. Almgre, E. G. Karlsson, *Cryo transmission electron microscopy of liposomes and related structures, Colloids and Surface A: Physicochem. End Engineering Astpects*, **2000**, *174*(1-2), 3-21.

filmed grid, for 60 seconds and spread carefully. The samples were immediately plunged into liquid ethane and kept at -180°C. All observations were made in the bright. Field mode at an acceleration voltage of 120kV.

2.3. *In vivo* experiments

2.3.1. Animal: Zebrafish strains and maintenance

Zebrafish (Danio rerio) were maintained and handled according to the guidelines from the Zebrafish Model Organism Database (http://zfin.org) and in compliance with the directives of the local animal welfare committee of Leiden University. Fertilization was performed by natural spawning at the beginning of the light period and eggs were raised at 28.5oC in egg water (60 ug/mL Instant Ocean sea salts). The stains AB/TL, *Tg(kdrl:GFP)*, *stab1*^{ibl3}, *stab2*^{ibl2} and *mrc1a.*$^{-7bp}$were used.[35,379,380]

2.3.2. Zebrafish intravenous injections and imaging

Glyco-liposomes were injected into 2-day old zebrafish embryos (52-56 hpf) using a modified microangraphy protocol as described previously. Briefly, 1 nl of the liposome formulation was injected into the Duct of Cuvier after embryos were embedded in 0.4% agarose containing 0.01% tricaine. Mannan isolated from *Saccharomyces cerevisiae* (Merck) was dissolved in milliQ water and 1nl was injected at 50mg/mL 15 minutes prior to liposome injections. After injection, embryos were mechanically removed from the agarose and scored for fluorescent signal throughout the vascular system. Embryos without fluorescence, or with damage to the yolk ball were excluded for further analysis. Subsequently, fish were randomly selected and imaged by confocal microscopy four hours post injection. Confocal z-stacks were captured on a Leica TCS SPE or LEICA TCS SP8 confocal microscope, using a 10x air objective (HCX PL FLUOTAR) or a 40x water-immersion objective (HCX APO L). In order to compare images between strains, microscopy settings (laser intensity, gain and offset) were identical between stacks and sessions. Whole-embryo images were a compilation of 3-4 overlapping z-stacks. Fiji distribution of ImageJ was used to process images.

3. Result and discussion

3.1. Synthetic procedure to obtain glycolipids

379 S. W. Jin, D. Beis, T. Mitchell, J. N. Chen, D. Y. Stainier, *Cellular and molecular analyses of vascular tube and lumen formation in zebrafish, Development*, **2005**, *132*(23), 5199-5209.

380 Y. Padberg, A. van Impel, M. van Lessen, J. Bussmann, S. Shulte-Marker, Meningeal lymphatic endothelial cells fulfill scavenger endothelial cell function and employ Mrc1a for a cargo uptake, bioRxiv, **2019**. http://dx.doi.org/10.1101/691477

6-O-Oleoyl-Glucose (**GM_C18**) and 6-O-Oleoyl-Mannose (**MM_C18**) were obtained by enzymatic reaction. Candida antartica lipase catalyzed the acylation of the 6-O'-hydroxyl group of glucose and mannose in acetone. The presence of 4Å molecular sieves significantly increased the conversion by the removal of water from the reaction mixture.[381,382] The structures of compounds were unambiguously assessed by ^{1}H NMR and ^{13}C NMR and High-resolution mass spectrometry (HRMS). The alpha conformation of the glucopyranoside is confirmed by the presence of spatial coupling between H^1 and H^2, as observed by NOESY-NMR. Furthermore, the 7:3 alpha/beta ratio of the mannose ester is determined by H-NMR and the preference for the alpha anomer is confirmed by NOESY-NMR, where it's possible to identify the coupling between H^1 and H^4.

2-O-Oleoyl-Fucose was synthesized non-enzymatically under basic conditions. 1.1 equivalents TBTU promoted esterification of L-fucose in pyridine, with 1.1 equivalents of oleic acids. After work up, the reaction mixture was crystallized from diethyl ether and pentane giving 2-O-monoesters **3a** in 10% yield after 4 days reaction time.[57] The starting L-fucose was not completely consumed during the 4 days of reaction time and the opened fucose ester was formed as a side product of this reaction and isolated by column chromatography (cyclohexane/ethyl acetate 6:4). Nuclear magnetic resonance ^{1}H NMR and ^{13}C NMR analysis were performed to characterize **FM_C18**. In this case, the coupling constant between H^1 and H^2 (7.9 Hz) and the chemical shift of the anomeric proton (4.40 ppm), as can be seen in the ^{1}H NMR, in combination with the chemical shift of the anomeric carbon (94.67 ppm) suggest a beta-L-fucose configuration (See **Supporting Information**).

3.2. Synthesis and characterization of glycol-liposomes

Glycolipid were synthesized as described previously and incorporated into the layer of DOPC liposomes by the thin-film method combined with extrusion at a molar ratio of 20 mol%. These glyco-liposomes obtained, were than characterized and analysed with NTA and DLS techniques (**Table 11**).

381 M. Oosterom Woudnberg-van, F. Van Ratwijik, R. A. Sheldon, *Regioselective acylation of disaccharides in tert-butyl alcohol catalyzed by Candida antartica lipase, Biotechnol. Bioeng*., **1996**, *49*, 328-333.

382 X. Zhang, T. Kobayashy, Y. Watanabe, T. Fujii, S. Adachi, R. Matsumo, *Lipase-Catalyzed synthesis of monolauroyl maltose through condensation of maltose and lauric acid, Food Sci Technol. Res*., **2003**, *9*, 110-113.

	DLS			*NTA*		
FORMULATION	**z-Average (nm)**	**PDI**	**Z-Potential (mV)**	**Mean (nm)**	**SD (nm)**	**Particle Conc. (E8/mL)**
BLANK SAMPLE	98.08 ± 1.019	0.081 ± 0.013	-16.4 ± 2.23	117.4 ± 1.0	25.5 ± 2.9	26.4
DOPC/MM_C18	97.17 ± 0.465	0.070 ± 0.013	-16.0 ± 1.59	93.4 ± 2.2	21.2 ± 4.6	2.98
DOPC/GM_C18	100.6 ± 0.153	0.079 ± 0.020	-20.0 ± 0.814	105.6 ± 1.5	30.8 ± 2.0	5.98
DOPC/FM_C18	94.05 ± 0.254	0.098 ± 0.014	-20.4 ± 2.74	110.5 ± 1.3	41.7 ± 1.7	2.93

Table 11. Mean Size and Size distribution of glycol-liposomes from NTA an DLSW MeasurementsPDI polydispersity index; SD standard deviation calculated by NTA software, Conc. Concentration in particles E8/mL as measured by NTA. Numbers represent average values standard deviation (n= 3 measurements).

DLS showed a Z-average of about ~100 nm with a PDI < 0.1 and a Z-potential -18 mV for all the glycol-liposome formulations. (**Figure 18.**).

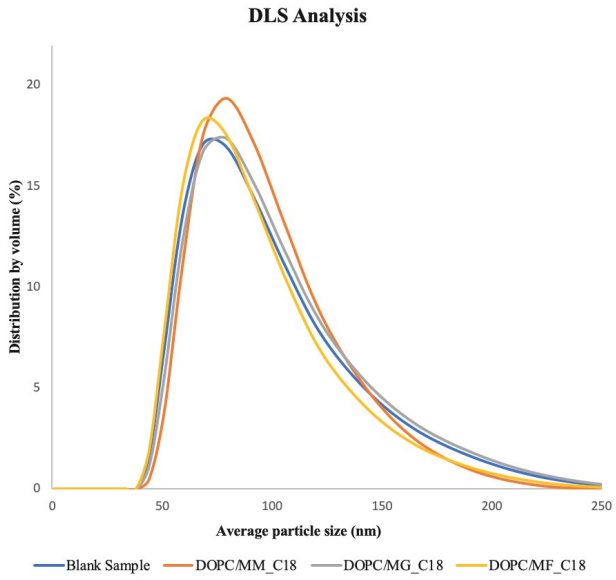

Figure 18. A representative volume-based particle size distribution of glyco-liposomes formulations.

The mean value observed with NTA (~106.72 nm) was slightly higher than the Z-ave given by DLS for the blank sample, glucose and fucose liposomes (**Figure 19.**).

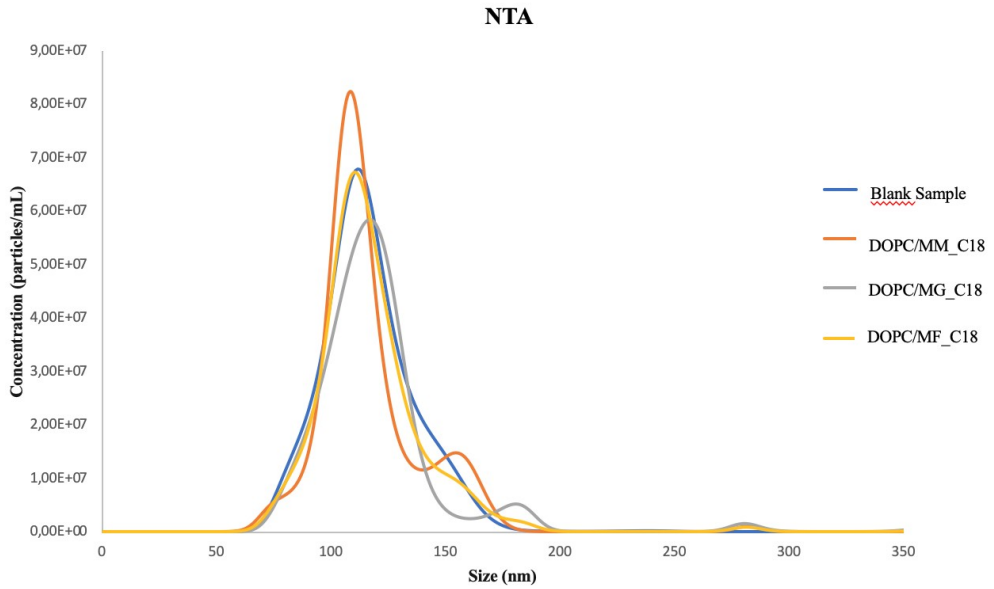

Figure 19. Particle size distribution of liposomes from NTA. The determined particle concentration is reported y-axis.

Nevertheless, a good consistency in liposome size distributions between NTA and DLS analysis was observed. The data obtained shown a homogeneous particle size distribution for all glycol-liposome formulations.

Cryo-TEM images confirmed the formation of liposomes with an approximate size of 130–150 nm as illustrated by representative DOPC/MM_C18 glyco-liposomes.

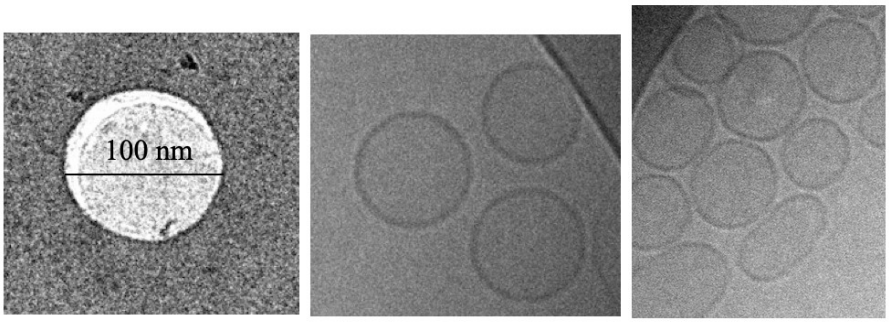

Figure 20. Cryo-TEM images of DOPC/MM_C18 glyco-liposome formulation.

UPLC method, with ELSD and IR detectors, was used to quantify lipids within the DOPC/MX_C18 glyco-liposome adjuvant system. Standard solution of DOPC (0.5 to 0.0039 mg/mL), MM_C18 (0.5 to 0.0039 mg/mL), MG_C18 (0.222 to 0.0017 mg/mL), MF_C18 (0.214 to 0.0016 mg/mL) and DPPE-Rho (0.05 to 0.0003 mg/mL) were prepared in methanol. Solutions were injected into the UPLC system prior to each measurement in order to establish the calibration curves and as a reference check. For quantification, established calibration

curves were used. The system was flushed with 100% acetonitrile with 0.1% TFA (solvent B) before each use for 8 min until a stable baseline was observed. **Figure 21.** shows the chromatograms of the different glyco-liposome formulations.

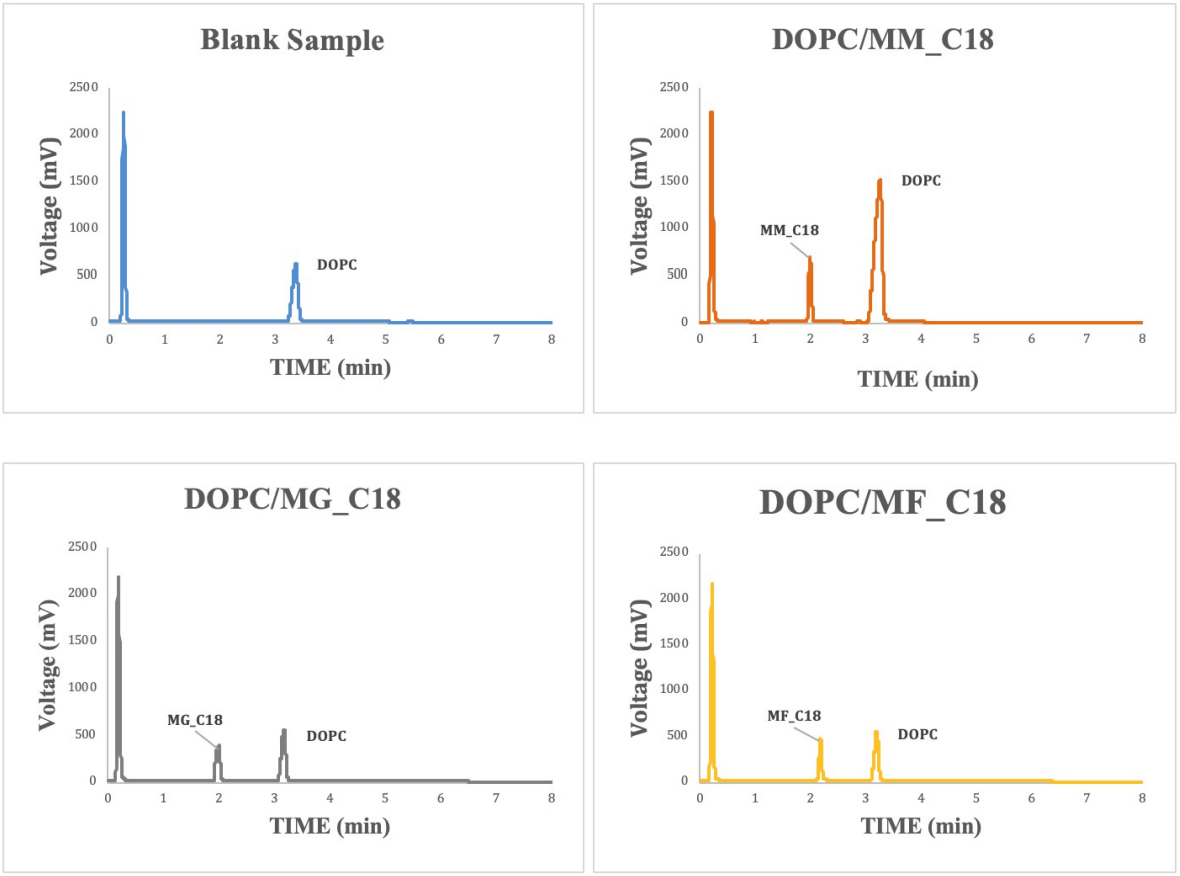

Figure 21. ELSD-detected UPLC chromatogram of glycol-liposome formulations.

Elution peaks were well separated with a stable baseline. The DOPC/MX_C18 liposome formulations were quantified by integration of the area under the curve of the standards (**Table 12.**).

Formulation	DOPC (MM)	MX_C18 (mM)	Rho-DPPE (mM)
BLANK SAMPLE	1.076	/	0.0107
DOPC/ MG_C18	1.064	0.531	0.0114
DOPC/MM_C18	1.109	0.476	0.0116
DOPC/MF_C18	1.082	0.583	0.0109

Table 12. Total mM concentration of glycoliposomes

The final concentration of DOPC and MG_C18/MM_C18/MF_C18 were about 1.6 mg/mL. Lipid quantification revealed a good average recovery values, after extrusion method, for each

of the lipids of the glico-liposome formulations. The lipid recovery was in the range of 95-99% (Data show in **Supporting information**).

3.3. *In vivo* analysis

Of the myriad nanoparticles reported as potential drug delivery vectors, liposomes are the most widely investigated and the major class of nanoparticles approved for clinical use.[383,384] So far, the ability to predict the fate of liposomes following intravenous injection based on lipid composition alone has been limited. Moreover, the opacity of mammalian models precludes limited comprehensive assessment of the dynamic behavior of liposomes *in vivo*. Recent studies have shown that the small and transparent zebrafish embryo allows for the direct observation of circulatin NPs, including liposomes, and their interaction with cells.[385,386,387,388] T

hese studies show key aspects of NPs behavior, including uptake by MPS, are conserved between zebrafish and mammals. We therefore selected this model to identify the influence of glycolipid composition on liposome biodistribution and the mechanisms of liposome uptake by cells. Fluorescently labeled glycol-liposomes (100 nm in diameter and without encapsulated drugs) were injected intravenously into the duct of Cuvier of Zebrafish embryos at 52-56 h post-fertilization (hpf), a stage which most organ systems are established. Injected embryos were imaged using confocal microscopy at 4 h post injection (hpi), and confocal micrographs were generated for the entire embryo (whole osganism level) as well as from a region caudal to the coaca (tissue level) (**Figure 22.**).

3.3.1. Distribution of glyco-liposomes in zebrafish embryos

As a first evaluation of *in vivo* functionality of the generated liposomes, 2-day old zebrafish embryos were intravenously injected with the liposomal formulations as described previously.

383 T. M. Allen, P. R. Cullis, *Liposomal Drug Delivery Systems: From Concept to Clinical Applications. Adv. Drug Delivery Rev.*, **2013**, *65*, 36−48.

384 L. Sercombe, T. Veerati, F. Moheimani, S. Y. Wu, A. K. Sood, S. Hua, *Advances and Challenges of Liposome Assisted DrugDelivery, Front. Pharmacol*., **2015**, *6*, 286.

385 L. Evensen, P. L. Johansen, G. Koster, K. Zhu, L. Herfindal, M. Speth, F. Fenaroli, J. Hildahl, S. Bagherifam, C. Tulotta, L. Prasmickaite, G. M. Maelandsmo, E. Snaar-Jagalska, G. Griffiths, *Zebrafish as a Model System for Characterization of Nanoparticles against Cancer, Nanoscale,* **2016**, *8*, 862−877.

386 F. Fenaroli, D. Westmoreland, J. Benjaminsen, T. Kolstad, F. M. Skjeldal, A. H. Meijer, M. Van Der Vaart, L. Ulanova, N. Roos, B. Nyström, J. Hildahl, G. Griffiths, *Nanoparticles as Drug Delivery System against Tuberculosis in Zebrafish Embryos: Direct Visualization and Treatment, ACS Nano,* **2014**, *8*, 7014−7026.

387 X. Y. Jiang, C. D. Sarsons, M. J. Gomez-Garcia, D. T. Cramb, K. D. Rinker, S. J. Childs, *Quantum Dot Interactions and Flow Effects in Angiogenic Zebrafish (Danio Rerio) Vessels and Human Endothelial Cells, Nanomedicine,* **2017**, *13*, 999−1010.

388 S. Sieber, P. Grossen, P. Detampel, S. Siegfried, D. Witzigmann, J. Huwyler, *Zebrafish as an Early Stage Screening Tool to Study the Systemic Circulation of Nanoparticulate Drug Delivery Systems in Vivo, J. Controlled Release*, **2017**, *264*, 180−191.

Compared to control liposomes, all formulations containing glycolipids displayed an altered biodistribution, 4 hours post injection (hpi, **Figure 22.**).

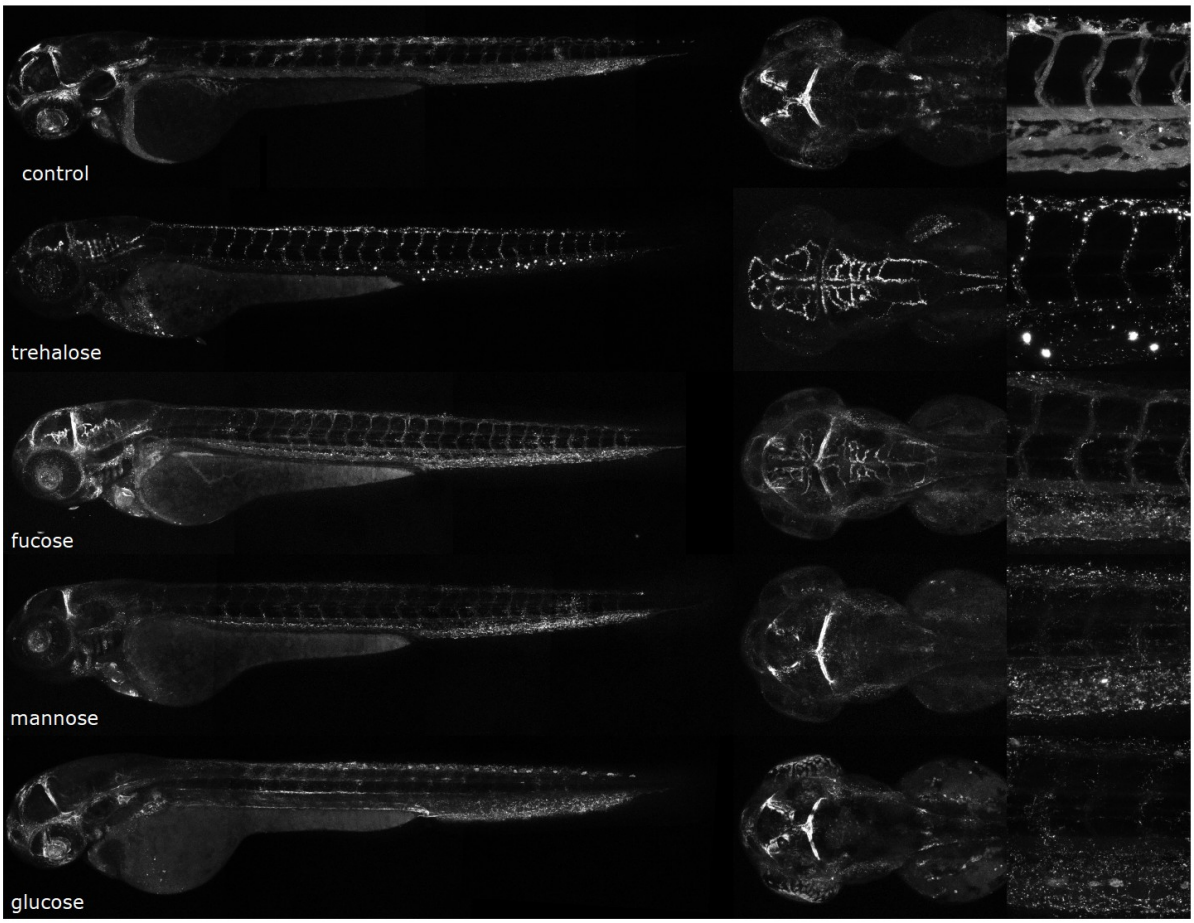

Figure 22. Confocal microscopy images. On the left: whole-embryo view of liposome distribution in zebrafish embryos; on the right: micrographs from the region caudal.

While control liposomes composed of DOPC were still mostly circulating throughout the vascular system, with significant extravasation and limited uptake by plasma-exposed macrophages. Enrichment of DOPC was also liposomes was observed on the dorsal head vasculature and in the first aortic arch artery, but no clearance by scavenger endothelial cells – homologous to liver sinusoidal endothelial cells, was observed.

This result is identical to the previous analysis of this formulation in zebrafish embryos. Addition of trehalose-C18 to DOPC-liposomes dramatically changed their biodistribution, with an almost complete plasma clearance at 4hpi. In embryos injected with this formulation, localization to the dorsal head vasculature and first aortic arch artery was absent. Instead, liposomes were cleared much more efficiently by plasma-exposed macrophages – homologous to liver Kupffer cells in mammals.

Importantly, a strong enrichment of trehalose-containing liposomes was observed on the endothelial cells that comprise the zebrafish blood-brain-barrier.[389] These cells are present throughout the brain vasculature and within the dorsal aspect of the intersegmental vessels where these are in contact with the spinal cord.

For fucose-containing liposomes, we observed a similar but weaker enrichment compared to trehalose-containing liposomes at the blood-brain barrier. Also, at 4hpi an important part of the injected dose was still present in circulation, and their distribution was similar to control liposomes, with the exception of increased clearance by scavenger endothelial cells.

Importantly, clearance by scavenger endothelial cells was most prominent for liposomes containing mannose, suggesting an additionally pathway to the nanoparticle charge-mediated clearance observed previously. This was confirmed by colocalizing mannose-containing liposomes with endothelial cells in the *kdrl:GFP* transgenic line (**Figure 23.**).

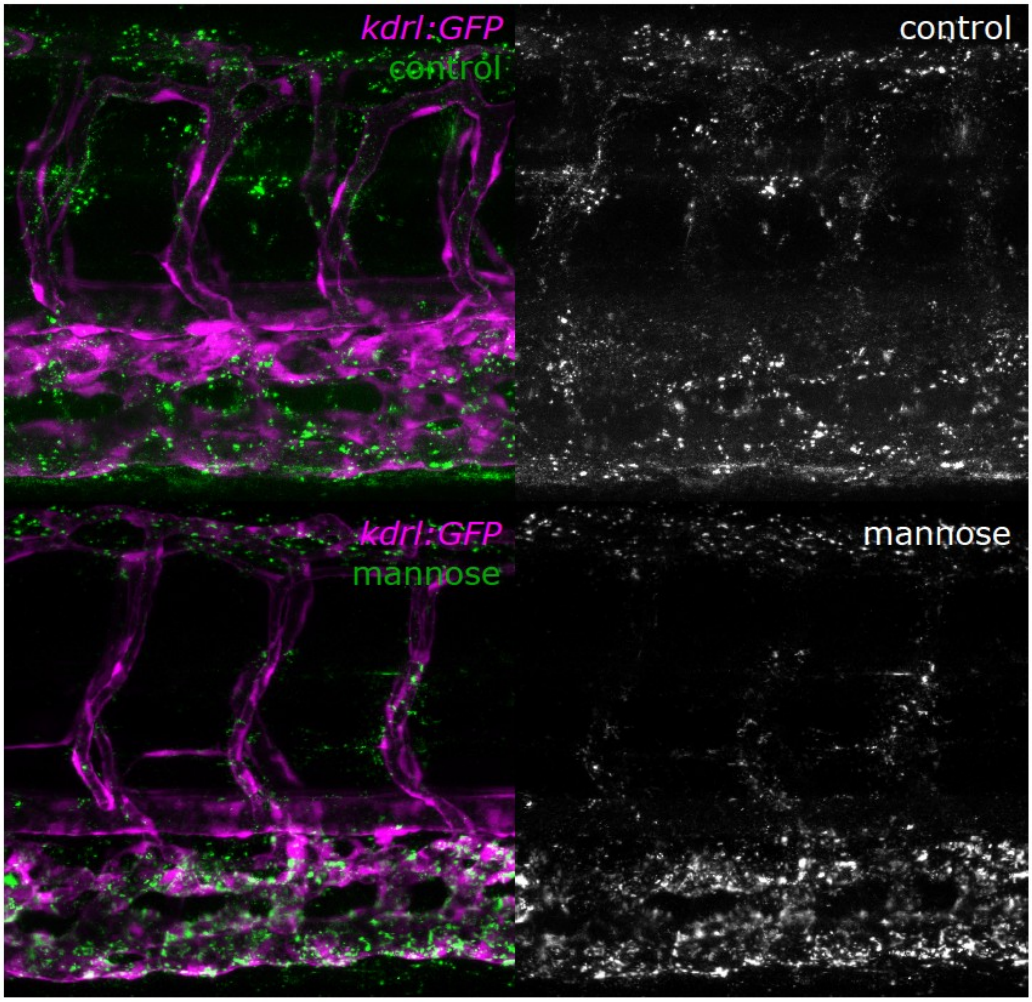

389 C. Quinonez-Silvero, K. Hubner, W. Herzog, *Development of the brain vasculature and the blood-brain barrier in zebrafish, Dev. Biol.*, **2019**. https://doi.org/10.1016/j.ydbio.2019.03.005

Figure 23. Tissue level view of liposome distribution in kdrl:GFP transgenic embryos, 4 h after injection. Liposome accumulation is observed in the entire caudal vein (CV), and on the dorsal side of the PCV (dPCV, arrows).

Mannose-containing liposomes displayed clearance rates that were faster than those observed for fucose-containing liposomes (but not as rapid as trehalose-containing liposomes) and did not display enrichment at the blood-brain barrier. Also, in mannose-containing liposomes, we observed enrichment at the dorsal head vasculature and the first aortic arch artery, common cardinal vein (CCV), posterior cardinal vein (PCV), and caudal vein (CV)**,** similar to control embryos (**Figure 24. A, B**).

This suggests that cells in these vessels mediated clearance through the DOPC-component of the liposomes, but only if the circulation time is long enough to permit this happening. For example, trehalose-containing liposomes, clearance by the blood-brain-barrier endothelial cells and macrophages is so rapid that the slower clearance by the first aortic arch artery and dorsal head vasculature is precluded from visibility. Finally, glucose-containing liposomes displayed a biodistribution that was similar to mannose-containing liposomes, but with less efficient clearance by scavenger endothelial cells, and an enrichment at the lateral line (**Figure 24. B**).

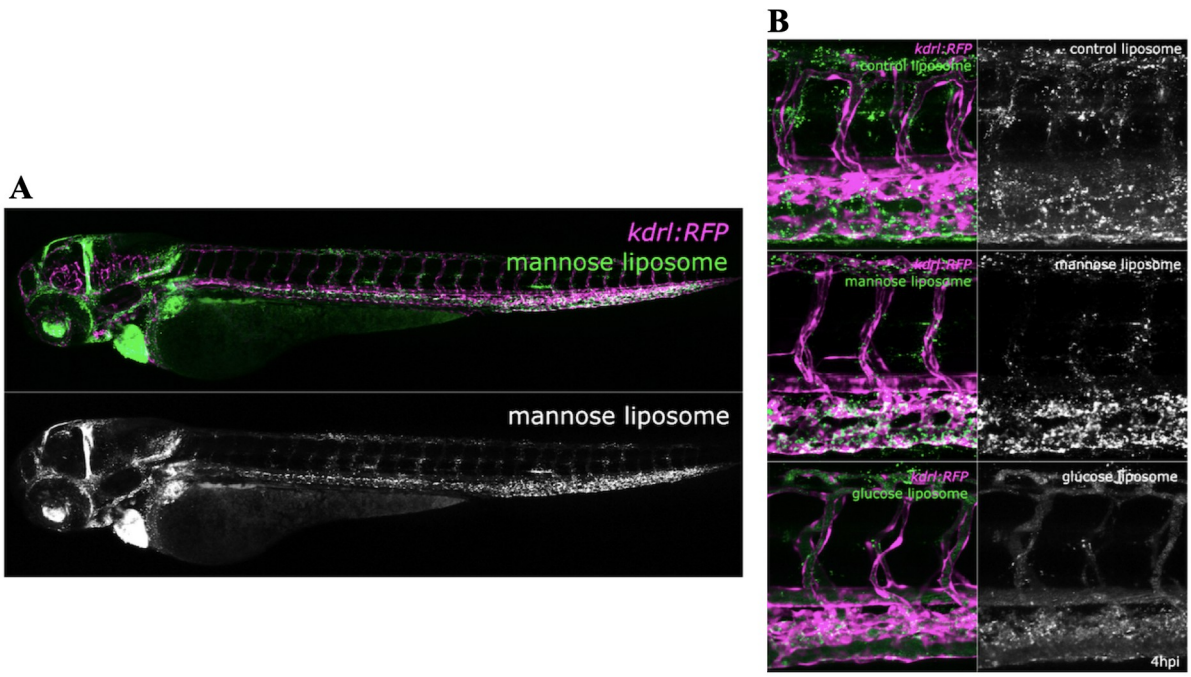

Figure 24. A) Whole-embryo view of mannosylated liposome distribution in kdrl:GFP transgenic embryos, 4 h after injection. Liposome accumulation for DOPC/MM_C18 formulation is observed in the dorsal head vasculature, aortic arch artery, common cardinal vein (CCV), posterior cardinal vein (PCV), and caudal vein

A

(CV). B) Tissue level view of liposome distribution in kdrl:GFP transgenic embryos, 4 h after injection with control, mannosylated and glucosilated liposomes at 52-56 hpf. Liposome accumulation is observed on the dorsal aorta (DA).

This was somewhat surprising given the very strong expression of the glucose-transporter Glut1 at the brain barrier, and suggest that this transporter can interact with glucose only in its free form.

3.3.2. Clearance mechanism of mannose-containing liposomes on SECs

The precise intracellular colocalization of fluo-DOPC with glycolipipds liposomes in SECs indicated the use of a shared receptor for endocytosis. We have previously identified the clearance mechanism of anionic nanoparticles by scavenger endothelial cells in zebrafish embryos, which we found to be dominated by the class H scavenger receptor *stab2*. Recently, we have identified *stab1* as an endothelial receptor that has a less prominent but still important role for anionic nanoparticle clearance (Arias-Alpizar, in preparation).

The finding that mannose-containing liposomes were cleared by scavenger endothelial cells (SECs), homologous to liver sinusoidal endothelial cells (LSECs), without having an overall (anionic) charge, suggested the presence of at least one other mechanism by which these cells can clear the blood of circulating nanoparticles. Besides *stab1* and *stab2*, the mannose receptor *mrc1a* is another receptor that is highly expressed on zebrafish scavenger endothelial cells and mammalian liver sinusoidal endothelial cells (LSECs). The mannose receptor is a highly efficient clearance receptor for mannosylated proteins of diverse nature, and although the interaction is most efficient when the mannose groups are part of a glyocosylation structure, this receptor is still an important candidate receptor for the mannose-containing liposomes.

Based on these, we have been trying to understand if the clearance of our mannosylated liposomes is specifically mediated by Stabilin-1, and -2 or by *mrc1a* receptors of SECs. Firstly, to test if *mrc1a* receptor was involved in liposome uptake by SECs, zebrafish embryos were pretreated with mannan, a competitive inhibitor of *mrc1a*.[390] Subsequent DOPC/MM_C18 liposome injection resulted in a striking loss of liposome uptake by SECs, offset by an increase in circulating liposomes, and an inhibition in macrophage uptake(**Figure 25.**).

390 T. Kawasaki, R. Etoh, I. Yamashina, *Isolation and Characterization of a Mannan-Binding Protein from Rabbit Liver, Biochem. Biophys. Res. Commun.*, **1978**, *81*, 1018−1024.

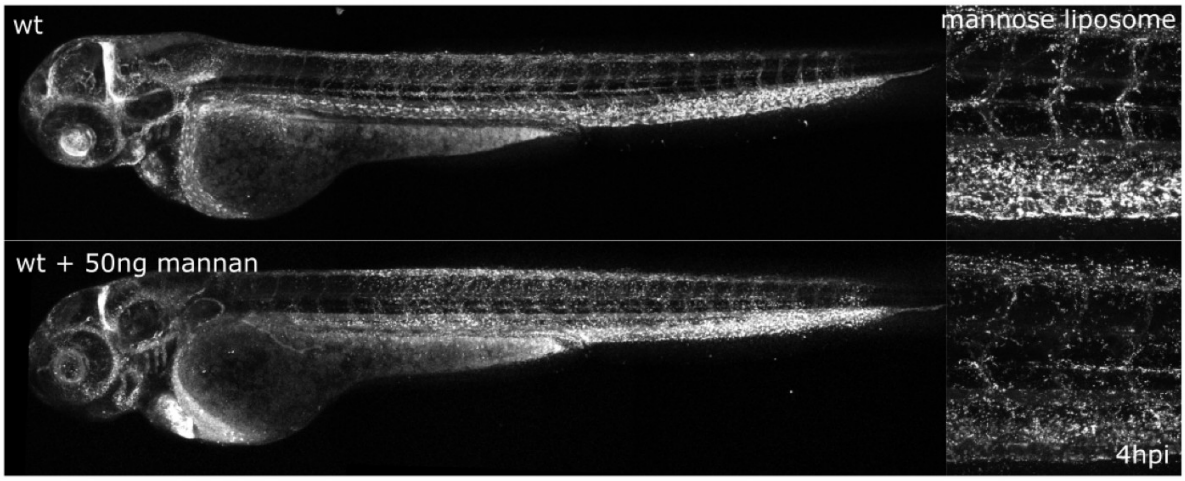

Figure 25. Confocal microscopy images. On top: whole-embryo view of mannosylated liposomes distribution in zebrafish embryos; on the bottom: confocal microscopy images of whole-embryo view of mannosylated liposomes distribution in zebrafish pretreated with mannan.

In contrast, injection of dextran sulfate, a competitive inhibitor of scavenger receptors Stabilin-1 and -2, did not inhibit liposome uptake by SECs, and the DOPC/MM_C18 liposomes were immediately removed from circulation.[391,392] (**Figure 26**)

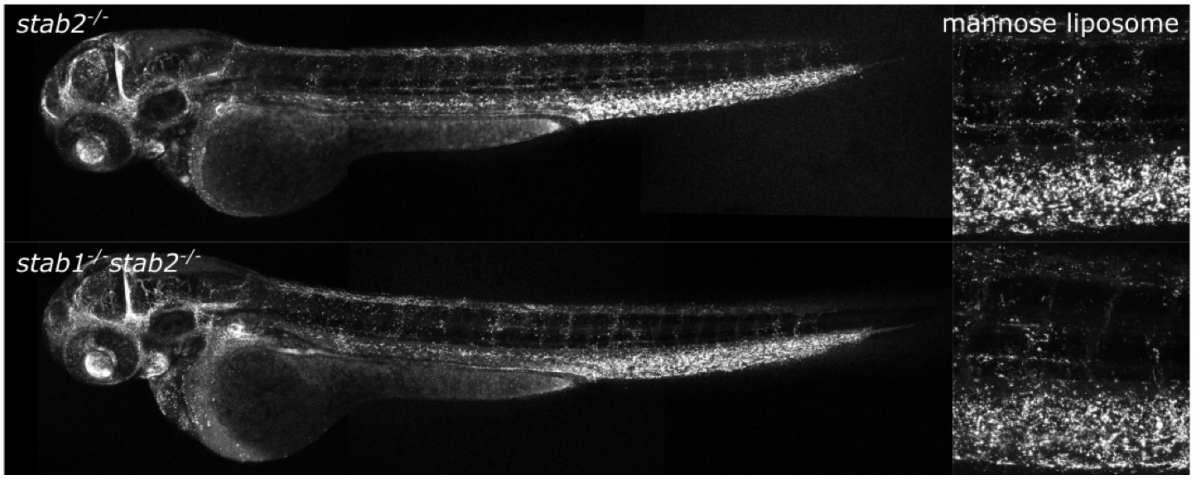

Figure 26. Confocal microscopy images of whole-embryo view of mannosylated liposomes distribution in zebrafish lacking Stab-1 and -2.

These studies confirmed that the mannose receptor *mrc1a* mediates the clearance of our mannosylated liposomes in zebrafish embryos lacking stab-1 and Stab-2.

4. Conclusion

391 E. N. Harris, P. H. Weigel, *The Ligand-Binding Profile of HARE: Hyaluronan and Chondroitin Sulfates A, C, and D Bind to Overlapping Sites Distinct from the Sites for Heparin, Acetylated Low-Density Lipoprotein, Dermatan Sulfate, and CS-E, Glycobiology,* **2008**, *18*, 638−648.

392 Y. Tamura, H. Adachi, J. Osuga, K. Ohashi, N. Yahagi, M. Sekiya, H. Okazaki, S. Tomita, Y. Iizuka, H. Shimano, R. Nagai, S. Kimura, M. Tsujimoto, S. Ishibashi, *FEEL-1 and FEEL-2 Are Endocytic Receptors for Advanced Glycation End Products, J. Biol. Chem*., **2003**, *278*, 12613−12617.

In summary, synthetic sugar fatty acid esters of glucose, mannose and fucose, were synthesized and fully characterized by spectroscopy techniques. These compounds were incorporated into fluorescent DOPC liposomes. After intravenous injection in zebrafish embryos, compared to control liposomes, all formulations containing glycolipids displayed an altered biodistribution, 4 hours post injection.

In particular, control liposomes composed of DOPC, where no clearance by scavenger endothelial cells was observed. Addition of trehalose-C18 to DOPC-liposomes dramatically changed the biodistribution, of all glyco-liposomes. An almost complete plasma clearance at 4hpi was observed for them. Furthermore, trehalose-liposome formulation has shown a strong accumulation on the endothelial cells that comprise the zebrafish blood-brain-barrier. For fucose-containing liposomes, we observed a similar but weaker enrichment compared to trehalose-containing liposomes at the blood-brain barrier. Besides, fucosylated liposomes shown a clearance similar to the blank sample, used as control. Mannose-containing liposomes displayed clearance rates that were faster than those observed for fucose-containing liposomes (but not as rapid as trehalose-containing liposomes) and did not display enrichment at the blood-brain barrier. Moreover, glucose-containing liposomes displayed a biodistribution that was similar to mannose-containing liposomes, but with less efficient clearance by scavenger endothelial cells.

After that, SECs targeting was prevented in embryos preinjected with mannan and in **mrc1a** mutants, but not stab1/stab2 mutants showing precise specificity towards the mannose receptor. We have successfully generated a LSECs-targeted liposomal drug delivery system with precise and *in vivo* confirmed specificity towards LSECs through interaction with the **mrc1** receptor.

The use of the embryonic zebrafish as a model organism, and the ability to visualize nanoparticle−cell interactions at high resolution in living organisms, has been essential in this process. We therefore propose that the embryonic zebrafish, with its established extensive genetic toolkit, is a valuable preclinical *in vivo* model allowing screening, optimization, and mechanistic understanding of nanoparticle biodistribution, predictive of their behavior in mammals.

Supporting Information

6-O-Oleoyl-Glucose (1a)

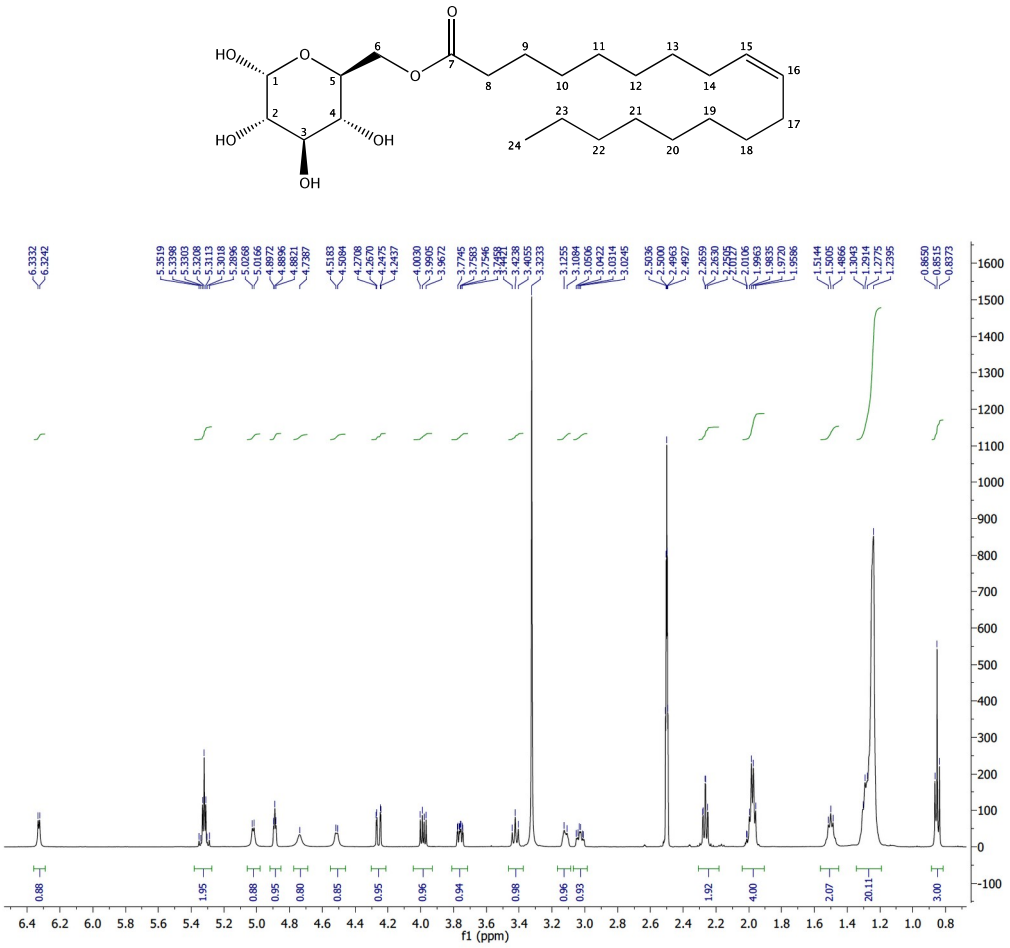

Fig.S 4. ^{1}H NMR spectrum of glucose-oleate in DMSO.

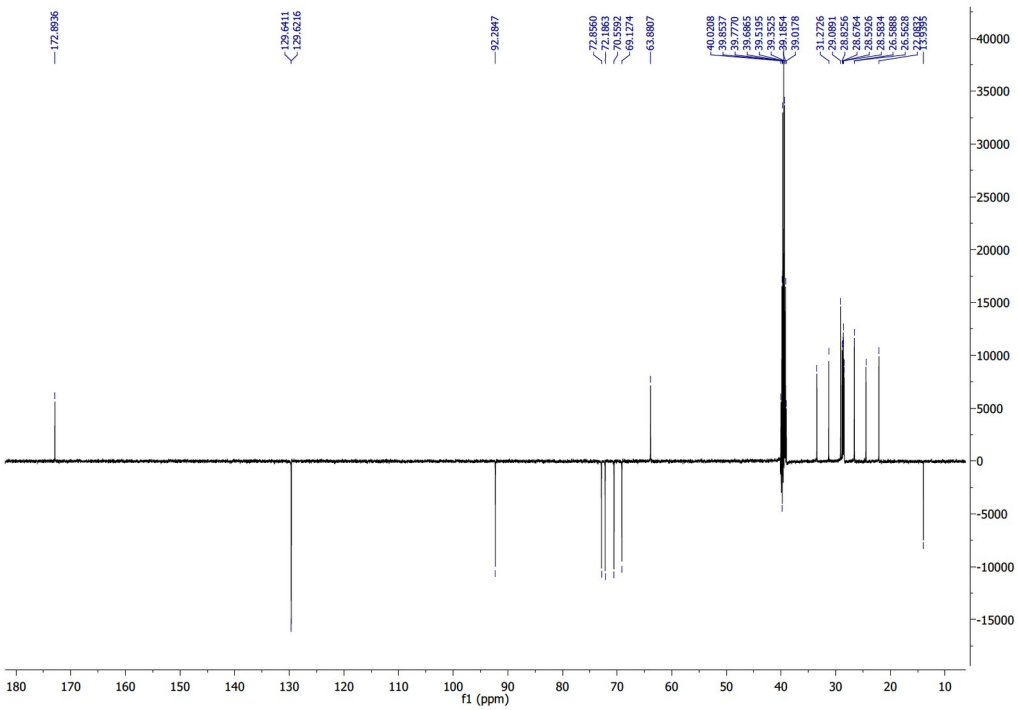

Fig.S 5. ^{13}C NMR- DEPT spectrum of glucose-oleate in DMSO.

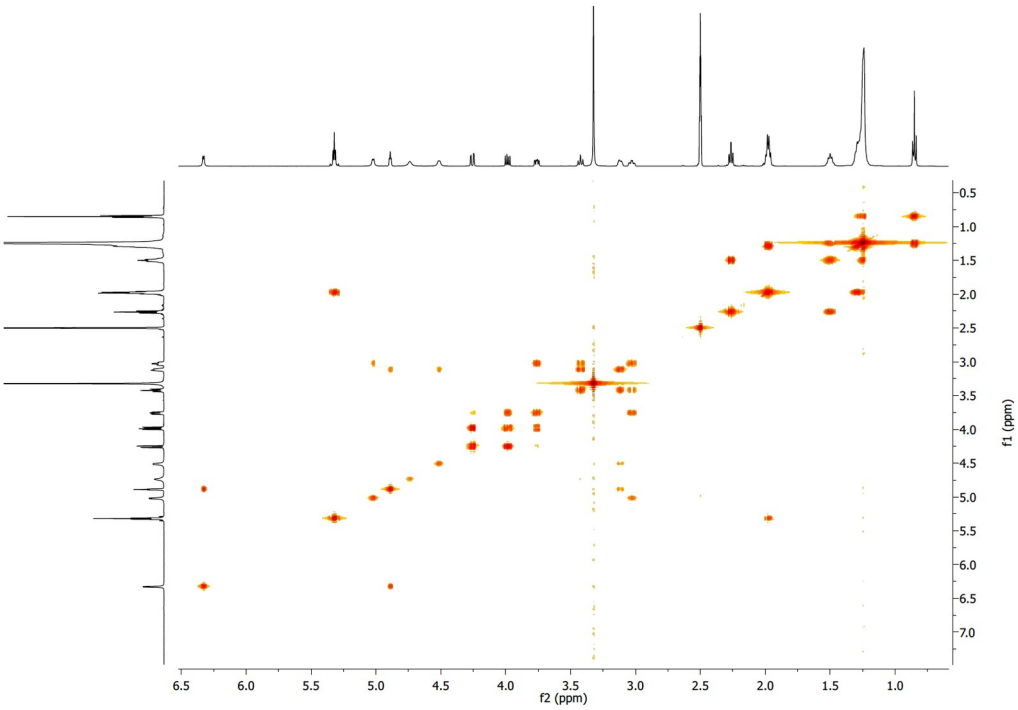

Fig.S 6. COSY NMR spectrum og glucose-oleate in DMSO.

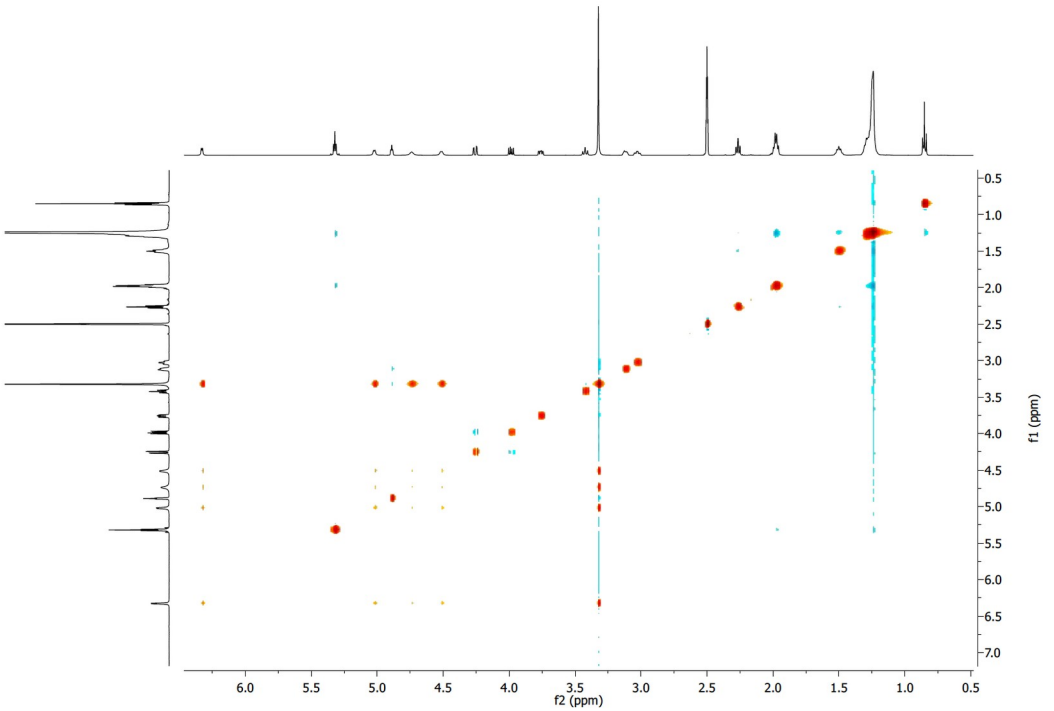

Fig.S 7. NOESY NMR spectrum of glucose-oleate in DMSO.

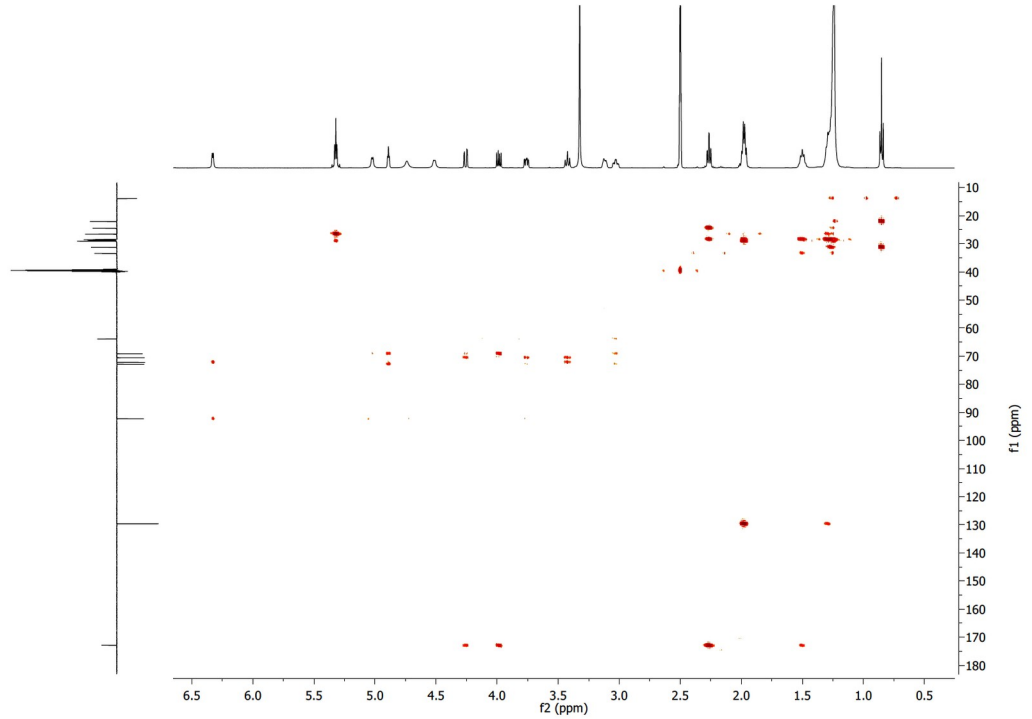

Fig.S 8. HMBC NMR spectrum of glucose-oleate in DMSO.

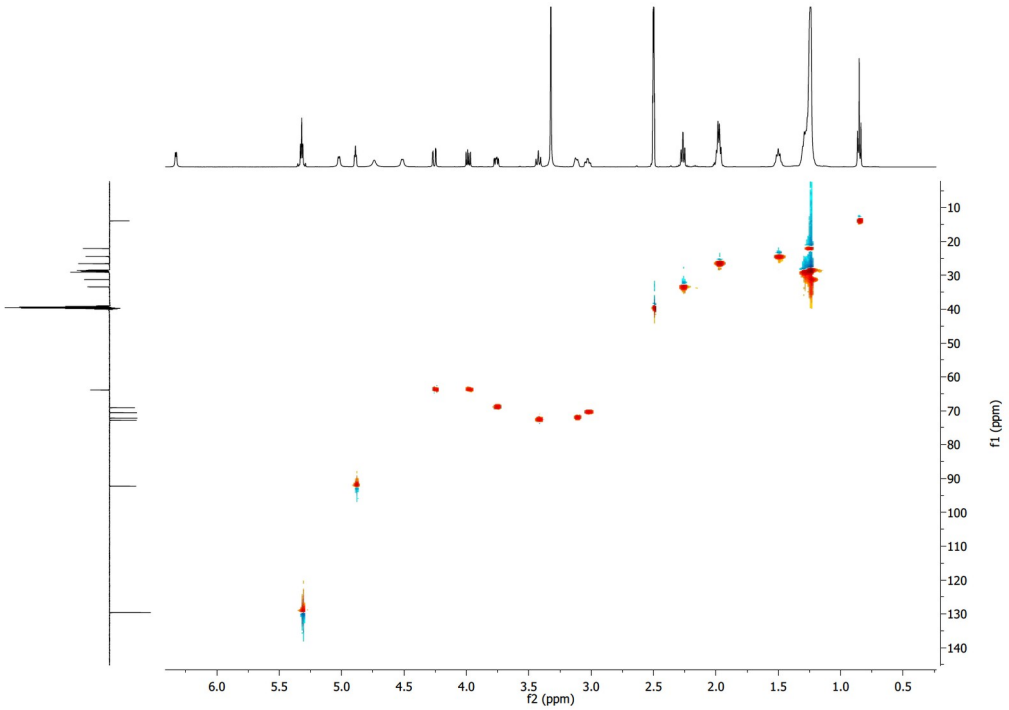

Fig.S 9. HSQC NMR spectra of glucose-oleate in DMSO.

6-O-Oleoyl-Mannose (2a)

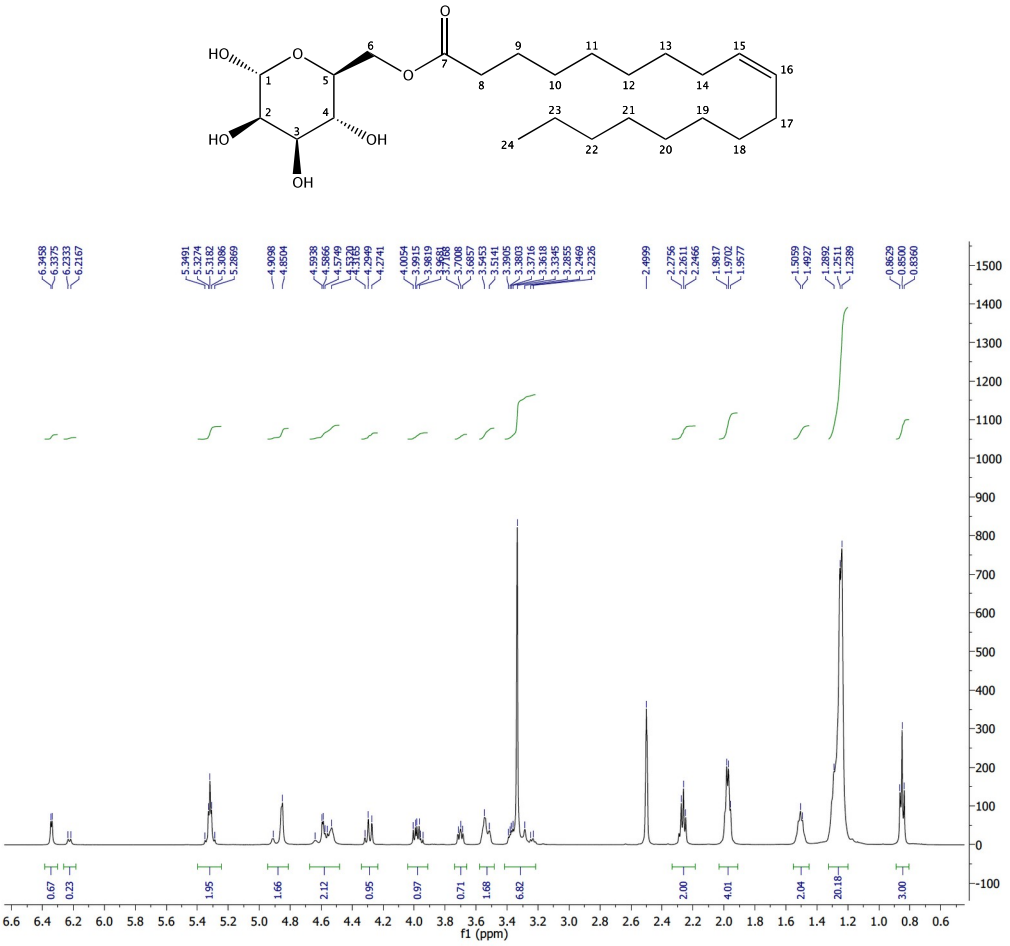

Fig.S 10. [1]H NMR spectra of mannose-oleate in DMSO.

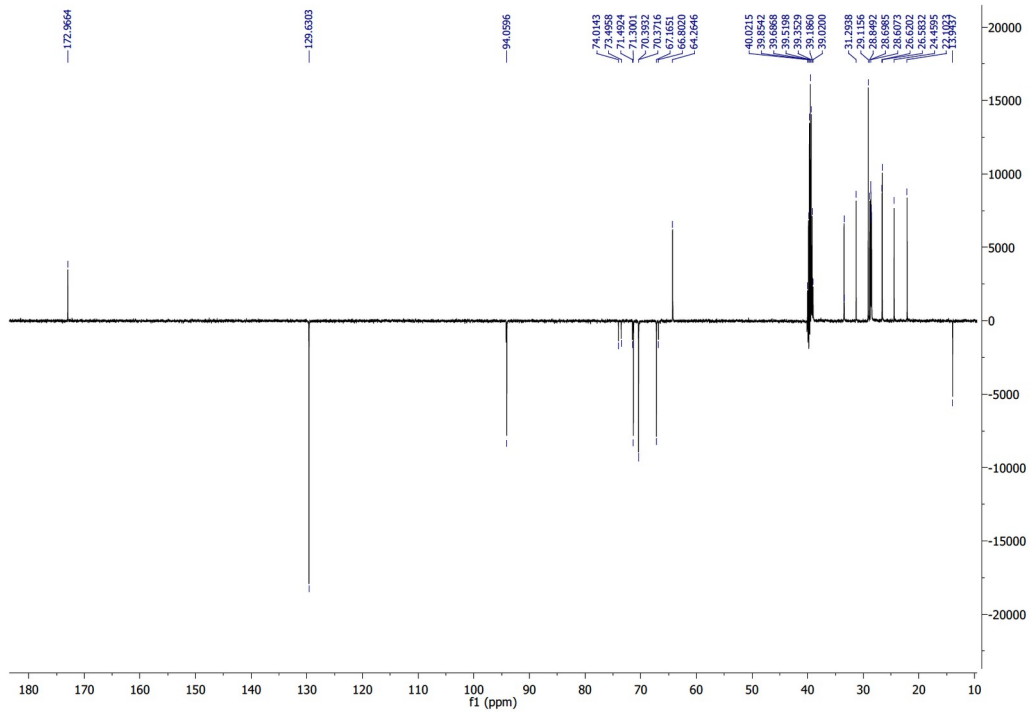

Fig.S 11. [13]C NMR-DEPT spectra of mannose-oleate in DMSO.

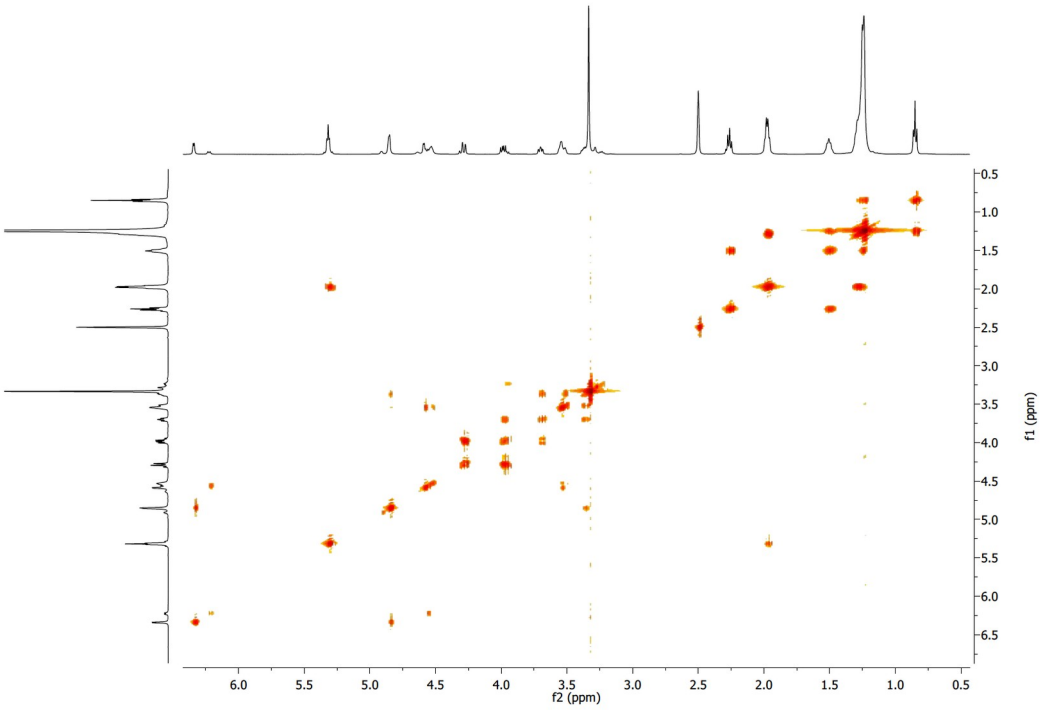

Fig.S 12. COSY NMR spectra of mannose-oleate in DMSO.

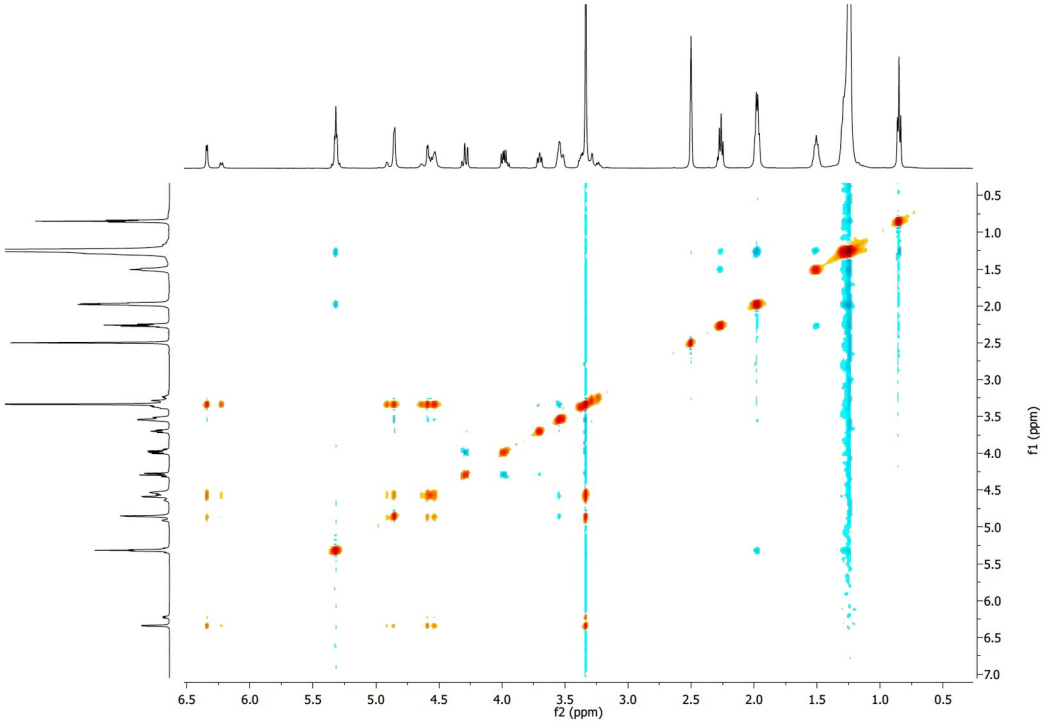

Fig.S 13. NOESY NMR spectra of mannose-oleate in DMSO.

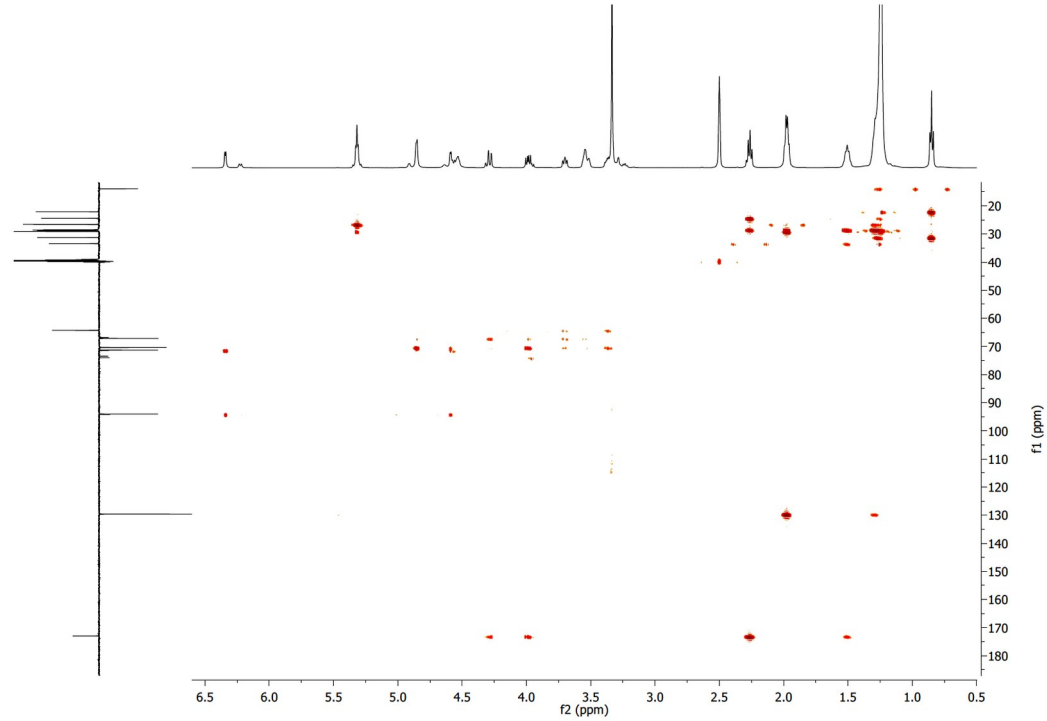

Fig.S 14. HMBC NMR spectra mannose-oleate in DMSO.

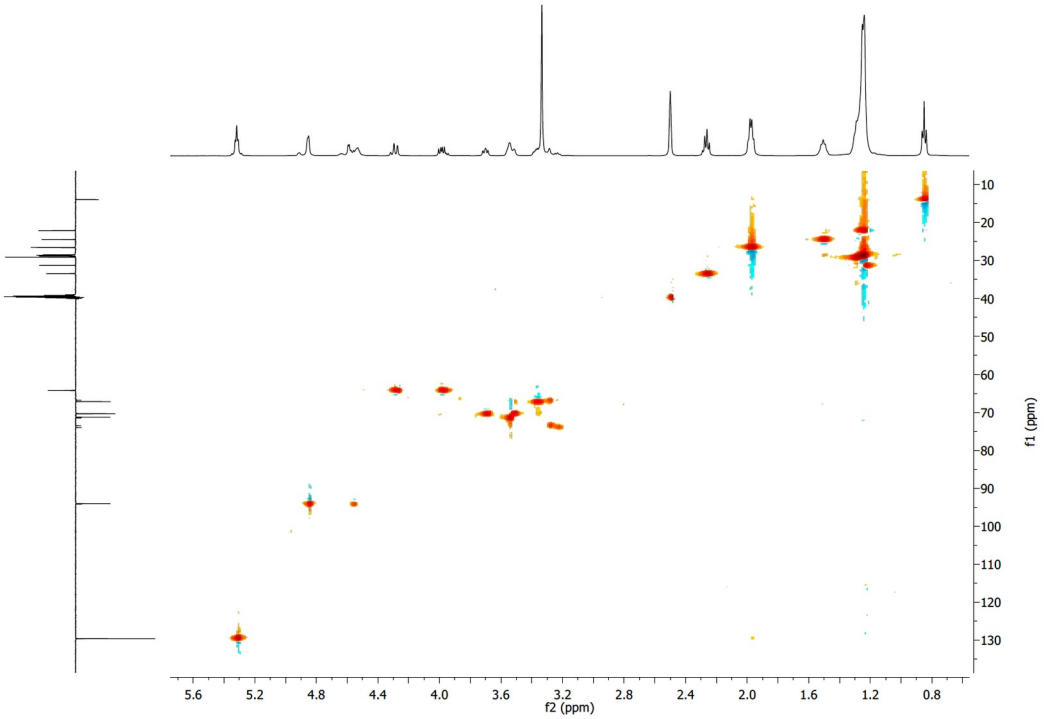

Fig.S 15. HSQC NMR spectra of mannose-oleate in DMSO.

2-O-Oleoyl-Fucose (3a)

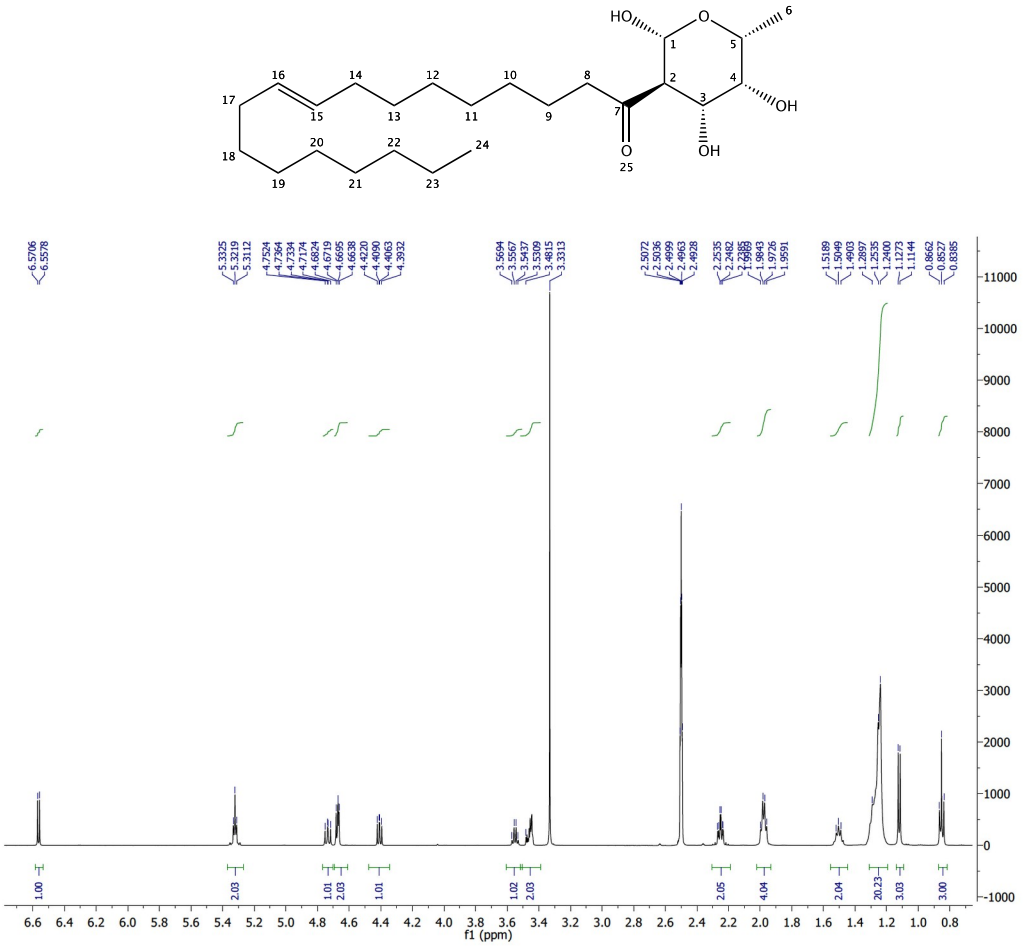

Fig.S 16. [1]H NMR spectra of fucose-oleate in DMSO.

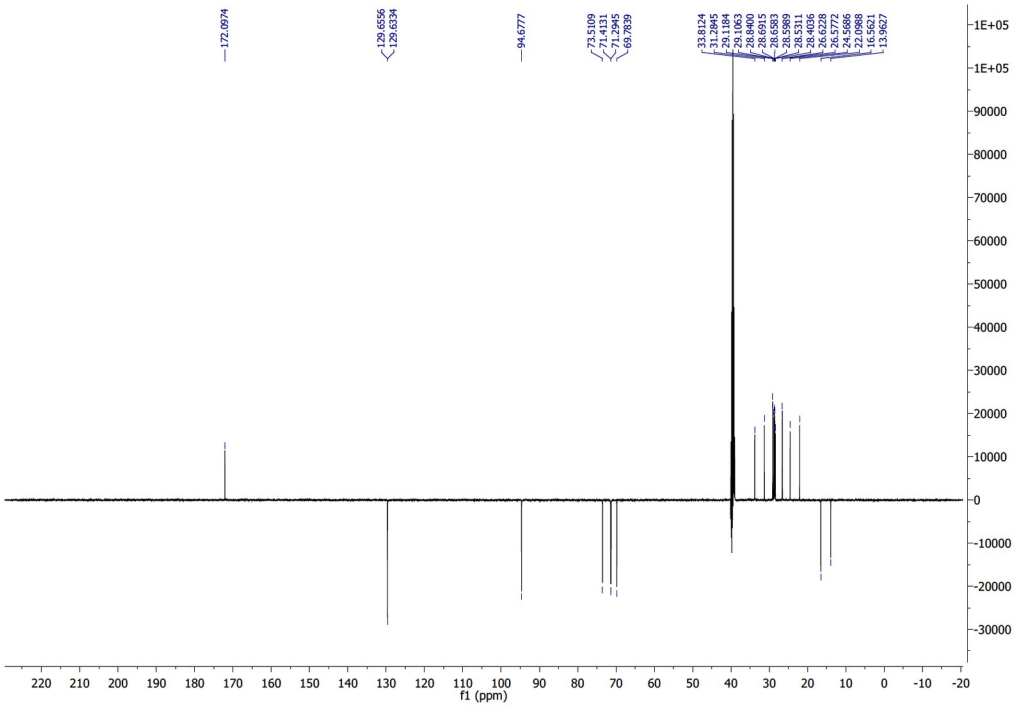

Fig.S 17. [13]C NMR-DEPT of fucose-oleate in DMSO.

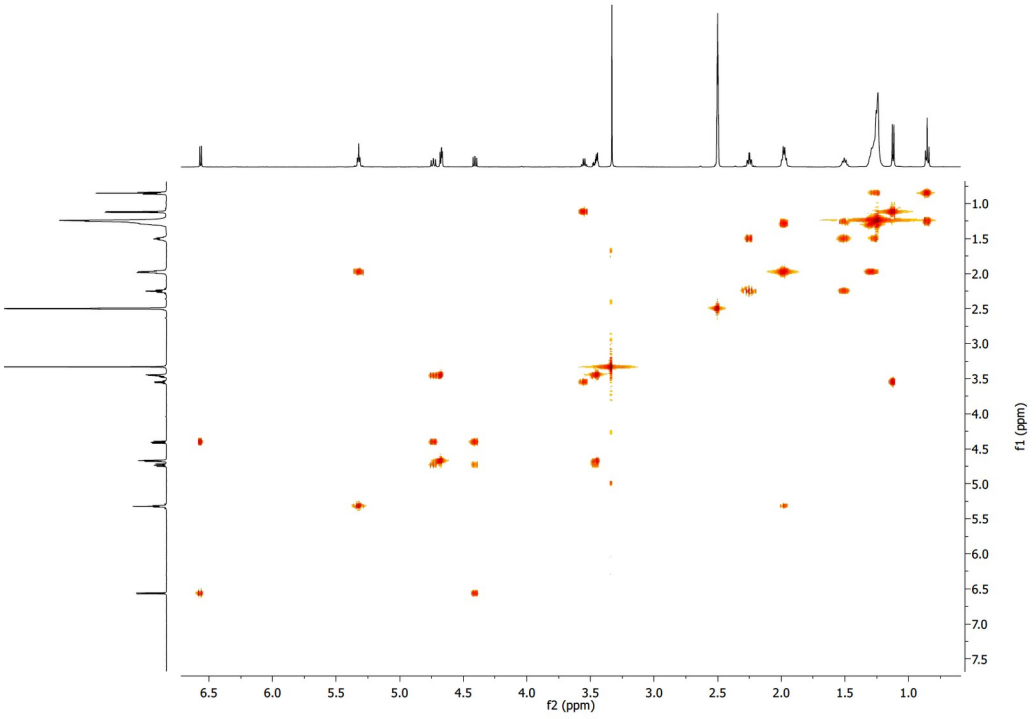

Fig.S 18. COSY NMR spectra of fucose-oleate in DMSO.

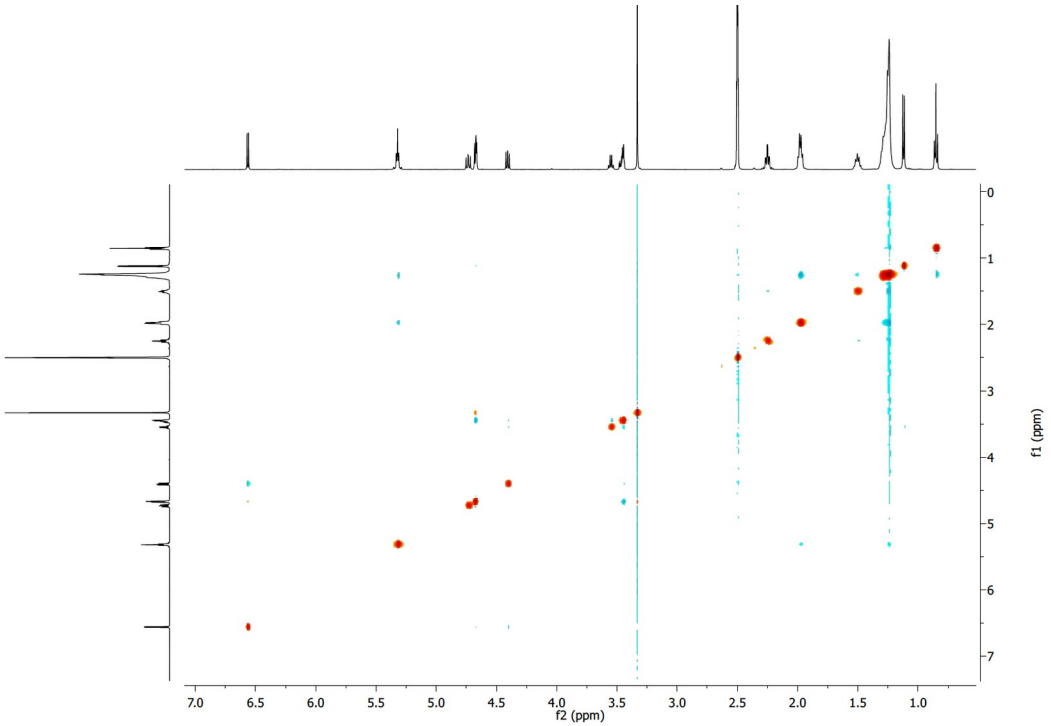

Fig.S 19. NOESY NMR spectra of fucose-oleate in DMSO.

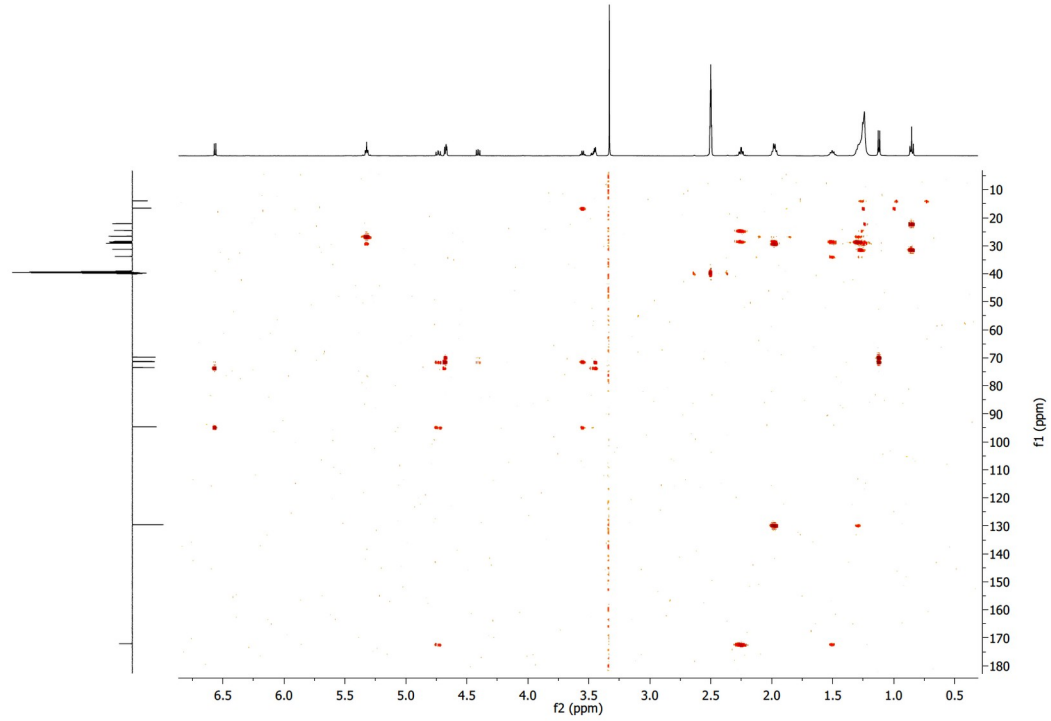

Fig.S 20. HMBC NMR spectra of fucose-oleate in DMSO.

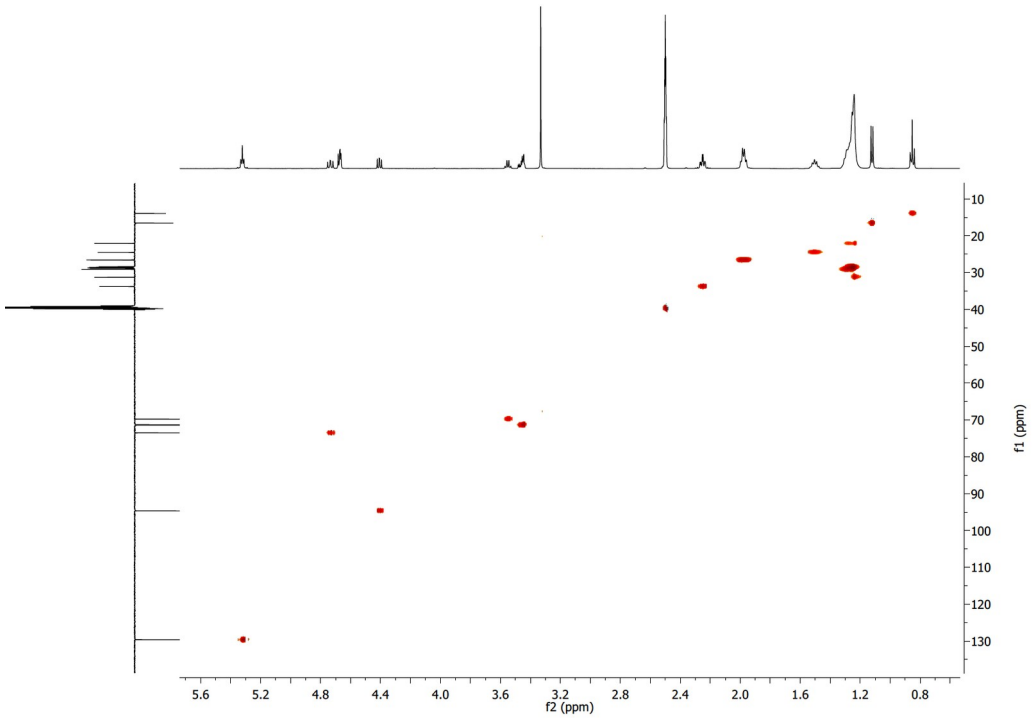

Fig.S 21. HSQC NMR spectra of fucose-oleate in DMSO.

Liposome stability on time

The colloidal stability, measured as the change in average particle size of the formulations as a function of time was evaluated during storage for 60 days at 4 °C. The show that the average particle size of glycol-liposome formulations was not affected by the storage temperature or the time. All glycol-liposomes are stable.

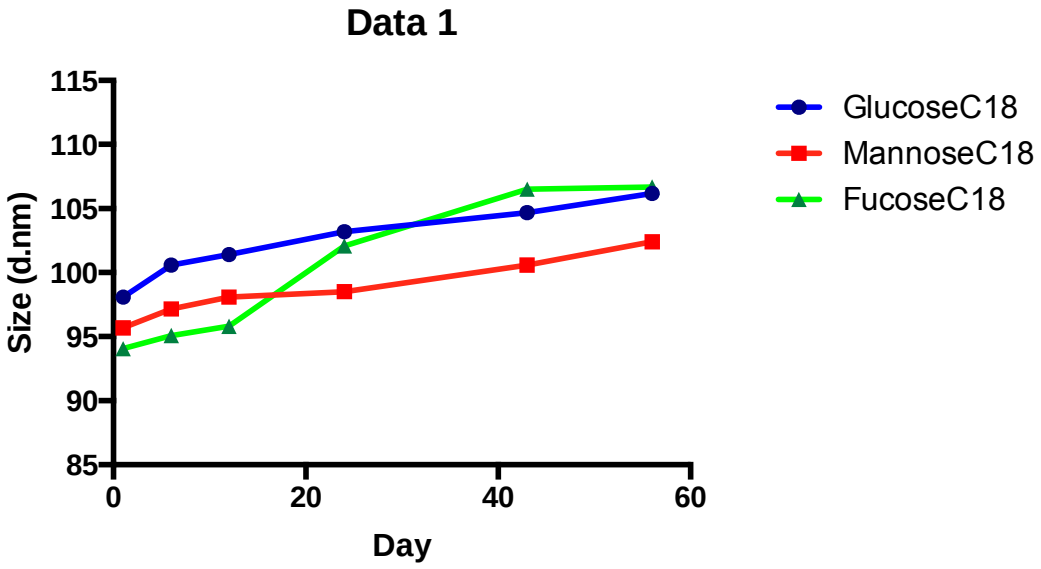

Fig.S 22. Average particle size (z-average) of DDA/TDX liposomes stored at 4 °C.

Lipid Recovery before and after extrusion

	DOPC	Glycolipid	Rho-DPPE
DOPC/MG_C18	96%	94%	98%
DOPC/MM_C18	93%	93%	99%
DOPC/MF_C18	96%	96%	97%

Conclusion and perspectives

Nanotechnology has been extensively explored in the past decade to develop a myriad of functional nanostructures to facilitate the delivery of therapeutic agents for various medical application. The development of highly selective and effective nanoparticles (NPs) for drug delivery has brought new hope for the treatment of various diseases. As a delivery vehicle, NPs with size range of 10-150 nm have demonstrated many advantages compared with the conventional approaches to the uses of drugs. Indeed, these systems face issues concerning stability in physiological media, sensitive toxicity, poor specificity followed by an uncontrollable release of therapeutics, low bioavailability, and drug resistance induction, which sensitively decrease the therapeutic efficiency of many conventional drug systems. The development of novel nanoparticles-based drug delivery systems can help solve some of these challenges by employing materials shaped by evolution. Thereby in this thesis the potential of different type of nanoparticles was evaluated with the aim to design and develop of novel biocompatible nanosystems for drug delivery.

Recent years have witnessed and intense research on polymeric materials for biomedical application mainly applied in the nanomedicine field for the formulation of innovative nanocarrier systems. Among the large variety pf available polymers, only a limited number have received so far regulatory approval for biomedical application. Among them, poly(ethylene glycol) (PEG), poly-ε-caprolactone, and poly-δ-decalactone are few examples of the polymers approved by the US Food and Drug Administration (FDA). As results, an extraordinary variety of nanocarrier systems with different properties can be easily obtained by selecting the polymer with the desired characteristic.

According to this information, in the ***Section I***, the effect of polymer molecular weight, surface charge and surface hydrophilicity is evaluated in the engineering of novel polymeric micelles PMs of synthetic di-block copolymer mPEG-PCL in terms of size, homogeneity, drug to polymer ratio, and entrapment efficiency of anti-glaucoma drug Metazolamide (MTZ). mPEG-PCL PMs bearing the hydrophobic drug, MTZ, were formulated by the thin film hydration method. This technique has allowed as to obtain mPEG-PCL of different molecular weights of 3, 4, and 5.5 kDa. Dynamic light scattering revealed that the average diameter of the PMs was maintained below 100 nm, due to the great aqueous solubility of the copolymer, resulting in decreasing the interfacial tension and the formation of small particles. Drug loaded polymeric micelles possessed negative charge with Z-potential values fitted

between -2.42 ± 0.42 and −14.1 ± 1.10 mV. The observed negative charge is due to ionized carboxyl groups of PCL segment. The percent of MTZ entrapped within micelles was found to be in the range of 57.05 and 93.91%. Based on these findings, NM3 of optimum maximum EE% (93.91%) and lowest particle size values of 60.39 nm and the highest desirability ratio (DR= 0.832) was selected for further investigation.

The successful entrapment of MTZ inside NM3 polymeric micelles has been proven by complete vanishing of drug melting peak in DSC thermogram and the possible formation of hydrogen bonding between MTZ and mPEG-PCL copolymer in FT-IR spectrum. TEM images of NM3 revealed that this formulation was spherical. Moreover, *in vitro* release study of MTZ from selected PMs was compared to MTZ-solutions. The results showed that MTZ-PMs had a biphasic release profile with an initial burst effect of more than 50% MTZ followed by a sustained drug release for 8 h. In contrast, MTZ solution was completely released within 4 h. indicating the capability of PMs of significantly sustaining MTZ release.

MTT assay and histopathological assessment were carried out to verify ocular tolerability as well as Draize irritancy test. The obtained data indicates that NM3 was physiologically tolerated and do not cause ocular cytotoxicity *in vivo*. Besides, the Draize test displayed a good ocular tolerability of MTZ-PMs. *In vivo* studies were conducted on rabbits to evaluate the ocular tolerability and to evaluate anti-glaucoma activity in glucocorticoid-induced glaucoma model. No signs of ocular damage or clinical abnormalities were detected in the cornea, iris, conjunctiva or pupil region of the rabbit.

Furthermore, a pronounced reduction in IOP of glaucomatous eyes upon for sub-conjuntival injection of selected MTZ-PMs NM3 formulation, compared to MTZ solution was observed. The characterization of the prepared PMs and the results of release, *in vitro* MTT assay, hemocompatibility, Draize test, and *in vivo* histology experiments showed favorable nanosized, reasonable entrapment efficiency, sustained drug release, and superior ocular tolerability. Better *in vivo* inhibitory effect of MTZ-PMs was achieved compared to simple MTZ. solution on glaucoma induction in experimental rabbits. These data suggest that, these newly developed nanoformulations have characteristics which are appropriate for ocular nanodelivery of MTZ.

The ***Section II***, reports the formulation and characterization of a new class of nanocarriers, called hybrid/mixed/chimeric liposomes. By combining the specific function of each material, new hybrid nanocomposite materials can be fabricated. For instance, liposomes and polymeric

NPs are the two most widely studied drug delivery platforms and attempts have been made to combine the advantages of both systems. Liposomes have been widely studied and used as nanovectrors in the past decades.

The benefits of liposomal formulations include the ability to carry hydrophilic drugs inside the aqueous vesicles and to carry hydrophobic drugs within the lipid bilayer membranes, high biocompatibility that provides perfect shield to protect drugs from internal and external environment, and easy surface modification with other molecules such as PEG and targeting ligand to achieve prolonged systemic circulation lifetime and targeted drug delivery, respectively. However, the applications of liposomes are typically limited by some unfavourable features such as relatively complicated fabrication steps associated with liposome preparation and purification, low loading efficiency for hydrophobic drugs, busts release kinetics of encapsulated drugs, and instability during storage leading to short shelf-life. On the other hand, biodegradable polymeric nanoparticles have shown great therapeutic potential as a drug delivery nanocarrier.

These PNPs can carry hydrophobic drugs, as we have seen before, with higher loading capacity than liposomes. Drug release from polymeric nanoparticles is usually dominated by polymer degradation and drug diffusion, which can be controlled by choosing proper polymers with desirable degradation rates and binding affinity with the encapsulated drugs. Moreover, PNPs can be prepared by self-assembry of the block copolymers through a simple manufacture method, which allows cost-effective large-scale fabrication of the particles. Despite all these appealing deatures, PNPs have not gained much success as liposomes, presumably due to their moderate circulation lifetime and potential biocompatibility issues. Recently, efforts have been made to combine the positive attributes of both liposomes and PNPs into a single hybrid delivery systems.

According to these facts, the central goal of this study was to create novel self-assembled and functional hybrid synthetic/biological macromolecular nanostructures and enrich basic understanding on behavioural motifs, as well as widen the application potential of nanostructured polymeric colloidal systems. In particular, a synthetic block copolymer polyethylene glycol-co-poly(delta-decalactone) ($mPEG_x$-PDL_y) was incorporated into 1,2-dipalmitoil-sn-glycore-3-phosphocholine (DPPC) and 1,2-diasteroyl-sn-glycero-3-phosphocholine (DSPC) lipid bilayers.

In the present study, a series of nanosystems were built by combining phospholipids DSPC or DPPC with one of the mPEGx-PDL block copolymers. The interactions between the polymer and the lipids were investigated using DSC and the effect of the composition and molecular weight of the block copolymers on these interactions was evaluated. In particular, DSC analysis revealed the thermotropic effect of the copolymers on the DSPC or DPPC types of membranes in two different weight ratios, 9:0.1 and 9.05. The most promising chimeric systems, in terms of thermotropic behaviour, were chosen to be developed as liposomes. Based on the enthalpy of the main transition, those were DSPC:polymer (9:0.5).

The resulted chimeric liposomes were developed in PBS solution since this medium simulates well the physiological environment in terms of pH and ionic strength, and were studied in regards with their physicochemical properties, their colloidal stability and their *in vitro* toxicity. Regarding the size and PDI of chimeric liposomes, we observed a high dependence on the nature of the utilized copolymer. In particular, the hydrophilic-to-hydrophobic balance of the copolymer affected those parameters greatly. In the case of mPEG1.9, the length variation of PDL did not alter the liposomal diameter, leading to a size of 90 nm, while the PDI was also stable at 0.270, indicating homogeneity of the systems. These properties were promising for further *in vitro* investigation of these chimeric nanoparticles. MTT assay was used to quantify the viability of cells exposed to four different chimeric liposome types. Of all liposomes tested the DSPC:mPEG$_{1.9}$-PDL$_{24}$ appeared to be the most toxic *in vitro* for HEK-293 cells, with the other formulations being more tolerable, especially at certain concentration.

As a result, depending on their thermodynamic, physicochemical and toxicity profiles, chimeric polymer-grafted liposomes could be promising candidates for further *in vitro* and *in vivo* investigations for future drug delivery applications. Furthermore, the described functionality of these new proposed nanosystems may have a high impact to the emerging need of innovative platforms based on nanotechnology. To the best of our knowledge this is the first time that a chimeric liposome composed of a PEG-PDL block copolymer is prepared and characterized.

The first objective of ***Section III*** was to selectively produce novel glycolipids, in particular, fatty acid sugar esters, using substrates originating from renewable resources. Fatty acid sugar esters, belonging to glycolipids, are amphiphilic, non-toxic, non-ionic and biodegradable molecules that consist of a hydrophilic carbohydrate moiety and one or more fatty acids as a lipophilic moiety. These molecules showing high emulsifying, stabilizing and detergent

properties and they find applications in different food, cosmetic and pharmaceutical products as well as in drug formulation and delivery.

As surfactants they may play a role in the solubilization or stabilization of drugs in different preparations and they can also be included in formulations to modify the bioavailability of drugs and to be used as drug delivery systems. Liposomes are vesicular drug delivery systems that have an aqueous solution core surrounded by a hydrophobic membrane, in the form of a lipid bilayer, developed with the purpose of loading poorly soluble drugs, thus providing an enhanced solubility and a long-term bioavailability of the therapeutic in the systemic circulation. The aim of the present work was to design and to characterize a novel drug delivery system, by combining the advantages of phospholipid-based carriers (liposome) and synthetic sugar fatty acid esters. In the designing and developing a new biocompatible nano-based drug delivery system for human, preclinical screenings with animal models are an essential part of gaining insight nanoparticle behavior including liposome biotoxicity, biodistribution and the mechanisms of liposome uptake by cell.

To this end, Zebrafish was used as a model to study the glycol-liposome biodistribution and their resistance or not against macrophages. Zebrafish is a biological homologous to humans, inexpensive, amenable to modifications, and optically transparent, and hence have many advantages over other animal models. With zebrafish embryo models, we have been able to study dynamic behavior of fluorescent glycol-liposomes *in vivo* after intravenous injection.

Three different glycolipids (MX_C18) were synthetized by one reaction step. Oleic monoesters of Glucose (MG_C18) and Mannose (MM_C18), were obtained by enzymatic reaction using Novozym 435.[393] Fucose oleic monoester was synthesized by chemical reaction under basic condition, using Pyridine and 2-(1H-Benzotriazole-1-yl)-1,1,3,3-tetramethylaminium tetrafluoroborate (TBTU) as catalyst.[394] The complete ^{1}H-NMR and ^{13}C NMR assignments of the compounds were carried out by using DEPT, HMBC, HSQC, NOESY and ^{1}H–^{1}H COSY spectra.

The synthetic glycolipid was incorporated into the lipid bilayer of DOPC fluorescent liposomes in order to obtain a novel biocompatible nanosystem for drug delivery. Glyco-liposomes of 100 nm, <0.1 PDI and Z-potential of about -18 mV were obtained. These nanocarriers were used to identify the influence of glycolipid composition on liposome

393 D. Coulon, A. Ismail, M. Girardin, B. Rovel, M. Ghoul, *Effect of different biochemical parameters on the enzymatic synthesis of fructose oleate, Journal of biotechnology*, **1996**, *51*, 115-121.

394 B. Tang, K. H. Row, *Recent developments in deep eutectic solvents in chemical sciences, Monatshefte für Chemie-Chemical Monthly*, **2013**, *144*, 1427-1454.

biodistribution and the mechanisms of liposome uptake by cells. Furthermore, liposome clearance by macrophages was studied using transgenic zebrafish embryos, lacking Stab-1, Stab-2 and mrc1a receptors, with fluorescently labeled glycol-liposomal formulations. The ultimate goal was tested the glico-liposomes mannose (mrc1) receptor-specificity and study their potential for delivery to LSECs in our recently zebrafish embryo model after intravenous injection.

After IV on 2-days old zebrafish, the distribution of the injected glyco-liposomes were examined by fluorescence confocal microscopy at 4 h after injection. At 4 hpi, we observed differential distribution of glyco-liposomes in various blood vessels and macrophage/monocyte population. For DOPC liposomes, used as control, we observed a long circulation time and most clearance was performed by macrophages. Translocation through the vessel wall (extravasation) was evident for all Glyco-lipsomes except for the mannosylated liposomes, which had circulation time shorter than that other glycol-liposomes. Accumulation on the walls of the vessel in the blood-brain-barrier of the zebrafish was observed for DOPC-trehaloseC18 and DOPC_MF_C18. After that, SECs targeting was prevented in embryos preinjected with mannan and in **mrc1a** mutants, but not stab1/stab2 mutants showing precise specificity towards the mannose receptor. We have successfully generated a LSECs-targeted liposomal drug delivery system with precise and *in vivo* confirmed specificity towards LSECs through interaction with the **mrc1** receptor.

The work described in this thesis was focused on the synthesis, physicochemical characterization and biological evaluation of three novel biocompatible nanosystems for drug delivery. The results obtained here are interesting and encourage further studies on these nanocarriers in order to fully understand their peculiar characteristics.

Curriculum vitae and list of publications

Curriculum vitae

Francesca Biondo was born on the 14th of January 1989 in Gallipoli, (LE), Italy. She attended the high school "Liceo Scientifico *Quinto Ennio*" in Gallipoli, and she graduated with 100/100 in 2008. She received her master degree 99/100 in Chemistry and Pharmaceutical Technology at University of Urbino Carlo Bo in 2016, whit a master thesis in Chemistry. Title of the thesis: "*Oxidative Carbonylation reactions promoted by diaryl α–diimines palladium (II) complexes*". She obtained the licence to practice as pharmacist in 2016. In the same year, she started a PhD program in Pharmaceutical Technology at University of Urbino, under the supervision of Prof. Luca Casettari. Her research focuses on the design and development of novel biocompatible nanosystem for drug delivery, and on the synthesis and characterization of new materials for innovative pharmaceutical application. In 2018/2019 she was a visiting PhD student at Leiden Academic Centre for Drug Research (LACDR), Division of BioTherapeutics at Leiden University, The Netherlands, under the supervision of Prof. Dr. Wim Jiskoot and Ass. Prof. Jeroen Bussmann. During these nine months she worked on formulation, characterization, biodistribution and Drug Delivery efficiency studies of Sugar Fatty acid ester-based liposomes in Zebrafish embryos. She participated in several educational courses and international conferences and schools. During her PhD program she acquired new skills in the field of innovative drug delivery systems, such as nanoparticles, micelles, liposomes, polymer (Ring opening polymerization (ROP)) and several analytical techniques including NMR spectroscopy, Chromatography techniques, TLC, LC, GC, and HPLC & UPLC/UHPLC instrumentation with a wide variety of detection capture (UV, DAD, RI, MS, ELSD), Liposome formulation techniques, Dynamic Light Scattering (DLS), Nanoparticle Tracking Analysis (NTA), Differential Scanning Calorimetry (DSC), Transmission Electron Microscopy (TEM), Analytical quality control (CAPA, GAMP,GMP, GCP).

List of Publications

Francesca Biondo, Stefan Romeijn, Laura Marino, Wim Jiskoot, Luca Casettari, Jeroen Bussmann. "*Glycolipid-mediated liposome targeting in zebrafish embryos*". (Under Submission, ACS Nano 2019/2020);

Simone Lucarini, Raffaella Campana, Alessio Merli, Francesca Biondo, Gianfranco Favi, Andrea Duranti. "*Synthesis and evaluation of sugar-based aliphatic and aromatic esters as antimicrobial and antibiofilm agents*" (Under Review Food Chemistry, 2019);

Enas Elmowafy, Heba Gad, Francesca Biondo, Luca Casettari, Mahmoud E. Soliman. "Exploring optimized methoxy poly(ethylene glycol)-block-poly(ε- T caprolactone) crystalline cored micelles in anti-glaucoma pharmacotherapy" Int. J. Pharm., **2019**, 566, 573-584, https://doi.org/10.1016/j.ijpharm.2019.06.011;

Natassa Pippa, Athanasios Skouras, Nikolaos Naziris, Francesca Biondo, Mattia Tiboni, Hector Katifelis, Maria Gazouli, Costas Demetzos, Luca Casettari. "*Incorporation of PEGylated δ-decalactone into lipid bilayers: thermodynamic study and chimeric liposomes development*". *J. Liposome Res*., **2019**, https://doi.org/10.1080/08982104.2019.1625377;

Raffaella Campana, Francesca Biondo, Francesca Mastrotto, Wally Baffone, Luca Casettari. "*Chitosans as new tools against biofilms formation on the surface of silicone urinary catheters*". *Int. J. of Biol. Macromol*., **2018**, https://doi.org/10.1016/j.ijbiomac.2018.07.088.

Oral presentation

Francesca Biondo, Stefan Romeijn, Laura Marino, Wim Jiskoot, Luca Casettari, Jeroen Bussmann. "Glycolipid-mediated liposome targeting in zebrafish embryos". XIII A.It.U.N. Annual Meeting, AAPS Italian University Network Student Chapter **2019** New Challenges in self-assembling drug delivery systems. 13-14/06/2019, Camerino (Italy).

Conference proceedings

- Controlled Release Society Annual Meeting & Exposition, 2019, Valencia, Spain;
- XIII A.It.U.N. Annual Meeting, AAPS Italian University Network Student Chapter 2019 New Challenges in self-assembling drug delivery systems, 2019, Camerino, Italy;
- 3rd European Conference on Pharmaceutics, 2019, Bologna, Italy;
- 11th World Meeting on Pharmaceutics, Biopharmaceutics and Pharmaceutical Technology, 2018, Granada, Spain;
- MIPOL2018 - Milan Polymer Days, 2018, Milan, Italy.

Poster

Francesca Biondo, Stefan Romeijn, Laura Marino, Wim Jiskoot, Luca Casettari, JeroenBussmann "*Biodistribution and drug delivery efficiency of Sugar Fatty Acid Esters-Liposomes in Zebra Fish*". 3rd European Conference on Pharmaceutics, 2019, Bologna.

Francesca Biondo, Ghada M. El-Zaafarany, Laura Fagioli, Samar Mansour, Mahmoud E. Soliman, Lisbeth Illum, Gehanne A.S. Awad, Luca Casettari "*Oxcarbazepine brain targeting via direct nose-to brain delivery using a emulsome-thermogel system: from in-vitro toin-vivo studies*". Edition XI World Meeting on Pharmaceutics, Biopharmaceutics and Pharmaceutical Technology, 2018, Granada.